THE EFFECT OF ACCESS ROAD CONSTRUCTION ON THE HYDROLOGY OF WETLANDS IN ROCK BARREN LANDSCAPES

Jessica Vu, B.Sc.

A Thesis Submitted to the School of Graduate Studies in Partial Fulfillment of the Requirements for the Degree of Master of Science

McMaster University MASTER OF SCIENCE (2019) Hamilton, Ontario

(School of Geography and Earth Sciences)

TITLE: The effect of access road construction on the hydrology of wetlands in rock barren landscapes

AUTHOR: Jessica Vu, B.Sc.

SUPERVISOR: Dr. James Michael Waddington

OF PAGES: 110

ABSTRACT

Dense networks of access roads can be found across the Canadian landscape. Though necessary for natural resource and mineral exploration projects, access roads are linear disturbances that can alter hydrological processes operating within the landscape. While this has previously been studied in many landscapes, research has not been conducted in wetland-dominated depressional landscapes of the Precambrian shield. As such, four wetlands were instrumented with paired monitoring wells and piezometer nests to assess hydrological change upstream and downstream of the road cut-through. In all four wetlands, the road obstructed the movement of lateral flow, resulting in ponding upstream as water was discharged to the surface. Downstream of the road, the wetland experienced a lowered water table due to reduced water inputs, especially during drought conditions. The difference between the upstream and downstream water table position (ΔWT) was largest when the culvert was placed 20 cm above the surface, indicating that large water inputs and prolonged flooded conditions was required for water to be permitted downstream. Conversely, the ΔWT was smallest when the culvert was embedded 50% into the subsurface, confirming a previous suggestion (Phillips, 1997) that partial burial is the ideal culvert placement to maintain drainage patterns. In wetlands with comparable culvert placements (perched on the moss surface), the ΔWT was smallest in the wetland that received not only water input from lateral flow, but from groundwater discharge and overland flow as well. This suggests that multiple water sources are important to provide water to the bisected unit downstream of the road cut-through. Furthermore, wetlands with a groundwater connection and deeper depression

depths were capable of maintaining a water table during drought conditions, and as such were not subjected to long-term aerobic conditions that can result in peat degradation. In general, the ΔWT was higher in the wetland during the fall rewetting than during the drought. Provided that culvert design was standardized throughout the road network, wetlands that received a greater contribution of overland flow would be at a greater risk for flooding and subsequently hydrological change. As such, a GIS model was created to assess the relative flooding potential of wetlands using criteria (catchment area, proportion of rock cover, stream order, surface water connection) that represents the first-order controls on runoff in Precambrian shield landscapes (T3 template; Buttle, 2006). The model output was evaluated using field data, where wetlands were ranked based on its water table position during the winter period when snowmelt was assumed to occur. The model was capable of assessing the hydroperiod of different wetland types, where the highest and lowest flooding potential was associated with marshes and bogs, respectively. A higher flooding potential was also associated with deeper depressions, which have been shown to have a higher hydroperiod (Didemus, 2016). The flooding potential of wetlands was variable throughout the landscape, and was not correlated with a particular wetland metric (i.e. wetland type, wetland area). The model results suggest that wetlands can be assessed based on flooding potential, in conjunction with other traditionally used wetland metrics. As such, an understanding of the hydrological function of wetlands, and proper selection of culvert design and wetlands for road crossing can be completed in order to minimize hydrological change associated with the construction of access roads.

TABLE OF CONTENTS

ACKNOWLEDGEMENTS

I would first like to thank my supervisor, Mike, for his ongoing support throughout my academic career. Even as an undergraduate student you have had the utmost confidence in my ability to do this whole research thing, and for that I am forever grateful to you. I would also like to thank the AECOM staff at HIWEC, Henvey Inlet Wind LP., as well as the contractors and personnel on site, for their technical and logistical support during the field season.

This work would not have been possible without the help from several individuals. To Katie Black, thank you for being so supportive throughout my entire field season. From bushwhacking through the woods that could possibly be inhabited by mountain lions (thanks Bob for the concern), to those ridiculous fall fieldwork trips, and numerous booters and chip stand runs, you have always maintained such a positive infectious attitude. You have definitely been the rose to my thorn (those were dark days…) during this process. To Chantel Markle, Lorna Harris, Sophie Wilkinson and Paul Moore, thank you for answering my never-ending questions and curiosity. An extra apology goes out to Alex Furukawa for dealing with the brunt of my questioning bombardment and phone calls, for the hours spent procrastinating, for keeping life in the Picarro, and for that last week of fieldwork in late November. Who knew so much could go wrong in one week! I would also like to thank Becky Janssen, Danielle Hudson, Ian Martin and Keegan Smith for their invaluable assistance in the set-up of my sites and data collection during the field season. To the best crew at our sketch house on Isabella, thank you for your company, for

sacrificing your fingers and thumbs to one syringe filter during our Gossip Girl filtering sessions (sorry Dan but this is a horrible show), and for keeping me in the loop during that notorious Bingo night. A huge shout out goes to Nicole Sandler for being my little cheerleader during the final year of my Masters. There is nothing quite like the bond you make with people during fieldwork, and I am fortunate to leave having formed these long lasting friendships.

To my friends and family, thank you for your ongoing support and love throughout this process. To Jackie Zurowski who has been worried about me since day 1, you can rest easy now that I'm finished! To my brother, Jacob, you're a bum. I'm still bitter you moved to the west coast best coast. To my parents, thank you for everything.

LIST OF TABLES

LIST OF FIGURES

LIST OF APPENDICES

CHAPTER 1: INTRODUCTION

1.1 Northern peatlands

Northern peatlands have acted as a persistent sink of atmospheric carbon dioxide (CO_2) for millennia owing to their wet anoxic conditions that constrains the decomposition of organic material. The long-term accumulation of peat material resulting from lowered decomposition rates can be attributed to a number of interrelated hydrological and ecological feedbacks that act together to regulate the response of peatlands to external forcings (Waddington et al., 2015). The water table depth (WTD) – decomposition feedback is of particular interest due to its role in the organization of the peat matrix. During periods of seasonal drought, exposure of peat soils to aerobic conditions enhances decomposition rates, resulting in a progression of finer pores with depth due to the collapse of large pores. A negative feedback regime to decomposition is formed as smaller pore spaces found in the newly organized peat matrix requires larger tensions to dewater, and as such are capable of withstanding evaporative demands. Not only does the hydrophysical structure of peat soils vary with depth, it varies spatially as well. The moss surface is made up of a mosaic of microforms that are commonly divided into hummock and hollow species (Wagner and Titus, 1984). The development of microtopography arises from fine-scale moisture gradients that promotes the establishment of *Sphagnum* hummock species that form elevated mounds above deeper water table positions, and *Sphagnum* hollow species that are capable of withstanding flooding conditions (Hogg, 1993).

1.2 Hibernation habitat

Sphagnum hummocks are commonly used as hibernation habitat by the threatened eastern Massasauga rattlesnake (EMR) at the northern extent of their range (Johnson et al., 2000; Shine and Mason, 2004). A critical zone (termed the resilience zone) exists within the hummock that allows EMRs to overwinter between the advancing frost line and fluctuating water table (Smolarz et al., 2018), where the survival rate of EMRs is dependent on the water table position and the timing and duration of snow events. Fluctuating water levels during overwintering can be detrimental to populations of EMRs as it results in flooding within the hibernacula and exposes the snake to sub-freezing conditions leading to dehydration and desiccation (Costanzo, 1988). Although EMRs have a tolerance to short-term flooding events, they are unable to withstand long-term flooding due to obstacles related to osmotic and ionic balance, and oxygen demand (Costanzo, 1989). For instance, in the winter of 2001, a den in central Manitoba experienced flooding as a result of unusually heavy rainfall, resulting in the death of 123 snakes (Shine and Mason, 2004). While numerous ecohydrological feedbacks operate in peatlands to regulate water table fluctuations, there exists uncertainty to the response of these systems to extreme disturbance (Waddington et al., 2015). The maintenance of hydrological function of wetlands is especially important as rattlesnakes at the northern extent of their range display a high fidelity to hibernation sites, indicating a lack of suitable overwintering sites (Johnson et al., 2000; Harvey and Weatherhead, 2006). The loss of one suitable habitat due to hydrological disturbance can be detrimental to population of EMRs.

1.3 Hydrological processes operating in bedrock systems

1.3.1 Runoff

Wetlands in near-northern Ontario are found in low-lying bedrock depressions and topographic valleys over relatively impermeable bedrock. These wetlands are traditionally considered isolated, in the sense that they do not exhibit continuous connection of flow (Oswald et al., 2011). Hydrological connectivity with the surrounding landscape occurs due to overland flow during periods of 'fill-and-spill', a process that is initiated when water input exceeds the storage capacity of the depression (Spence, 2003). Once the storage capacity is exceeded, water discharges from the depression at the lowest bedrock elevation (termed the sill) as surface flow. Runoff generated by upland depressions in turn contributes overland flow to downstream hydrological response units (HRU), resulting in a progression of water table rise moving downslope within the catchment (Buttle and Sami, 1992; Branfireun and Roulet, 1998). Each HRU therefore has three functions: to store water within the depression, to generate runoff during periods of fill-and-spill, and to contribute water to allow coupling between the wetland and landscape (Spence, 2003).

1.3.2 Storage

The water storage dynamics of wetlands is dependent on the morphometric characteristics of the depression; where depressions with deeper depths, greater volumes, and a larger surface area were capable of maintaining a water table for longer periods of time (termed hydroperiod; Brooks and Hayashi, 2002). This was determined by assessing the number of times the depression maintained a water table to the total number of visits (Snodgrass et al., 2000), where a value of 1 indicates that standing water was present during every visit. The results of this study

indicated that the hydroperiod index was greater than 0.8 for vernal pools deeper than 50 cm with larger surface areas, and below 0.5 for pools shallower than 35 cm with smaller surface areas. Similarly, the hydroperiod for wetlands formed over unfractured bedrock depressions was 1.0 for depressions with a depth greater than 60 cm, even amidst drought conditions (Didemus, 2016). The underlying geology also plays a role in the water storage dynamics of wetlands (Gay, 1998). In systems that are supplied by rainwater and surface waters, the hydroperiod is limited by the rate of evaporation and water demands of the vegetation. In groundwater-fed systems, however, groundwater inflow provides some supply of water throughout the dry season and sustains baseflow within the depression (Leibowitz and Brooks, 2008; Ketcheson, 2005). As such, water contributions to wetlands play an important role in their water storage dynamics.

1.3.3 Landscape connectivity

HRUs within the landscape become coupled when saturated portions of the catchment expand in response to rainfall. Only a portion of the catchment is actively involved in runoff generation (Hewlett and Hibbert, 1967), and only a portion of that water reaches the outlet (termed contributing area). The ability of the landscape to propagate runoff to the outlet is dependent on the spatial arrangement of HRUs and their location relative to one another (Buttle et al., 2004). For instance, runoff is more likely to reach the outlet if it travels shorter distances between the HRU and the outlet (Bracken and Crooke, 2007). In contrast, wetlands become decoupled with the landscape when the storage capacity of the depression cannot be exceeded (Branfireun and Roulet, 1998; Spence, 2003; Tromp-van Meerveld and McDonald, 2006).

1.3.4 Rainfall

Precipitation is a major source of water input contributing to wetlands by falling directly into the depression, or indirectly as surface runoff from the catchment. Once water enters the depression, it is partitioned into storage, evapotranspiration, runoff, or bedrock infiltration (Spence and Woo, 2003). The timing, duration and intensity of rainfall determines how the event is partitioned. If rainfall exceeds the evapotranspiration demands of the atmosphere, the event will be stored within the depression; if rainfall exceeds the storage capacity of the depression, the event will generate runoff; and given a high enough rainfall intensity, water infiltration into fractured bedrock can be restricted, resulting in higher runoff rates (Tromp-van Meerveld and McDonald, 2006). It is no surprise that larger events produce more runoff and hydrological connectivity within the catchment than smaller rain events (Lehmann et al., 2007). However, the timing and duration of rainfall also plays an important role in initiating and propagating runoff. High intensity events on a dry catchment will not initiate runoff due to high infiltration rates (Fitzjohn et al., 1998; Bracken and Crooke, 2007). Low intensity events following a previous rain event, however, will generate runoff as the catchment is wet and transmission losses are low. Therefore, increased soil moisture (following previous storm events) will result in a higher probability of hydrological connectivity within the catchment.

1.3.5 Snowmelt

The largest runoff event typically occurs during the spring freshet when a large quantity of snowmelt is released to the landscape over a relatively short period of time (Ketcheson, 2015). During the spring freshet, the storage capacity of the depression is typically at full saturation, and as such, the wetland is unable to moderate streamflow (Gray et al., 1984; Spence et al., 2011). In

the summer, antecedent moisture condition within the depression is typically low, and thus minimal overland flow is generated as precipitation is primarily partitioned into storage and evapotranspiration. Having a large snowmelt can potentially eliminate the storage deficit of a depression, as it results in higher antecedent moisture conditions in the late spring/early summer (Spence, 2000). Spence and Rouse (2002) suggested that the dominant control on summer evaporation rates was the size of the spring freshet, where the snow water equivalent (SWE) determines the rate of groundwater recharge and size of groundwater flow. Therefore, the timing and duration of snowmelt has implications for streamflow at different times of the year.

1.3.6 Groundwater flow

It was previously assumed that vertical flow through peatlands is insignificant due to the heterogeneous and anisotropic distribution of hydraulic conductivity in peat soils (Ivanov, 1981; Ingram, 1982). However, Reeve et al. (2002) observed that vertical flow does occur, where the primary control on groundwater exchange within wetlands is the permeability of the mineral soil. Peat formed under permeable soils will drive peat pore-water to recharge, whereas peat formed over impermeable soil has negligible vertical flow and will be dominated by lateral flows. Therefore, the hydrogeology and presence of sediment determines whether water movement is dictated by lateral or vertical flow.

1.4 Thesis framework

Historically, environmental protection has been placed on wetlands due to the large amount of ecosystem services that are provided (Lemly, 1995). Due to developmental pressures in near-northern Ontario, it is unrealistic to avoid wetlands altogether. It is, however, possible to improve

mitigation measures and the site selection process such that hydrological impact within wetlands is minimized. The objective of this research was to investigate access road construction in wetland-dominated depressional landscapes in order to guide wetland crossings best management practices. The first manuscript assesses the spatial variability of hydrological impact in wetlands with various site characteristics and culvert design. The water source and hydrophysical properties of the wetland were characterized through the use of stable isotopes, hydrodynamic data, and soil cores. Paired monitoring wells and piezometer nests were installed upstream and downstream of the road cut-through to assess differences in hydrological processes on either side of the disturbance. The result of the first manuscript was used to provide the foundation for the second manuscript. From the first manuscript, it was observed that the hydrological impact of road cut-through in wetlands manifested itself through a higher water table position upstream and a lower water table downstream of the disturbance. This water table difference (ΔWT) was greatest during the fall rewetting, suggesting that the wetland experience prolonged flooding conditions during periods of high water input. Therefore, a GIS approach was taken to assess the flooding potential of wetlands due to contributions of overland flow, where a higher flooding potential was indicative of wetlands that would be at risk for greater hydrological change. Easily accessible spatial data such as DEM (obtained from LiDAR), and ELC (obtained from image classification) was used to create the model. The model output was evaluated using field data and wetland metrics such as depression depth, wetland type, and wetland area.

CHAPTER 2: HYDROLOGICAL RESPONSE OF WETLAND-FILLED BEDROCK DEPRESSIONS SEVERED BY ACCESS ROADS

2.1 INTRODUCTION

One of the most widespread forms of modification to the physical environment in the past century is the construction of access roads (Noss and Cooperrider, 1994). Although necessary for the development and operation of natural resource and mineral exploration projects, access roads are linear disturbances that can have a cumulative impact on the landscape (see Trombulak and Frissell, 2000). The most notable consequence associated with access roads is the fragmentation of habitat. The creation of edges arising from linear features can alter the vegetation community of the interior habitat due to increased light infiltration, changes in temperature, and exposure to wind (Findlay and Bourdages, 2000; Delgado et al., 2007; Tew and Hesselberg, 2017). As a result, there is a loss of biodiversity due to reduced resources and increased competition amongst species (Haddad et al., 2015). Not only do access roads change the ecological function of the landscape, it changes the hydrological function as well. Topography changes associated with the construction of access roads have been observed to divert natural drainage patterns, thereby altering the timing and magnitude of runoff within the catchment (Megahan, 1972; Wemple, 1996). Given that hydrology is the primary control on the form, function and development of wetlands (Mitsch and Gosselink, 1993), hydrological change associated with access road construction can change the trajectory of wetland systems.

Wetlands are often avoided during the construction of access roads, as it is a difficult and costly venture (FP Innovations, 2011). While longer roads are seen as an alternative to wetland crossing, there reaches a point where the distance associated with avoiding wetlands becomes too great. Considering that the natural resource and mineral exploration sector contributes to 11% of Canada's economy (NRC, 2018), and wetlands make up 13% of the Canadian landscape, it is no surprise that complete wetland crossing avoidance is unattainable. Wetland crossings in near-northern Ontario are of particular concern as populations of the threatened eastern Massasauga rattlesnake (EMR) utilize *Sphagnum* hummocks found in moss-forming wetlands for overwintering (Johnson et al., 2000; Shine and Mason, 2004). Furthermore, EMRs at the northern extent of their range display a high fidelity to hibernation sites, indicating a lack of suitable overwintering habitat (Johnson et al., 2000; Harvey and Weatherhead, 2006). The maintenance of hydrological function of wetlands during development is therefore especially critical, as the loss of one suitable habitat can be detrimental to the entire population of EMRs.

In the case where wetlands do need to be crossed, mitigation measures (such as culverts) can be implemented such that hydrological processes are maintained. The design and installation of culverts, however, needs careful consideration in order to adequately allow the movement of flow downstream. Culverts can be perched on the moss surface, partially embedded, or completely submerged into the wetland (Philips, 1997). The spacing between culverts can also be quite variable, ranging between 15 – 100 m apart when multiple culverts are used. While it has been established that hydrological disturbance is associated with the construction of access roads, the impact is not uniform across the landscape. In Manitoba and Saskatchewan, practitioners observed tree dieback alternating between the upslope and downslope of the road

due to ponding of lateral flow (FP Innovations, 2011). This indicates a meandering nature of surface and subsurface flows within the wetland, where the access road alternated between bisecting and paralleling water flow. Mader (2014) also observed different severity of ponding in wetlands with a similar length of road cut-through and culvert design. In the Peace River area, practitioners demonstrated that ponding was eliminated when culverts were evenly and closely spaced 60 m apart (FP Innovations, 2011). Conversely, in eastern Canada a spacing of 20 m was sufficient to minimize hydrological change in forested wetlands (Mader, 2014). Therefore, a standard culvert design cannot be applied to every landscape and is instead assessed on a site-by-site basis. As such, the hydrological function of wetlands should likely be assessed prior to road cut-through such that proper mitigation measures are selected to minimize hydrological change. The objective of this research is therefore threefold: to assess hydrological function of wetlands in the Henvey Inlet Wind Energy Centre (HIWEC), to examine hydrological response of wetlands upstream and downstream of access road cut-through, and to identify site properties and culvert design that can minimize potential impacts to the wetland form and function.

2.2 METHODOLOGY

2.2.1 Study area

HIWEC is located along the eastern shore of Georgian Bay approximately 80 km south of Sudbury, Ontario (Figure 2-1). The climate is characterized as cool-temperate and humid, with a mean annual temperature of -12.0°C in January, and 19.4°C in July (1981 – 2010; Environment Canada, 2015). The annual precipitation is 759 mm as measured in the Monetville Station located approximately 30 km northwest from HIWEC (Environment Canada, 2015). The growing season ranges from 183 to 219 days (AECOM, 2016).

2.2.1.1 Geology

HIWEC – situated on the southwestern part of the Grenville Province of the Canadian Shield – is composed of a complex suite of highly foliated migmatitic gneisses of granitic to granodioritic composition (Kor, 1991). The upper 10 to 20 m of the exposed bedrock is highly fractured, with hydraulic conductivities ranging from 4×10^{-7} to 8×10^{-4} m s^{-1} (AECOM, 2015). Longitudinal bedrock ridges run throughout the study area along a northeast to southwest axis. Mineral soil can be found in thin discontinuous deposits along the exposed bedrock, as well as thicker deposits under wetlands in low-lying areas and bedrock valleys. The mineral soil originates from the final Late Wisconsinan glacial advance and retreat (Kor and Delorme, 1989), and consists of glaciolacustrine deposits, ice-contact stratified deposits, and tills (OGS, 2003).

2.2.1.2 Vegetation

HIWEC is located within the Georgian Bay Ecoregion, and is dominated by mixed forest comprising of Eastern White Pine, Red Pine, Eastern Hemlock, Black Spruce, White Spruce, Balsam Fir, Jack Pine, Tamarack, Yellow Birch and Sugar (Crins et al., 2009). Wetlands can be found scattered throughout HIWEC within bedrock depressions, and as large complexes within topographic valleys. The wetlands are surrounded by uplands, where tree stands are commonly found along the bedrock perimeter. The different wetland types found at HIWEC are swamps, marshes, fens, and bogs. Fens and bogs are dominated by peat mosses such as *Sphagnum* spp.

2.2.2 Instrumented wetlands

Four wetlands were randomly selected within HIWEC with each wetland fulfilling the following criteria: bisected by a newly constructed access road, contains a culvert, and has *Sphagnum*

hummocks. The four wetlands varied in terms of physical properties as well as culvert design (Table 2-1). Two wetlands (201, 202) were formed in narrow isolated bedrock depressions and had a shallow deposit of organic soil (40 – 50 cm). Conversely, 203 and 205 were formed in wider bedrock depressions and had a thicker organic soil deposit (75 – 80 cm). Furthermore, 205 was formed in an isolated bedrock depression, and 203 was apart of a larger wetland complex. There were no tree stands in 201, 202 and 203, resulting in open cover throughout the wetland. A sparse distribution of tamarack stands can be found in 205.

2.2.3 Sampling design

Nested hydrological equipment was installed in *Sphagnum* hummocks in a transect parallel (PL) to the road (~ 3 m away from the road) and a transect perpendicular (PR) to the road (~ 15 m from the road). In the case where the wetland was formed in a narrow bedrock depression (201, 202), a transect parallel to the road was not installed, and instead a single nest was installed at the culvert (C). Each side of the road cut-through consisted of 2 – 4 nests. The nested equipment consisted of a well installed into the mineral soil below the wetland, and 2 – 5 piezometers placed at various depths (25 cm, 50 cm, 75 cm, 100 cm, and base of the depression), depending on the thickness of the organic material. Each side of the wetland was considered upstream (US) or downstream (DS) based on the water table position. The piezometers were labeled based on the wetland number, the location of the nested equipment, followed by the depth. The wells followed a similar labeling scheme with the exclusion of the depth measurement. For example, 205-DS-C refers to a well installed in the downstream side of the wetland 205, at the nest closest to the culvert. All pipes were constructed from PVC (4.5 cm diameter for wells, 2.25 cm diameter for piezometers) with the slotted portion covered with a well sock to prevent sediment

and other material from entering the pipe. The wells had slotted PVC that extended from the base of the depression to 10 cm above the moss surface. The piezometers were created with 10 cm of slotted PVC centered at the desired depth, and un-slotted PVC for the remaining pipe. Subsurface stratigraphy was recorded at each material change (organic soil, mineral soil) during the installation process. The pipe-top elevation was measured using a Smart Leveler (Digital Leveling Systems, Smyma TN, USA, accuracy = 2.3 mm) and adjusted to a common stationary datum (culvert) within each wetland.

2.2.4 Data collection and analysis

2.2.4.1 Meteorological conditions

The sampling period for this study was from May 17 – October 24, 2018. A barologger (Solinst Junior Levelogger, Solinst, Georgetown ON, CA, accuracy = ± 0.1%) was suspended in an empty well casing to measure changes in atmospheric pressure at 15-minute intervals, as well as changes in air temperature. Rain events were captured using a tipping bucket rain gauge installed at 203, and checked with manual rain gauges located at 201, 202, 203 and 205. Manual rain gauges were placed at the nest closest to the culvert in an open area to avoid interception from the canopy cover.

2.2.4.2 Water level

The water level of the wells and piezometers were measured manually at least once a week using a dip-meter (Solinst Beeper Tape, Solinst, Georgetown ON, CA, accuracy = ± 0.1%) over a sampling period of May 17 – July 17, and August 28 – October 24. Manual measurements were not collected from July 17 – August 28 due to site restrictions. The height of the pipe from the

moss surface was measured with every water level measurement to account for changes in peat compression and shrinkage. Pressure transducers (Solinst Junior Levelogger, Solinst, Georgetown ON, CA, accuracy = ± 0.1%) were deployed in each wetland within the wells located at the culvert to allow measurement of continuous water level at 15-minute intervals both upstream and downstream of the road. The pressure transducer measures the height of the overlying water column over a given point, as well as changes in atmospheric pressure. The data can be expressed relative to the surface (where moss surface = 0 cm) by subtracting the atmospheric pressure and the distance that the pressure transducer was suspended from the surface. Pressure offsets were corrected using manual water level measurements, and a moving average was used to gap-fill between two manual measurement points. The water table response to rainfall was assessed in each wetland using the pressure transducer and tipping bucket rain gauge. This was calculated using the difference between the initial and maximum water table position during each event. Storm events that were smaller than 1 mm in size were excluded.

2.2.4.3 Water quality

The temperature and electrical conductivity (EC) of the wells and piezometers were measured manually at least once a week using a handheld YSI device (YSI Pro 1030, YSI Incorporated, OH, USA, accuracy for conductivity = 1 uS cm^{-1}, temperature = ± 0.2°C). Electrical conductivity was internally corrected within the device to a reference temperature of 25°C. The YSI was calibrated using a one-point calibration for EC (80 mS cm^{-1}).

2.2.4.4 Water collection

Pore-water and mineral soil samples were collected on a monthly basis (June, July, September, November) within the piezometers, groundwater samples were collected from surficial bedrock wells opportunistically, and rain samples were collected in rainfall collectors (located at 202, 203 and 205) following a storm event. The rainfall collector was designed based on Gröning et al. (2012), with the addition of a mesh screening placed over the opening of the collector to keep out falling debris and material. Prior to pore-water, mineral soil and groundwater sampling, water was emptied from the pipe until the change in EC was less than 5%, or until three pipe volumes were removed. This discarded stagnant water and ensured that a representative sample at that depth was collected. Water samples were collected using a hand-held vacuum pump, tygon tubing, and 125 mL bottles (the latter two of which were environmentalized). The samples were filtered using a 0.45 um syringe filter into a 20 mL scintillation vial and kept with minimal headspace. All samples were filtered within 24 hours following collection, and kept refrigerated until analysis.

2.2.4.5 Isotope analysis

Water samples were analyzed for stable isotopes of hydrogen (δ^2H) and oxygen ($\delta^{18}O$) using the Picarro L-1102-I cavity ring-down spectroscopy (CRDS) isotopic water analyzer paired with a V1102-I vaporizer module and an HTC-PAL auto-sampler (Leap Technologies, Carrboro NC, USA). The isotopic composition of each sample was obtained by following a detailed methodology outlined by Furukawa (2018). Firstly, working standards (DSH, MDI, BSB305-DI, IWL) were calibrated to the international standards Vienna Mean Ocean Water 2 (VSMOW2) and Standard Light Antarctic Precipitation 2 (SLAP2) acquired from the International Atomic

Energy Association (IAEA, Vienna, Austria). The heavy working standard DSH ($\delta^{18}O$ = 0.10%, $\delta^{2}H$ = -2.23%) was sourced from deep-sea water; the light working standard IWL ($\delta^{18}O$ = -23.83%, $\delta^{2}H$ = -212.37%) was sourced from bottled iceberg water; and the medium working standard MDI ($\delta^{18}O$ = -6.51%, $\delta^{2}H$ = -46.97%) and BSB305-DI ($\delta^{18}O$ = -6.46%, $\delta^{2}H$ = 47.17%) were sourced from mixtures of reverse osmosis water from McMaster University. Four 1.5 uL injections of the water sample was injected into the Picarro, and then averaged to obtain the isotopic composition. MDI was injected after eight samples throughout the run to monitor drift. IWL, DSH, and BSB305-DI were injected at the beginning of every run to calibrate the data to the VSMOW2 scale. Following completion of the run, the dataset was checked for contamination using the ChemCorrect software (Picarro Inc., Santa Barbara CA, USA), and post-processed for drift and memory effects using a method outlined by van Geldern and Barth (2013). All results are reported in delta-notation ($\delta^{2}H$, $\delta^{18}O$) relative to the Vienna Standard Mean Ocean Water (VSMOW) and are expressed in per mil (%).

2.2.4.6 Hydrophysical properties

The hydrophysical properties of each wetland were characterized using soil from cores extracted from *Sphagnum* hummocks. Cores were taken with a 10 cm PVC pipe that was slowly lowered into the subsurface. Resistance was removed using a hand-held wool saw and scissors to minimize peat shearing and compression. Triplicate cores were taken at each site except 205 where only one core was collected due to a high density of shrubs and roots. The cores were cut with a band saw into 5 cm intervals and kept frozen until the sample was ready to be processed.

Bulk density

The samples were oven-dried at 65°C for at least 48 hours, or until the mass loss was less than 0.1 g day^{-1}. Bulk density was calculated using a standard method outlined by Freeze and Cherry (1979):

$$\rho_b = \frac{M_s}{V_T} \tag{1.1}$$

where ρ_b= bulk density (g cm^{-3}), M_s = dry mass of the soil (g), and V_T = volume of the sample (cm^3).

Organic matter content

The organic matter content of peat samples (expressed as a percentage) was determined by the loss-on-ignition (LOI) method as outlined by Payne et al. (2016). Crucibles were filled with approximately 5 cm^3 of material from each sample interval and subsequently burned in a muffle oven at 550°C for 4 hours. The percent organic matter content was calculated using:

$$\frac{weight\ of\ peat\ pre\ LOI - weight\ of\ ash\ post\ LOI}{weight\ of\ peat\ pre\ LOI} \tag{1.2}$$

Porosity

Porosity was calculated using:

$$n = 1 - \left(\frac{\rho_b}{\rho_d}\right) \tag{1.3}$$

where n = porosity, ρ_b= bulk density (g cm^{-3}), and ρ_d= particle density (g cm^{-3}). The particle density was estimated based on the relative organic/inorganic fractions, as well as the

organic/inorganic particle densities of 1.47 g cm^{-3} and 2.56 g cm^{-3}, respectively (Redding and Devito, 2006).

Saturated hydraulic conductivity

Bail tests were completed within each piezometer to measure saturated hydraulic conductivity (K_{sat}) in-situ. A pressure transducer was added into the piezometer prior to the start of the bail test to measure the initial water table position, as well as the water level response following the addition of 100 mL of water. The frequency of data collection ranged from 1 – 5 seconds for surficial moss (25 – 50 cm), 2 – 4 hours for denser decomposed moss (75 cm), and up to 24 hours for mineral soil. A barologger was used to correct for diurnal variation in atmospheric pressure. The saturated hydraulic conductivity was calculated using the Hvorslev (1951) method:

$$K_{sat} = \frac{r^2 \ln(\frac{L}{R})}{2\,LT_L} \tag{1.4}$$

where r = inner radius of the piezometer, L = length of well screen, R = outer radius of the piezometer, T_0 = time required for the water level to rise/fall to 37% of the initial change.

2.2.5 Statistical analysis

Statistical analysis was completed to identify differences (water source, hydrophysical properties, water table response to rainfall) between the four instrumented wetlands in order to conceptualize the hydrological function of the wetlands. Statistical analysis was also completed to assess whether hydrological processes within the wetland was different upstream and downstream of the road cut-through. All statistical analysis was completed in JMP 14 (SAS, Cary NC, USA). Datasets were first tested for normality using the Shapiro-Wilk test. Given that

the dataset failed the test for normality, the non-parametric tests were used. The water samples collected from the piezometers (pore-water, mineral soil) were separated into dry (June, July) and wet (September, November) conditions to assess whether the isotopic composition remained consistent with time using the Wilcoxon/Kruskal-Wallis test. There was no statistical difference between the water samples collected at different piezometer nests and as such all samples collected at a particular depth were aggregated together. The Wilcoxon/Kruskal-Wallis test was used to determine whether there was a difference between the surface soil samples (top 10 cm of the soil core) and deep soil samples (bottom 10 cm of the soil core) between the four wetlands. A generalized linear model was created to evaluate the relationship between the water table rise and the predictor variables (size of the storm event, initial water table position) in all four wetlands. A two-way interaction between the predictor variables was included if it improved the model performance (R^2).

To assess whether the bisected wetland had a different water table response upstream and downstream of the road, the Wilcoxon signed rank test was used. In all four wetlands the paired water table response (using mean water table positions from continuous logger measurements) was statistically significant ($p<0.0001$), indicating that each wetland can be separated into an upstream and downstream unit. In all subsequent analysis, all datasets that had a paired response (upstream and downstream of the road) was assessed for statistical significance using the Wilcoxon signed rank test. The manual measurements of EC and temperature from the well located at the culvert were aggregated together to assess changes in water quality measurements upstream and downstream of the road.

2.3 RESULTS

2.3.1 Meteorological conditions

The summer of 2018 was characterized by unusually dry conditions that persisted until August 24, followed by numerous consecutive rain events during the fall that added large water inputs to the landscape (Figure 2-2a). The average rainfall between May and August was 340 mm (1981 - 2010; Environment Canada, 2015) in comparison to the 170 mm of rain that fell during the summer. In total, 402 mm of rain fell over the duration of the study period. The largest rain event occurred on September 26 where 71 mm of rain fell over 22 hours (Figure 2-2a).

2.3.2 Isotope composition of rainwater

The results of the isotope analysis are shown in Figure 2-3 with summary statistics of $\delta^{18}O$ and $\delta^{2}H$ in Table 2-2 and 2-3, respectively. The Local Meteoric Water Line (LMWL) – created using rain samples collected from May 19 to November 8 – was $\delta^{2}H = 7.60\ \delta^{18}O + 9.90$. The isotopic composition of precipitation showed distinct seasonality, where more depleted (negative) values was recorded later in the fall (Figure 2-2c). Rain collected in November was the most isotopically depleted with an average $\delta^{18}O$ of -17.2% and $\delta^{2}H$ of -119.2%. Samples collected in August were the most enriched (positive) with an average $\delta^{18}O$ of -4.9% and $\delta^{2}H$ of -26.6%. Temperature effects were seen where a warming period in early October (average air temperature on October 2 = 17.6°C) coincided with more enriched rain samples (Figure 2-2). The line-conditioned deuterium-excess (d-excess) values was calculated using $\delta^{2}H - 8\ \delta^{18}O$ (Dansgaard, 1964). The d-excess values of the rain samples ranged from 7.3 to 20.0% with an average value of 12.9 ± 3.3%. All of the rain samples collected from September – November had

d-excess values above 10%, whereas 67.7% of the rain samples collected during the drought were above this threshold (Figure 2-d).

2.3.3 Stable isotopic profile of the peat and mineral soil

201

The isotopic composition of the mineral soil (75 cm, base) was consistent through time (Figure 2-5a). While the organic soil samples plotted along and below the LMWL (Figure 2-4a), it was more depleted than the mineral soil during the drought. During the fall rewetting, however, the organic material was enriched in $\delta^{18}O$ due to rain events. The top 50 cm were highly variable along the LMWL (Figure 2-4a).

202

Statistical analysis indicated that the isotopic composition at 25 cm was different between the dry and wet conditions (Wilcoxon/Kruskal-Wallis test, $p<0.005$). While there was no statistical difference between the dry and wet season for samples collected at 50 cm and base (Table 2-2), a small sample size could be producing a false p-value. As such, definitive conclusions could not be made. The isotopic signature of the mineral soil was more enriched during the fall rewetting than the drought (Figure 2-5b). This was the only wetland where the sample collected at the base was highly variable with time (Figure 2-4b). All of the pore-water and mineral soil samples plot along the LMWL, and were quite variable throughout the study period (Figure 2-4b).

203

The samples at the peat-mineral soil interface (75 cm) and mineral soil (100 cm, base) have a similar and consistent isotopic composition with time (Figure 2-5c). This was the only wetland where the isotopic signature of organic soil highly overlapped the mineral soil (Figure 2-4c). Within the top 50 cm, the pore-water at 25 cm and 50 cm did not differ significantly (Wilcoxon/Kruskal-Wallis test, p=0.37). Although both surficial samples (25 cm, 50 cm) plot along the LMWL, the 50 cm plots closer to the mineral soil (Figure 2-4c). During the fall rewetting, the top 50 cm was enriched in $\delta^{18}O$ with a mean value of -9.3% at 25 cm, and -10.0% at 50 cm. The top 50 cm was also highly variable during the fall rewetting (Figure 2-4c).

205

The top 25 cm of the peat profile was depleted in $\delta^{18}O$ during the drought and plotted consistently to the right and below the LMWL (Figure 2-4d). The isotopic signature at 50 cm (peat) and 75 cm (peat-mineral soil interface) was not statistically different (Wilcoxon/Kruskal-Wallis test, p=0.42; Figure 2-5d). However, the samples at 50 cm plot either along or below the LMWL, whereas the samples at 75 cm plot along the LMWL or overlapping the mineral soil (Figure 2-4d). During the fall rewetting, the isotopic composition of the top 75 cm was enriched in $\delta^{18}O$. The samples at 75 cm plot closer to the mineral soil, whereas the samples at 25 cm and 50 cm overlapped. The isotopic signature of the mineral soil (100 cm, base) was consistent through time (Figure 2-5d). All of the samples within the wetland (both organic and mineral soil) were tightly clustered together (Figure 2-4d). Unlike the other three wetlands, the isotopic composition of the top 50 cm was not highly variable along the LMWL during the fall rewetting (Figure 2-5d).

2.3.4 Groundwater dynamics

The piezometer nest furthest away from the road (PR) was used to assess the groundwater recharge-discharge relationship within the wetland, as the organic and mineral soil could be considered relatively undisturbed by construction activities. The vertical gradient (Δh) was assessed between the water table measured in the well, and the hydraulic head measured in the base piezometer installed at the same depth as the well. In some wetlands there was a lack of mineral soil (202-US), or insufficient area (203-DS) to allow for a transect perpendicular to the road. As such, only one vertical profile was examined for those wetlands. A positive value indicated that the hydraulic head was higher in the piezometer, and as such groundwater discharged into the wetland. Conversely, a negative value indicated that the hydraulic head was lower in the piezometer, and as such groundwater was recharged. In 201-US and 202-DS, there was a consistent recharge of groundwater (Figure 2-6a, 2-6b). Flow reversals occurred for 201-DS (Figure 2-6a), 203-US (Figure 2-6c) and 205-US (Figure 2-6d), where groundwater was recharged during the spring and fall rewetting, and discharged during the drought. The trend at 205-DS (Figure 2-6d) was quite unusual where groundwater was discharging during the spring, and recharging during the drought. The EC of the mineral soil (measured in the base piezometer installed in the mineral soil) was highest in 205-DS and lowest in 201-US (Figure 2-7). The EC was statistically similar between 203-US and 205-DS (Wilcoxon/Kruskal-Wallis test, $p=0.73$) and between 202-DS-PR and 201-DS-PR (Wilcoxon/Kruskal-Wallis test, $p=0.13$).

2.3.5 Bulk density

The general trend within all four wetlands was an increase in bulk density with depth (Figure 2-8). In 201 and 205, bulk density increased linearly with depth (R^2 of 0.93 and 0.94 for 201 and

205, respectively). Conversely, in 202 and 203 bulk density increased exponentially with depth (R^2 of 0.95 and 0.75 for 202 and 203, respectively). Though a sharp increase in bulk density was observed in 203 at a depth of 25 cm, this could be attributed to the wetland consisting of floating mats. The greatest increase in bulk density occurred between 45 – 50 cm, and 65 – 70 cm for 202 and 203, respectively. The bulk density within the top 10 cm of the core was significantly different than the bottom 10 cm in 201, 202 and 203 (Wilcoxon/Kruskal-Wallis test, $p<0.05$). The bulk density of the top 10 cm of the core was statistically different between 201 and 203 (Wilcoxon/Kruskal-Wallis test, $p<0.05$). The bulk density of the bottom 10 cm of the core, however, was not statistically different between all four wetlands.

2.3.6 Porosity

Within all four wetlands the largest porosity was observed in surficial samples, which then decreased with depth (Figure 2-9). The porosity of surface moss (0 – 10 cm) was statistically similar within all four wetlands with an average value of 0.98 ± 0.0003.

2.3.7 Saturated hydraulic conductivity

The saturated hydraulic conductivity (K_{sat}) for all four wetlands in both the organic and mineral soil decreased with depth (Figure 2-10). The peat-mineral soil interface was reached at 50 cm in 201 and 202, and at 75 cm for 203 and 205. In all four wetlands the K_{sat} at the peat-mineral soil interface was 1×10^{-6} m s^{-1}. There was no statistical difference between the four wetlands. The K_{sat} of the mineral soil within all four wetlands ranged from 2.3×10^{-8} to 3.2×10^{-5} m s^{-1}. In comparison, the K_{sat} of the fractured bedrock ranged from 4×10^{-7} to 8×10^{-4} m s^{-1}.

2.3.8 Water table position

A gradual water table decline occurred in all four wetlands from May 17 to August 24 (Figure 2-11). Throughout the entire study period, the water table position decreased by 35.7 cm in 201, 44.0 cm in 202, 33.6 cm in 203, and 55.7 cm in 205. The first wetland to lose its water table was 202 on July 10, followed by 201 on July 21. The downstream side of 201 lost its water table for 35 days (longest duration was 11 consecutive days), and 202 lost its water table for 30 days (longest duration was 2 and 11 consecutive days for the upstream and downstream side, respectively). The water table was maintained in 201-US, where the minimum position was reached on August 20 (WT_{min} = -26.7 cm). Although the deeper wetlands (203, 205) did not lose its water table during the study period, a minimum position was reached on August 5 (in 203; upstream WT_{min} = -48.8 cm, downstream WT_{min} – 64.2 cm) and on August 20 (in 205; upstream WT_{min} – 71.3 cm, downstream WT_{min} – 74.3 cm). Between August 25 and August 29 there were three rain events totaling 58.5 mm of rain that caused a large water table rise in all four wetlands. The water table rise was greatest for 202 (WT rise = 7.8 cm), followed by 203 (WT rise = 7.0 cm), 205 (WT rise = 6.3 cm), and lastly 201 (WT rise = 5.7 cm). However, the water table does not persist within the wetland until September 21.

The mean daily water table position between the two sides of the wetland was statistically different throughout the study period (Wilcoxon signed rank, $p<0.0001$; Figure 2-12). The difference between the upstream and downstream water table position was greatest in 201 (ΔWT_{max} = 28.3 cm), followed by 202 (ΔWT_{max} = 19.3 cm), 203 (ΔWT_{max} = 15.4 cm), and 205 (ΔWT_{max} = 8.3 cm). A larger ΔWT was observed during the fall rewetting for 201, 202 and 205. An opposite trend occurred for 203 where the ΔWT was on average higher during the drought than

fall rewetting. This was the only wetland where there was a negative ΔWT value, indicating that the downstream water table was higher than the upstream water table. The negative values occurred between August 26 and September 7, which coincided with large precipitation events. The wetland with the least amount of flooding was 205 (9 days), followed by 203 (44 days), 202 (46 days), and 201 (67 days). The upstream side of the wetlands flooded more frequently than the downstream side (Figure 2-13).

2.3.9 Water table response to rainfall

The water table response of wetlands to rainfall was a function of both the size of the storm event and to a lesser degree the initial water table position (Table 2-4). There was no interaction between the two predictor variables. In all four wetlands, there was a positive linear relationship between the initial water table position and the water table response during a rain event (Figure 2-14), suggesting that there was a greater water table rise moving deeper into the peat profile. For instance, at an initial water table position of -63 cm, the water table rose 33 cm for an 8 mm event in 203. For the same event, the water table increased by 13 cm at an initial water table position of -73 cm in 205. Furthermore, the slope of the regression line was largest in 203 and smallest in 205 (Figure 2-14), suggesting that these wetlands were the most and least responsive to rainfall, respectively. While the size of the rain event and the initial water table position can act as predictor variables for water table rise during rainfall, there was uncertainty that remained unaccounted for. The predictor equation determined from the generalized linear model explained more variability (R^2) in 202, followed by 201, 203 and lastly 205.

2.3.10 Vertical hydraulic gradient

Vertical hydraulic gradient was measured in the peat profile in the transect parallel to the road to assess the movement of water as it encountered a boundary with (C) and without (PL) a culvert. The vertical hydraulic gradient was assessed using the piezometers installed at 50 cm and 75 cm. At the road, the hydraulic gradient was positive upstream indicating discharge (Figure 2-15a). Conversely, the hydraulic gradient was negative downstream indicating recharge into the subsurface. The piezometer nest furthest away from the road (PR) was used to assess vertical hydraulic gradient in the absence of disturbance. The hydraulic gradient in the upstream side experienced flow reversals, where water was discharged during the spring/early summer (hydraulic gradient $_{average}$ = 0.1 ± 0.1) and recharged during the late summer/fall rewetting (hydraulic gradient $_{average}$ = -0.09 ± 0.1). In the downstream side, water was consistently recharged into the subsurface. The vertical hydraulic gradient at the culvert was measured only in 205, as the culvert was active for the majority of the study period. As water encountered the culvert, it was recharged upstream and discharged downstream (Figure 2-15c).

2.3.11 Water quality

The EC was significantly higher upstream of the road cut-through in 202, 203 and 205 (Wilcoxon signed rank, $p<0.005$ in 202, and $p<0.0001$ in 203 and 205; Figure 2-16). While the EC in 201 was higher downstream of the road, it was not statistically significant. There was no consistent trend in temperature within the four wetlands (as measured in the wells at the culvert). In some cases the downstream temperature was warmer than the upstream temperature (201, 205). In 202 and 203, the upstream temperature was warmer than the downstream temperature.

The difference between the upstream and downstream temperature was only statistically significant in 201 and 205 (Wilcoxon signed rank, $p<0.05$).

2.4 DISCUSSION

2.4.1 Hydrology of the HIWEC wetlands

The use of multiple tracers (EC, stable isotopes) and hydrodynamic data (hydraulic head) can be used to conceptualize the hydrology of wetlands (Clay et al., 2004; Hare, 2015; Bam, 2018). Unlike the wetland-filled depressions found approximately 50 km south in a well-researched site near Parry Sound, Ontario (see Didemus, 2016), a potential groundwater source was identified in the study area due to the presence of fractures within the upper 20 m of the bedrock (AECOM, 2015). The presence of fractures act as secondary permeability for groundwater movement in what would otherwise be impermeable bedrock (Singer and Cheng, 2002). Given that the mineral soil in the instrumented wetlands (Figure 2-10) fell within the range of K_{sat} values for the fractured bedrock, groundwater movement could be permitted between the wetland and underlying aquifer. This is crucial for wetlands that experience high summer evapotranspiration rates, as contributions from groundwater discharge can sustain a water table during prolonged drought conditions (Christensen, 2013). Therefore, identifying a groundwater connection is crucial to understanding the hydrological function of wetlands in the HIWEC.

The mineral soil and pore-water samples that clustered along the LMWL (Figure 2-3) indicated that these samples were derived from meteoric water, or mixed with a source consisting of higher $\delta^{18}O$ and $\delta^{2}H$ values. The fact that the isotopic signature of the mineral soil in the wetlands

remained unchanged through time (Figure 2-5) suggested that the soil was well mixed, has high storage, and/or was being fed from a constant water source. Although the isotopic composition of the mineral soil remained consistent within each wetland, it differed amongst the studied wetlands suggesting connection with different groundwater systems. The EC was also quite variable, where low values were found for 201 and 202 ($EC_{average}$ = 38 uS cm^{-1} and 48 uS cm^{-1}, respectively), and higher values for 203 and 205 ($EC_{average}$ of 241 uS cm^{-1} and 265 uS cm^{-1}, respectively; Figure 2-7). In comparison, the groundwater samples had an average $\delta^{18}O$ of -11.1% and $\delta^{2}H$ of -75.5%, and the EC ranged from 27 uS cm^{-1} to 303 uS cm^{-1}. Unfortunately, the bedrock wells were unavailable for repeated water sampling, and so definitive conclusions regarding the storage and recharge mechanism of the aquifer could not be determined. It is, however, worth noting that the groundwater samples consistently plot along the LMWL, suggesting aquifer recharge due to rapid infiltration of rainfall that was not subjected to fractionation (Figure 2-3). The low EC value of the mineral soil within the wetlands could therefore be an indicator of rainwater and/or short flow paths within the aquifer prior to discharging into the mineral soil (Datta et al., 1996). Conversely, larger EC values could indicate longer rock-water interaction resulting from longer flow paths and/or mixing with water of high solute content.

Assessing EC changes within the soil profile can confirm whether low EC values originated from rainwater as it infiltrated through the organic soil, or groundwater that traveled along a short flow path prior to being discharged into the mineral soil. The EC of the organic and mineral soil was statistically similar in 201-US and 202-DS (Figure 2-7) suggesting that while the isotopic

composition of the mineral soil remained unchanged through time, it was not sourced from groundwater. The hydrodynamic data indicated a consistent recharge of groundwater, further supporting this argument (Figure 2-6a, Figure 2-6b). Conversely, the EC of the mineral soil in 201-DS, 203-US and 205-US was consistently higher than values typically seen for rainwater (>30 uS cm^{-1}), suggesting that a groundwater connection existed within these wetlands (Figure 2-7). While the hydrodynamic data indicated that groundwater discharged into these sites during the drought (Figure 2-6), the lower EC values in 201-DS suggests that water traveled along a shorter flow path than in 203-US and 205-US (Figure 2-7). Nonetheless, a proportion of 201 received groundwater contributions during the drought. Not only does the vertical movement of water vary temporally, it varies spatially within the wetland as well. Siegel et al. (1995) found that connectivity to the regional groundwater system can cause flow reversals that become prolonged over several years. When this occurred, the EC increased from >60 to 200 uS cm^{-1} (400%). In comparison, Fraser et al. (2001) reported an increase in EC by 180 to 240 uS cm^{-1} (10 – 60%) during short flow reversals. Although 205-DS did not show long-term flow reversals (Figure 2-6d), it consistently had higher EC values (Figure 2-7), which could suggest a connection with different groundwater systems. A large hydraulic head difference between the water table and mineral soil (Δh_{max} = was 60.7 cm and 37.3 cm for 205 and 203, respectively) along with high EC values suggest a strong groundwater connection within 203 and 205. While it was determined that groundwater discharged into 201 at some point in time, the hydraulic head gradient was small (Figure 2-6a) and could therefore indicate small groundwater contributions. Lastly, there was a lack of evidence supporting that groundwater discharged into 202.

The wetland that did not have a groundwater signal (202) was the first monitored site to lose its water table (Figure 2-11b). Although a combination of both rainfall and (albeit small) groundwater contributions supplied water to 201 throughout the summer, it eventually lost its water table as well (Figure 2-11a). Water was replenished to the wetlands during the fall rewetting, where the water table response to rainfall was a function of both the size of the rain event and to a lesser degree the initial water table position (Table 2-4). While the two predictor variables does explain the water table response of wetlands to rainfall, uncertainty still remains. This uncertainty within the linear model could be attributed to the influence of groundwater contribution to the water table response of wetlands. For instance, the highest R^2 values were attributed to wetlands that had a weak groundwater signal (202). Conversely, the smallest R^2 value was associated with wetlands that had a strong groundwater signal (203, 205). Nonetheless, in all four wetlands the water table response to rainfall was greater moving deeper into the peat profile (Figure 2-14). Large pores found in surficial moss (Figure 2-9) are associated with higher drainable porosity values (Verry et al., 2011), resulting in minimal water table changes during rain events. Deeper into the substrate, decomposition of peat material occurs concomitantly with compressed pores (Figure 2-9) and increased bulk density (Figure 2-8), and as such require smaller water input to result in a water table response. For instance, the water table response to rainfall was greatest in wetlands where the bulk density increased exponentially with depth (202, 203; Figure 2-14). In contrast, the smaller water table response to rainfall occurred in wetlands where bulk density increased linearly with depth (201, 205; Figure 2-8). Therefore, not only does the water input of wetlands explain their hydrologic behaviour, but variations in hydrophysical properties as well.

2.4.2 Hydrological response of wetlands following road development

One of the most well established hydrological processes impacted by the addition of roads is the obstruction of lateral flow. Water that would otherwise flow downstream can end up ponded due to the presence of a less permeable boundary, resulting in a lowered water table downstream of the road, as this separate unit no longer received this water input. Although this was previously studied in other systems (Thomas and Megahan, 1998; La Marche and Lettenmaier, 2001; Mader, 2014), this hydrological response was no different for wetlands formed in bedrock depressions (Figure 2-11). While hydrological change occurred in all four instrumented wetlands, the degree of disturbance (as measured using ΔWT) varies both spatially and temporally (Figure 2-12), and could result from differences in site properties as well as culvert design (Table 2-1). Although the sample size was insufficient to allow for robust statistical analysis, site differences can be used to infer the importance of these properties.

Culverts are the most common mitigation measure used to maintain flow by allowing the movement of water downstream. The design and installation of culverts was quite variable throughout the study area (Table 2-1). In some cases, the culvert was situated 20 cm above the moss surface (201). In other instances, the culvert was perched on the moss surface (202, 203) or was embedded 50% into the moss itself (205). The culvert may be considered 'active' when the upstream water table exceeded the height of the culvert base. In 201, this meant that the water table would have needed to exceed 20 cm above the moss surface in order to permit flow downslope. Of the 161 days included in the study period, the culvert was only active for 16 of these days, or around 10% of the time. For the remaining duration of the study period, lateral flow was ponded upstream. One might suggest that ponding water can potentially be beneficial

as it maintained moisture within a portion of the wetland throughout this significant period of time. But along with prolonged drought conditions and weak groundwater connection, this obstruction of lateral flow resulted in complete losses of water table downstream during the growing season (Figure 2-11a). A lost of water table exposes the peat soils to aerobic condition, thereby resulting in peat degradation due to increased decomposition rates. As 201 had the largest ΔWT and was susceptible to complete loss of water, the culvert was the least effective (out of the four monitored wetlands) at minimizing the impact of disturbance, and the wetland is at risk for long-term hydrological change.

In wetlands where the culvert was perched on the moss surface (202, 203), the difference between the upstream and downstream water table position was smaller than what was seen for 201 where the culvert was embedded into the road (Figure 2-12). The average ΔWT was 9.7 cm and 4.7 cm for 202 and 203, respectively, compared to an average ΔWT of 20.4 cm for 201. Perching the culvert on the moss surface was therefore an improvement from embedding it into the road. A smaller ΔWT found in 202 and 203 could be attributed to a higher proportion of time that the culvert was activated. Of the 161 days included in the study period, the culvert was active for 28.6% and 27.3% of the time in 202 and 203, respectively. Unlike 201, the water table would only need to exceed the moss surface (WT > 0 cm) in order for lateral flow to be moved downstream. As such, the moss does not experience prolonged flooded conditions in order for connectivity to occur.

While the culvert size was smaller in 202 than in 203 (diameter of 50 cm in comparison to 100 cm, respectively), the ratio of culvert size to road cut-through was similar between the two

wetlands (0.03; Table 2-1). Furthermore, bulk density, porosity, K_{sat} and water table response to rainfall was statistically similar between the two wetlands, suggesting that there were no differences between the culvert design and hydrophysical properties of 202 and 203. Instead, the hydrological response of these wetlands to disturbance could be attributed to differences in water sources. Although 203 had a larger catchment (Table 2-1) and subsequently a larger volume of water that needed to be accounted for, this wetland had a smaller ΔWT. This suggests that lateral flow was not the only contributing water source to 203-DS. As determined from the hydrodynamic and tracer data, 203 was connected to the groundwater system, further highlighting the importance of a groundwater source to wetlands. The ΔWT was also smaller during the fall rewetting than during the drought, suggesting that the water table downstream of the disturbance increased during periods of overland flow. Moreover, while the culvert was active for ~28% of the time in both 202 and 203, 203-DS experienced a greater proportion of time flooded in compared to 202 (Figure 2-13). Therefore, multiple water sources, and the location of road cut-through play an important role in minimizing hydrologic differences upstream and downstream of the road.

The average ΔWT for 205 was 4.0 ± 2.2 cm, suggesting that the mitigation measure implemented in this wetland provided a consistent maintenance of flow between the bisected sides. The culvert at 205 was 50% embedded into the subsurface, allowing the upper half to handle storm flow, and the bottom half to manage slower subsurface flow (Phillips, 1997). Furthermore, the culvert was active for 120 days, minimizing the amount of flooded conditions within the upstream unit. (Figure 2-13) It has previously been suggested that partial burial is the optimal culvert placement (Phillips, 1997), as both perched culverts (202, 203) and completely

submerged culverts does not provide an open conduit for flow (FP Innovations, 2011). The results of this study support this suggestion, especially when developing in wetland-filled bedrock depressions. Lastly, while the EC was typically higher when water was ponded upstream, the difference between the upstream and downstream EC (ΔEC) was smallest in 205 (Figure 2-16). For example, the ΔEC was 68 ± 28 uS cm^{-1} and 65 ± 44 uS cm^{-1} for 202 and 203, respectively. In comparison, the ΔEC was 49 ± 34 uS cm^{-1} for 205, which suggests connection between the bisected wetlands results in the maintenance of water quality.

Although the culvert at 205 was the most effective at maintaining flow between the two bisected sides of the wetland, the difference between the water table position upstream and downstream of the road was statistically significant. Therefore, improvements can be made. In all four wetlands, the ratio of culvert size to road cut-through was small (0.03; Table 2-1), suggesting that the use of a single culvert could be problematic. As water encountered the road, slower subsurface flow becomes re-routed and discharged at the moss surface (Figure 2-15a). Downstream of the road, water was recharged into the subsurface. Although baseline vertical hydraulic gradient data was not recorded, the piezometer nest furthest away from the road (PR) was used to examine vertical water movement in the absence of disturbance. Similar to what was seen downstream of the road, water was consistently recharged into the wetland (Figure 2-15b). Conversely, water was recharged or discharged upstream of the road depending on the time of year. The vertical hydraulic gradient was small, however, indicating negligible vertical water movement and suggests that the trend of water discharging upstream (Figure 2-15a) was a consequence of the road. The effect of ponding was also shown by the EC values (Figure 2-16). The deeper peat layers are typically sourced from groundwater, and so when deeper subsurface

flows are re-routed, mixing occurred between the rain-fed and groundwater-fed layers. Downstream of the road, rainwater (with low EC) within the surficial moss gets recharged deeper into the subsurface. The higher EC values could also have originated from the accumulation of solutes as lateral flow moved through the catchment prior to ponding at the road.

An opposite trend occurred at the culvert where water was recharged upstream and discharged downstream of the road (Figure 2-15c). Although culverts act as an open conduit for water movement downstream (Shantz and Price, 2006), the use of a single culvert can concentrate flow to a particular spot and cause a pinch point (FP Innovations, 2011). Increasing flow velocity and turbulent action from concentrated flow can exceed the structural integrity of the pore structure, causing peat erosion and development of subsurface pipes due to preferential flow paths (Beven and Germann, 1982). Piehl et al. (1998) found that the proportion of soil erosion at the culvert outlet increased with culvert spacing, suggesting that peat erosion can be minimized with multiple closely spaced culverts. Moreover, water discharging downstream of the culvert can transmit water deeper into peat layers, which naturally wouldn't occur due to lower hydraulic conductivity found with depth (Holden et al., 2004; Figure 2-10). It has been suggested by Taylor and Tucker (1970) that the flow of water beneath the peat is a major initiator of erosion processes contributing to changes in the peat structure. As the hydraulic properties of peat are dictated by the structure and arrangement of pores, further changes could lead to long-term changes in wetland hydrology. Therefore, multiple culverts should be added in order to minimize concentrated flow and the formation of preferential flow paths.

The water table response to rainfall was statistically similar both upstream and downstream of the disturbance in all four wetlands. This indicates that the disturbance does not have a direct control on the water table rise during precipitation events. Instead, the disturbance has an indirect control by altering the initial water table position. Following road construction, the water table would be deeper downstream, and as such would be more responsive to rain events (Waddington et al., 2015). This was seen in 201 where a 47.7 mm storm event on September 25 resulted in a 10.7 cm water table rise upstream ($WT_{initial}$ = -18.3 cm) and a 20.6 cm water table rise downstream ($WT_{initial}$ = -43.2 cm). Although the upstream side should theoretically be less responsive to rainfall (as it has a higher initial water table position prior to the event), it was more prone to flooding due to the obstruction of lateral flow resulting in ponding at the road (Figure 2-13). Flooding can therefore represent a rapid rise of water table following rainfall, or when the water table exceeds the moss surface. Frequent flooding events (downstream) and a high water table (upstream) can have significant consequences on the succession of peatlands in disturbed sites. The large variability in water table promotes the establishment of *Sphagnum* lawn species that are capable of withstanding these conditions (Bocking, 2015). Over time, this fast growing moss can in-fill and smother pre-existing hummocks, leading towards the vegetative structure of a poor fen (Bocking, 2015). The succession of peatlands towards a fen was seen within 200 m of a linear disturbance in Alberta (Bocking, 2015), suggesting that the impact can propagate through the wetland complex. Moreover, *Sphagnum* hummocks are commonly used as overwintering habitat by EMRs at the northern extent of their range, suggesting a lack of suitable habitat in this geographic area (Shine and Mason, 2004). While a 4.0 cm water table difference might seem like a negligible change, the development of hummocks is dependent on the water table position (Titus and Wagner, 1984). The succession of

peatlands away from hummock-forming species and towards other microtopography is therefore problematic as it reduces the already limited site availability during this important life history. Thus, any hydrologic change has important implications for the future of these habitats, especially if they are to be maintained for SAR species.

2.5 CONCLUSIONS

The results of this study indicate that, unsurprisingly, culvert design plays a dominant role in allowing considerable flow and connection within bisected wetlands. Culverts need to be large enough, yet partially embedded to account for both surficial and subsurface flow. Furthermore, an adequate number of closely spaced culverts are needed to minimize the formation of preferential flow paths due to concentrated flow. While mitigation measures can be implemented to minimize hydrological change, the severity of disturbance varied depending on the site properties of the wetlands. For example, although 202 and 203 had a similar culvert design, the average ΔWT was larger in 202. It was suggested that the water table difference was minimized in 203 due to connection with groundwater system, and water contributions during periods of overland flow. Furthermore, while 203 and 205 had a similar storage capacity and hydroperiod, 205 was less responsive to rain events which was attributed to its hydrophysical properties. It is therefore important to understand the wetland systems that are being developed in. Instead of treating all wetlands as equal during the planning of a road network, assessing the hydrological function of the system can be completed prior to construction in order to minimize disturbance to sensitive habitat. Therefore, both culvert design and site properties are important to minimize the hydrological impact of road cut-through in wetland-filled bedrock depressions.

2.6 TABLES

Table 2-1: Description of the site characteristics and culvert design within the four instrumented wetlands.

Site	Peat depth (cm)	Catchment area (ha)	Length of cut-through (m)	Culvert size (cm)	Culvert placement
201	50	5.2	16	50	20 cm above moss surface
202	40	6.4	17	50	Perched on moss surface
203	75	7.6	31	100	Perched on moss surface
205	80	9.8	63	100	Buried 50%

Table 2-2**:** Descriptive statistics for pore-water and mineral soil $\delta^{18}O$ isotopic composition between the dry and wet season.

Site	Depth	Season	No of samples	Mean	Standard deviation	P value
201	25	Dry	6	-11.3	0.8	**<0.01**
		Wet	10	-9.1	1.3	
	50	Dry	8	-11.8	0.7	**<0.001**
		Wet	10	-9.8	0.7	
	75	Dry	5	-10.8	0.2	0.3
		Wet	8	-10.7	0.2	
	Base	Dry	7	-10.9	0.4	0.1
		Wet	7	-10.6	0.3	
202	25	Dry	4	-11.7	0.3	**<0.01**
		Wet	8	-9.4	1.0	
	50	Dry	2	-12.2	0.2	0.1*
		Wet	3	-9.5	0.2	
	Base	Dry	6	-11.7	0.5	**<0.05***
		Wet	5	-10.2	1.0	
203	25	Dry	7	-11.8	1.0	**<0.0005**
		Wet	12	-9.3	0.6	
	50	Dry	12	-11.3	0.8	**<0.0001**
		Wet	13	-10.0	0.6	
	75	Dry	12	-10.9	0.2	0.1
		Wet	12	-10.6	0.5	
	100	Dry	10	-11.1	0.1	0.08
		Wet	8	-11.0	0.2	
	Base	Dry	11	-11.2	0.6	0.1
		Wet	12	-10.7	0.6	
205	25	Dry	8	-10.8	0.4	**<0.01**
		Wet	6	-10.3	0.2	
	50	Dry	18	-11.6	0.4	**<0.0001**
		Wet	8	-9.8	0.2	
	75	Dry	13	-11.5	0.3	**<0.0005**
		Wet	8	-10.5	0.5	
	100	Dry	12	-11.1	0.2	0.3
		Wet	6	-11.1	0.1	
	Base	Dry	15	-11.3	0.1	0.3
		Wet	8	-11.3	0.2	

*Sample size is too small and may lead to false p-value
Bolded p-values are significant to $p<0.05$

Table 2-3: Descriptive statistics for pore-water and mineral soil δ^2H isotopic composition between the dry and wet season

Site	Depth	Season	No of samples	Mean	Standard deviation	P value
201	25	Dry	6	-77.5	4.5	**<0.01**
		Wet	10	-58.9	9.4	
	50	Dry	8	-78.3	5.2	**<0.005**
		Wet	10	-64.4	5.7	
	75	Dry	5	-71.9	2.7	0.3
		Wet	8	-70.8	1.6	
	Base	Dry	7	-71.8	3.2	0.7
		Wet	7	-70.2	1.7	
202	25	Dry	4	-80.2	1.6	**<0.01**
		Wet	8	-61.1	7.3	
	50	Dry	2	-82.2	1.9	0.1*
		Wet	3	-62.0	1.2	
	Base	Dry	7	-77.1	4.6	0.1*
		Wet	5	-67.6	6.9	
203	25	Dry	7	-80.7	6.8	**<0.0005**
		Wet	12	-60.6	4.5	
	50	Dry	12	-76.8	5.0	**<0.0001**
		Wet	13	-65.7	4.9	
	75	Dry	12	-72.9	1.3	0.3
		Wet	12	-71.7	2.1	
	100	Dry	10	-73.8	0.6	0.5
		Wet	8	-73.6	0.6	
	Base	Dry	11	-75.6	4.6	0.1
		Wet	12	-71.6	4.2	
205	25	Dry	8	-75.7	2.2	**<0.005**
		Wet	6	-67.3	1.8	
	50	Dry	18	-78.9	2.3	**<0.001**
		Wet	8	-64.3	1.4	
	75	Dry	13	-77.0	2.8	**<0.0005**
		Wet	8	-69.5	3.6	
	100	Dry	12	-74.5	0.6	0.1
		Wet	6	-73.9	0.6	
	Base	Dry	15	-75.7	0.7	0.1
		Wet	8	-75.0	1.0	

*Sample size is too small and may lead to false p-value
Bolded p-values are significant to $p<0.05$

Table 2-4: Generalized linear model of the water table response of wetlands to rainfall using the initial water table position and size of the rain event as predictor variables.

Predictor variables	201		202		203		205	
	F	*p*	*F*	*p*	*F*	*p*	*F*	*p*
Size of rain event	6.5	**<0.0001**	8.73	**<0.0001**	4.17	**<0.0005**	3.66	**<0.001**
Initial water table	2.36	**<0.05**	3.08	**<0.005**	6.31	**<0.0001**	3.98	**<0.0005**
Intercept	0.50	0.62	-0.81	0.42	-1.82	0.08	-0.58	0.56
R^2		0.69		0.84		0.65		0.57

Bolded p-values are significant to p<0.05

2.7 FIGURES

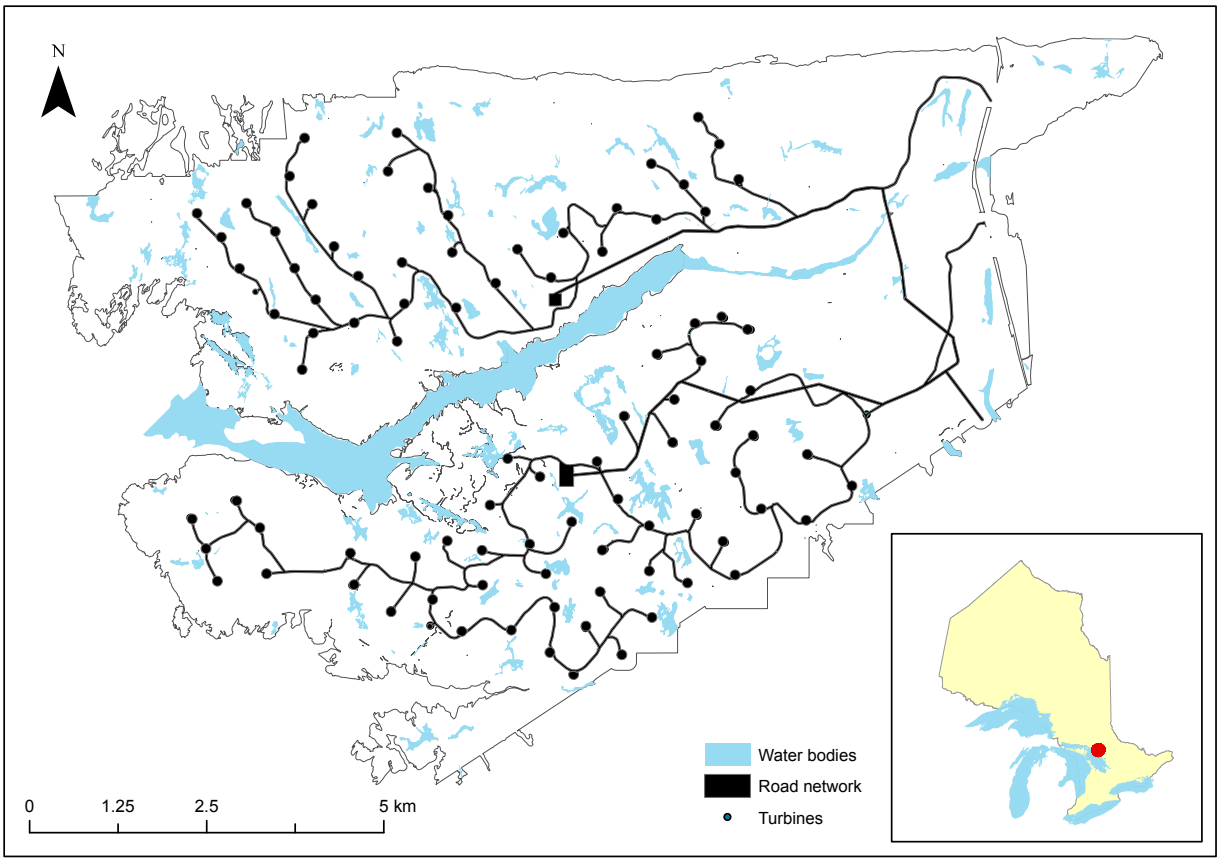

Figure 2-1: Map showing the boundary and road network of the study area as located on the Henvey Inlet First Nation Reserve 2, Ontario, Canada.

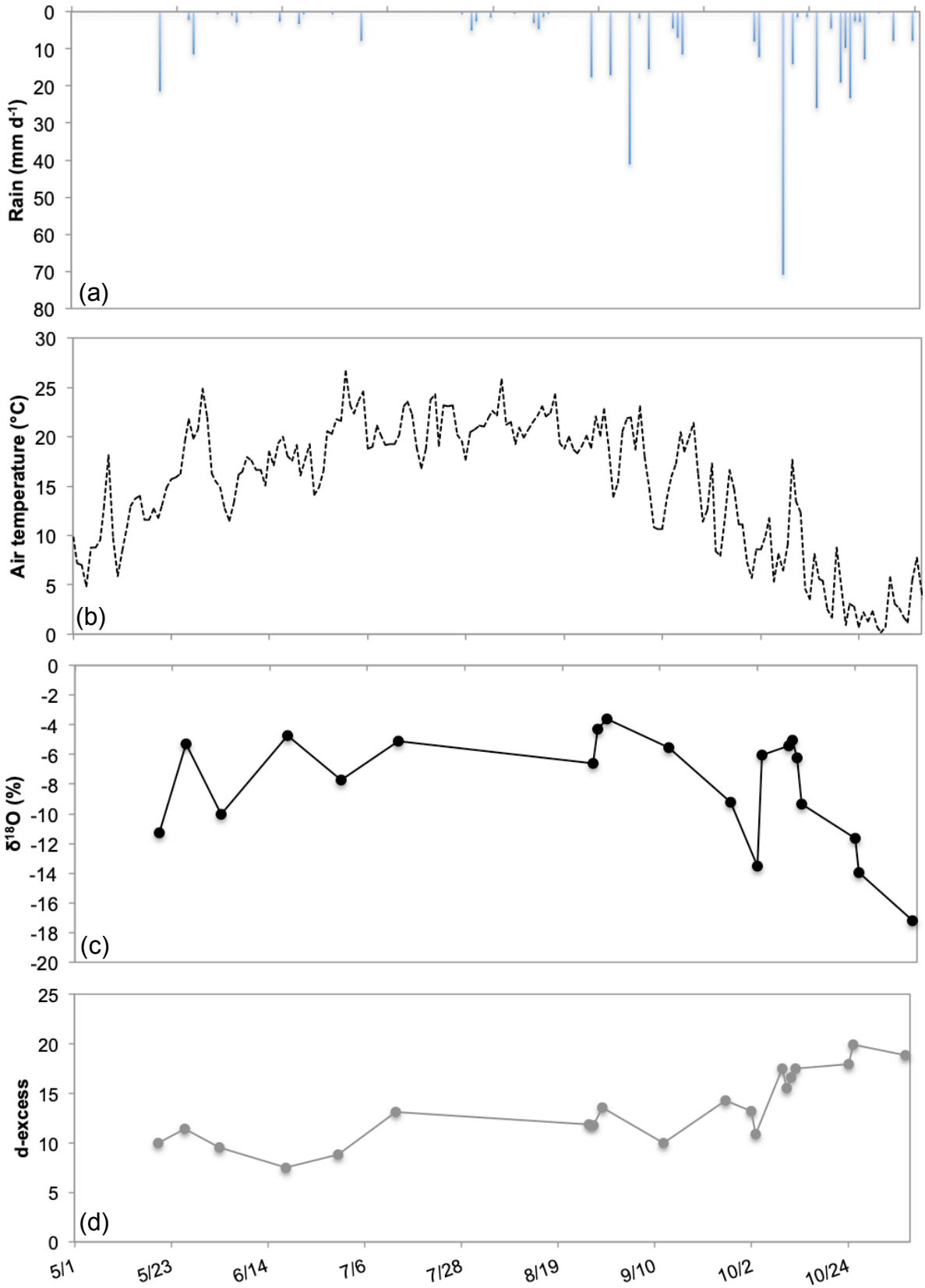

Figure 2-2: Meteorological conditions (rainfall, a; air temperature, b) and isotopic analysis ($\delta^{18}O$ isotopic composition, c; line-conditioned d-excess, d) of rain samples collected over the study period.

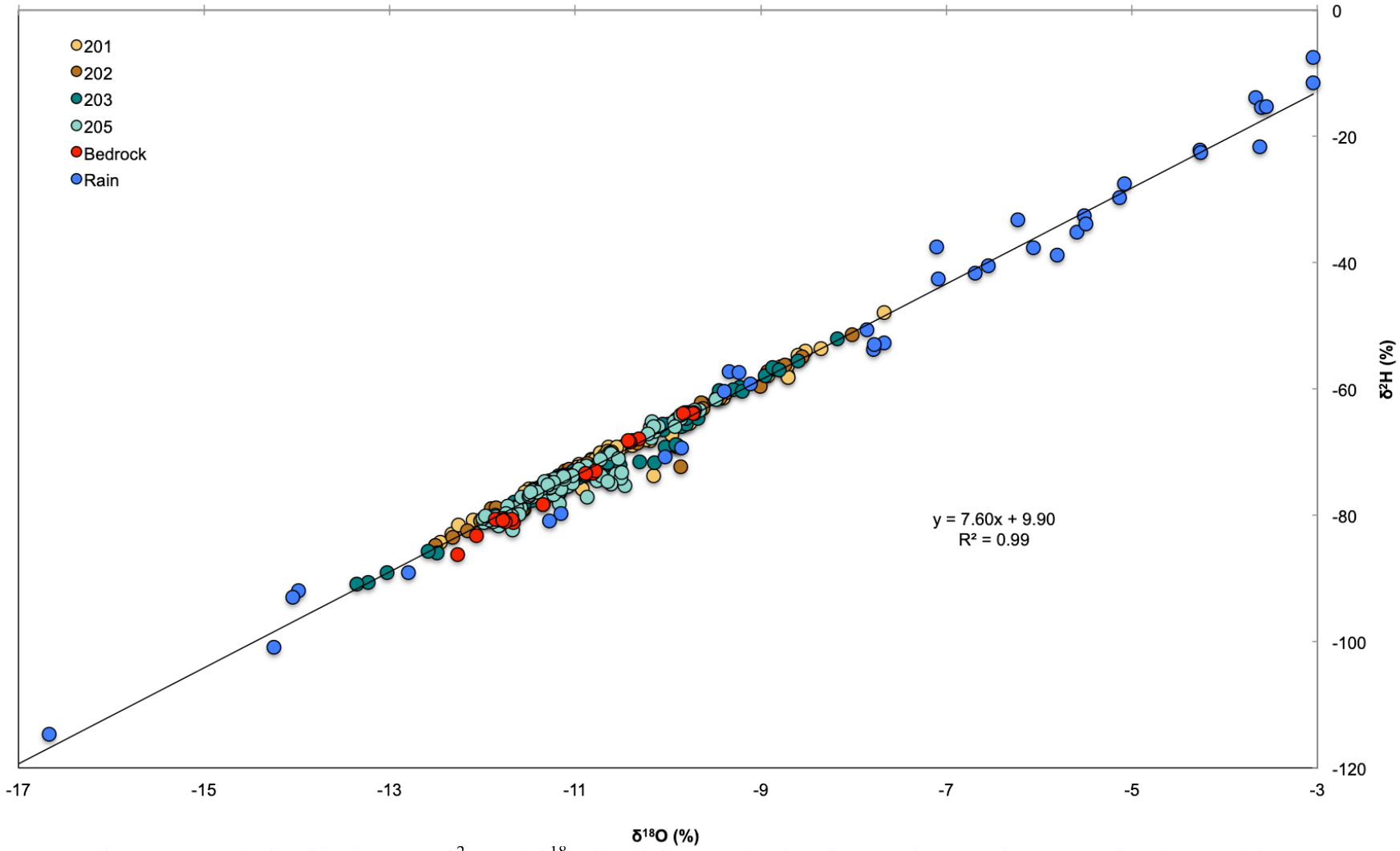

Figure 2-3: Relationship between δ^2H and $\delta^{18}O$ in all four wetlands. The Local Meteoric Water Line (LMWL) is represented by the linear regression line between δ^2H and $\delta^{18}O$, and was created using rain samples collected between May and November 2018. Both pore-water and mineral soil samples collected from the wetlands are displayed. The red circles represent groundwater samples collected from bedrock wells.

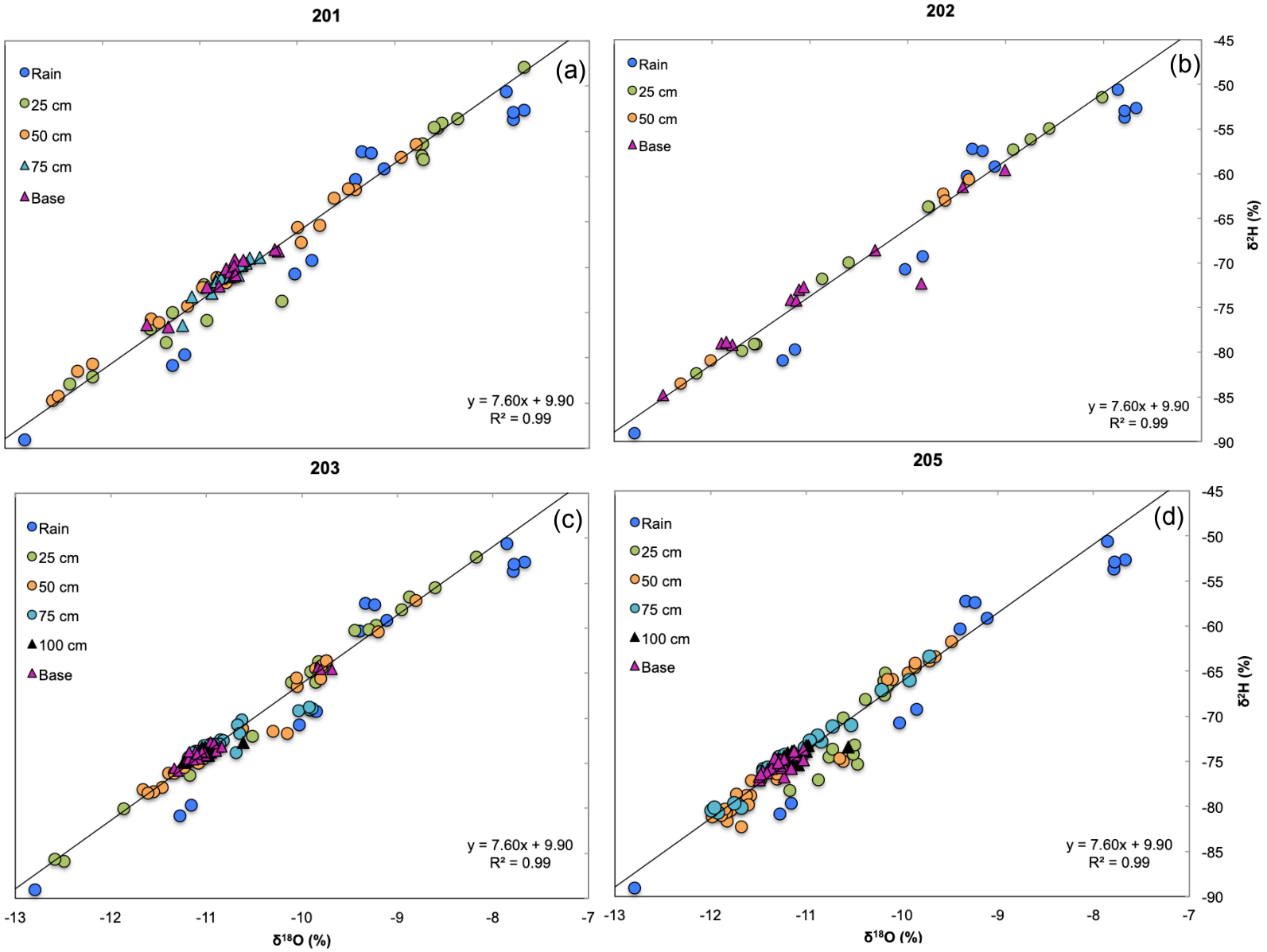

Figure 2-4 (a-d): Isotopic composition of pore-water (circles) and mineral soil (triangles) samples separated by depth for all four wetlands displayed relative to the LMWL

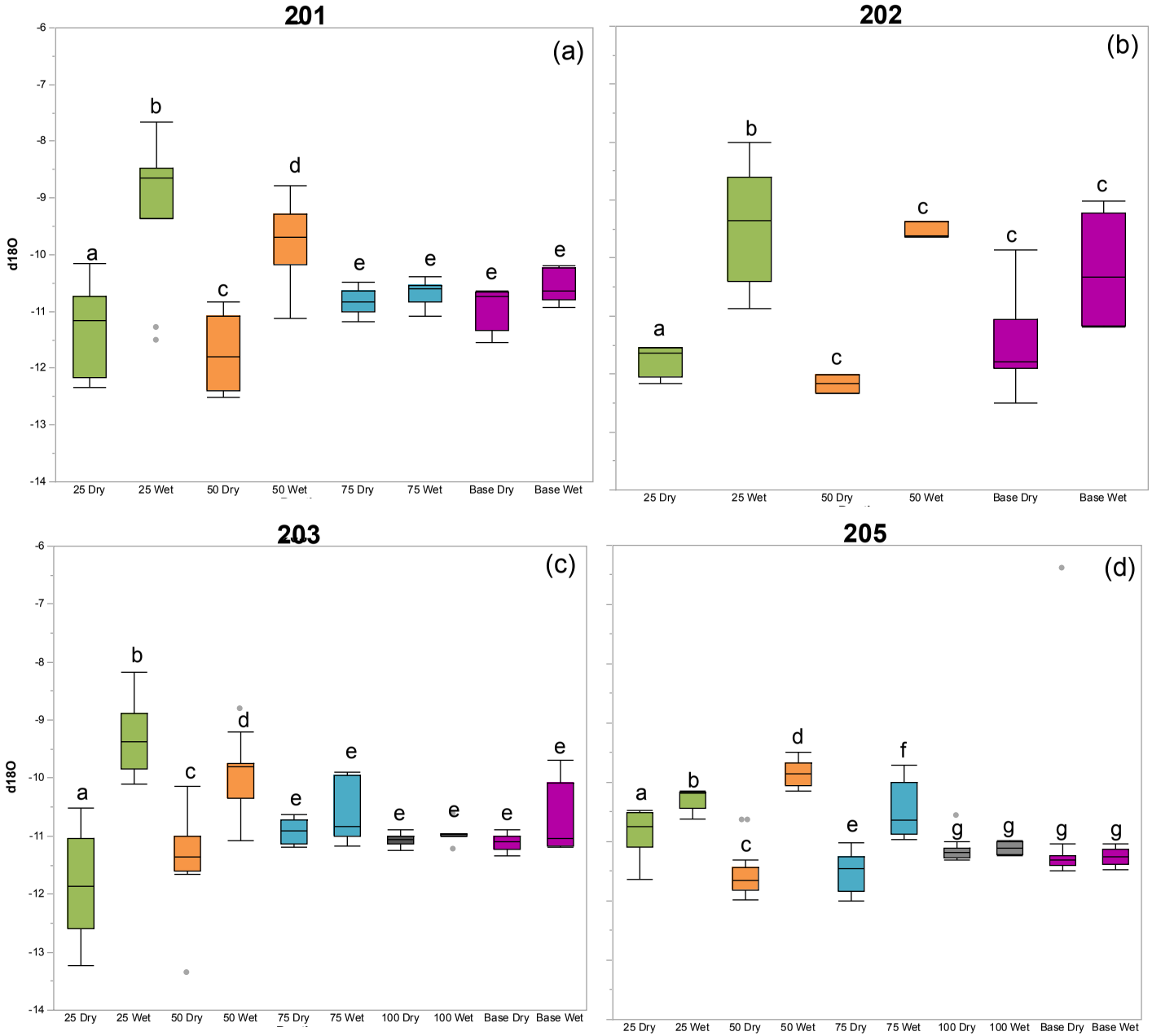

Figure 2-5 (a-d): $\delta^{18}O$ isotopic composition of pore-water and mineral soil samples for all four wetlands separated based on depth and season.

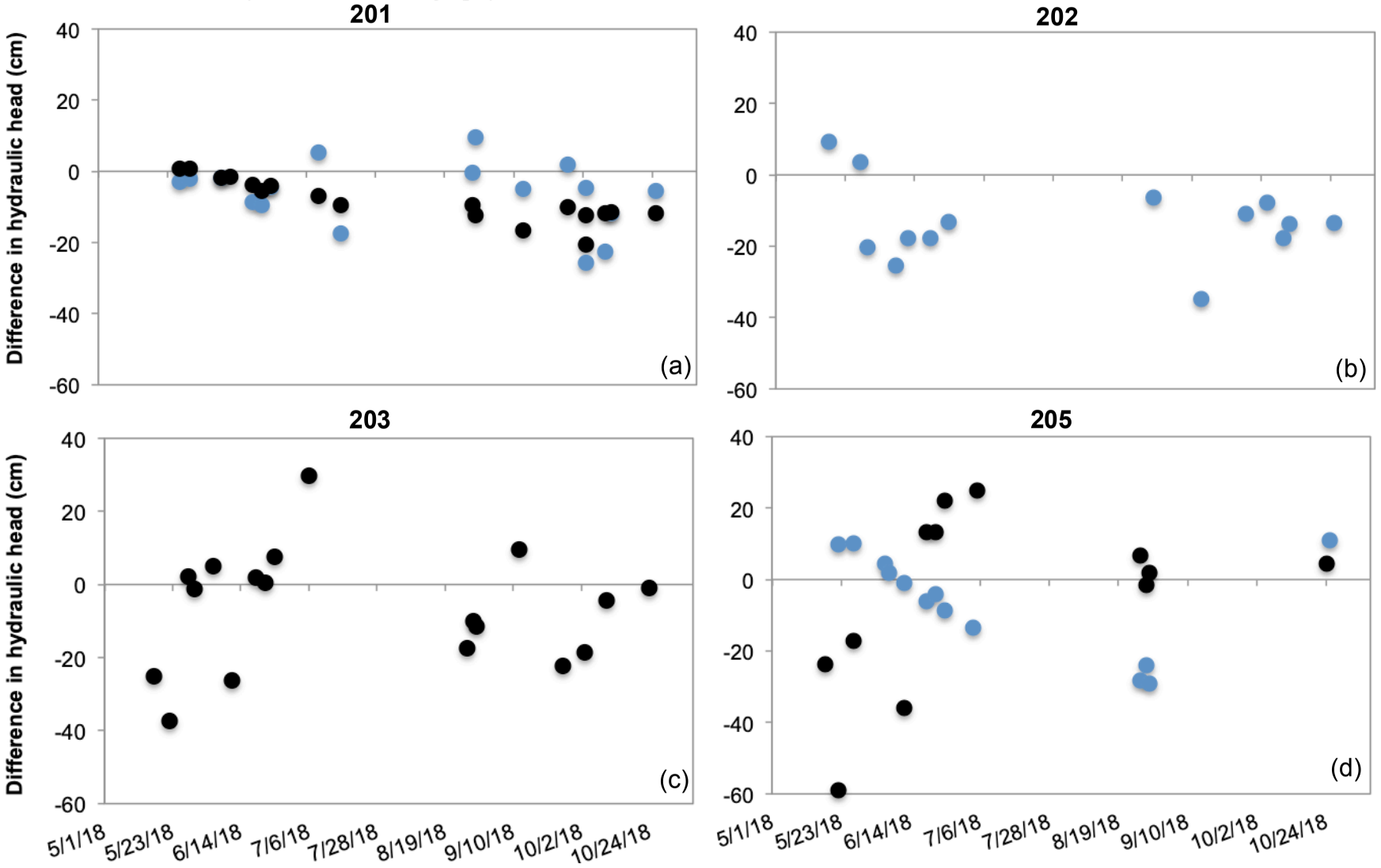

Figure 2-6 (a-d): Groundwater recharge-discharge relationship as assessed using the difference between the water table measured in the well and the hydraulic head measured in the base piezometer installed at the same depth. The nests were installed upstream (black circles) and downstream (blue circle) of the road cut-through. A higher hydraulic head measured in the well indicates groundwater recharge (negative value) and higher hydraulic head measured in the mineral soil indicates groundwater discharge (positive value) into the wetland.

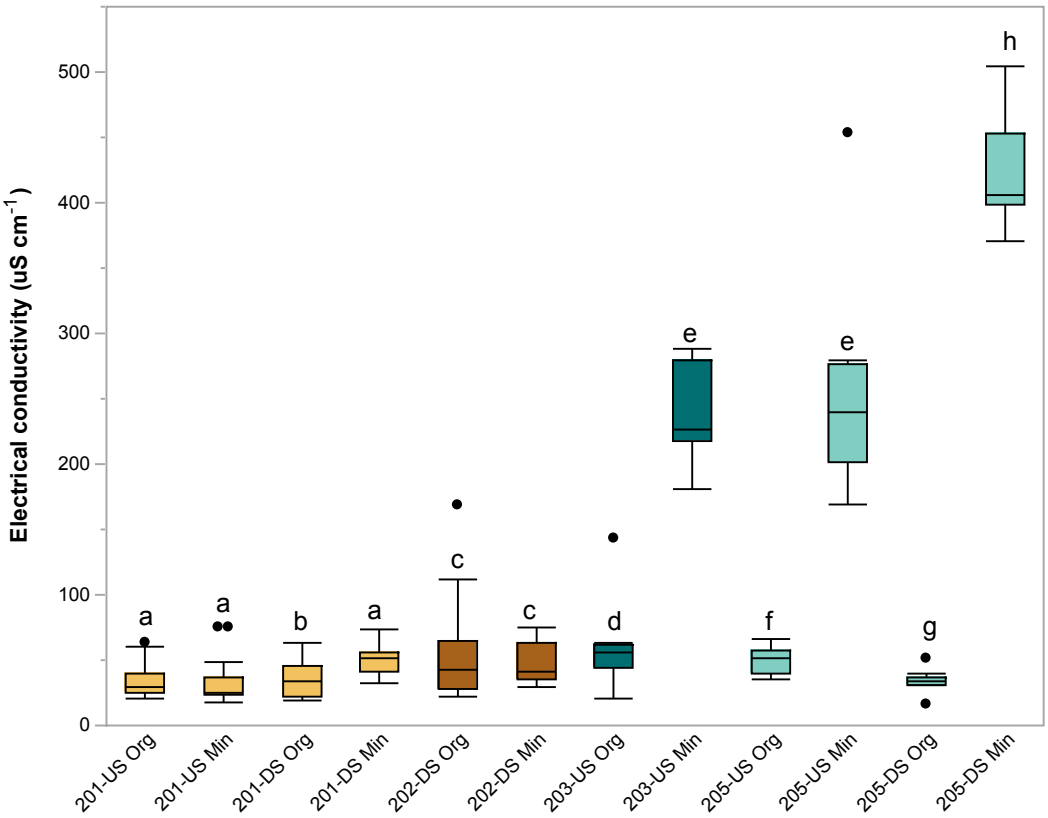

Figure 2-7: Electrical conductivity (uS cm^{-1}) of the organic (org) and mineral (min) soil measured in the piezometer nest located at PR. Letters denote statistical difference between the groups (Wilcoxon/Kruskal-Wallis test, $p<0.001$).

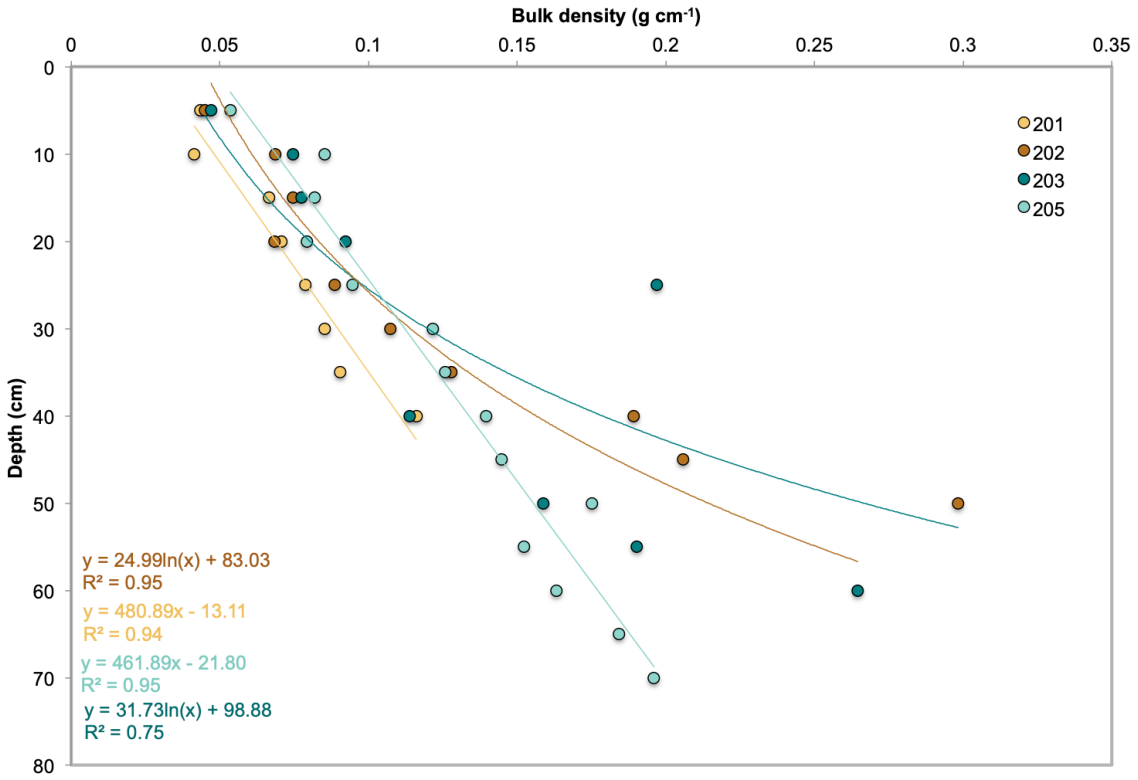

Figure 2-8: Depth profile of bulk density (g cm^{-3}) measured in 5 cm increments. The bulk density in 202 and 203 decreased exponentially with depth (R^2 of 0.95 and 0.75 for 202 and 203, respectively), whereas bulk density decreased linearly with depth in 201 and 205 (R^2 of 0.93 and 0.94 for 201 and 205, respectively).

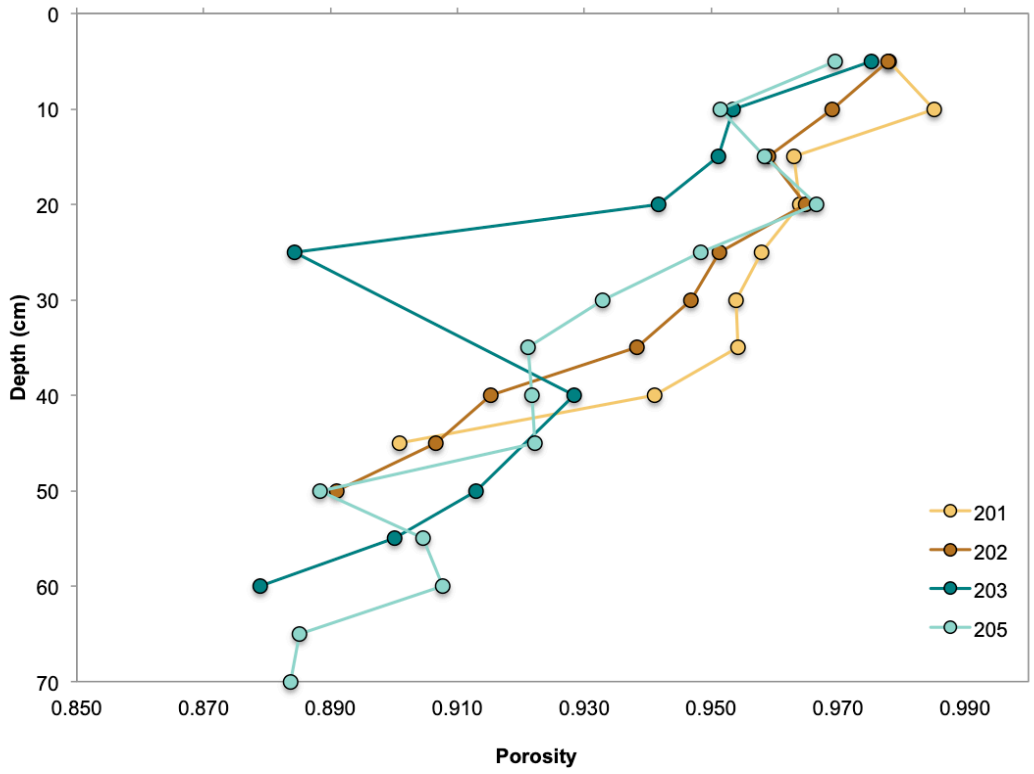

Figure 2-9: Depth profile of porosity measured in 5 cm increments.

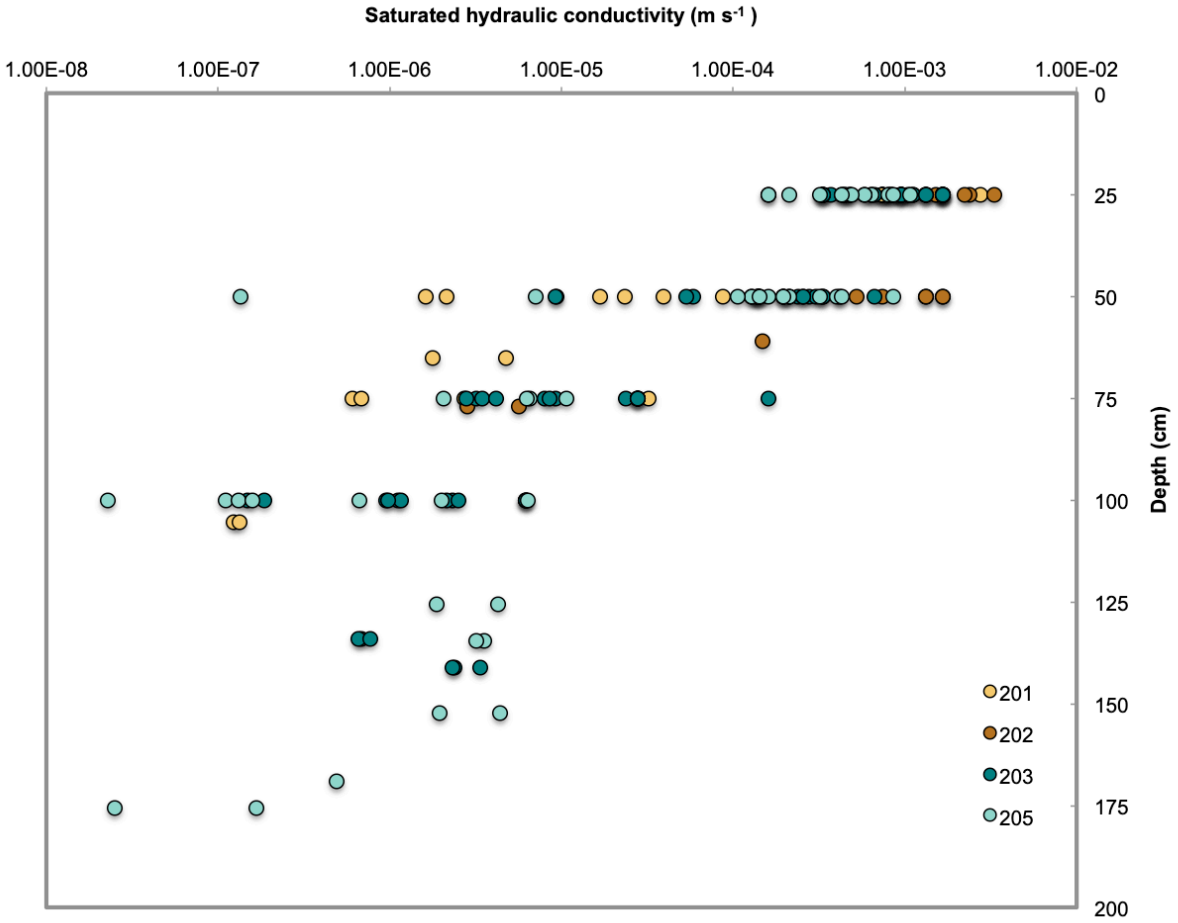

Figure 2-10: Saturated hydraulic conductivity (K_{sat}, m s^{-1}) of the organic and mineral soil measured using bail tests in-situ (Hvorslev, 1952). Triplicates were taken within each piezometer when possible.

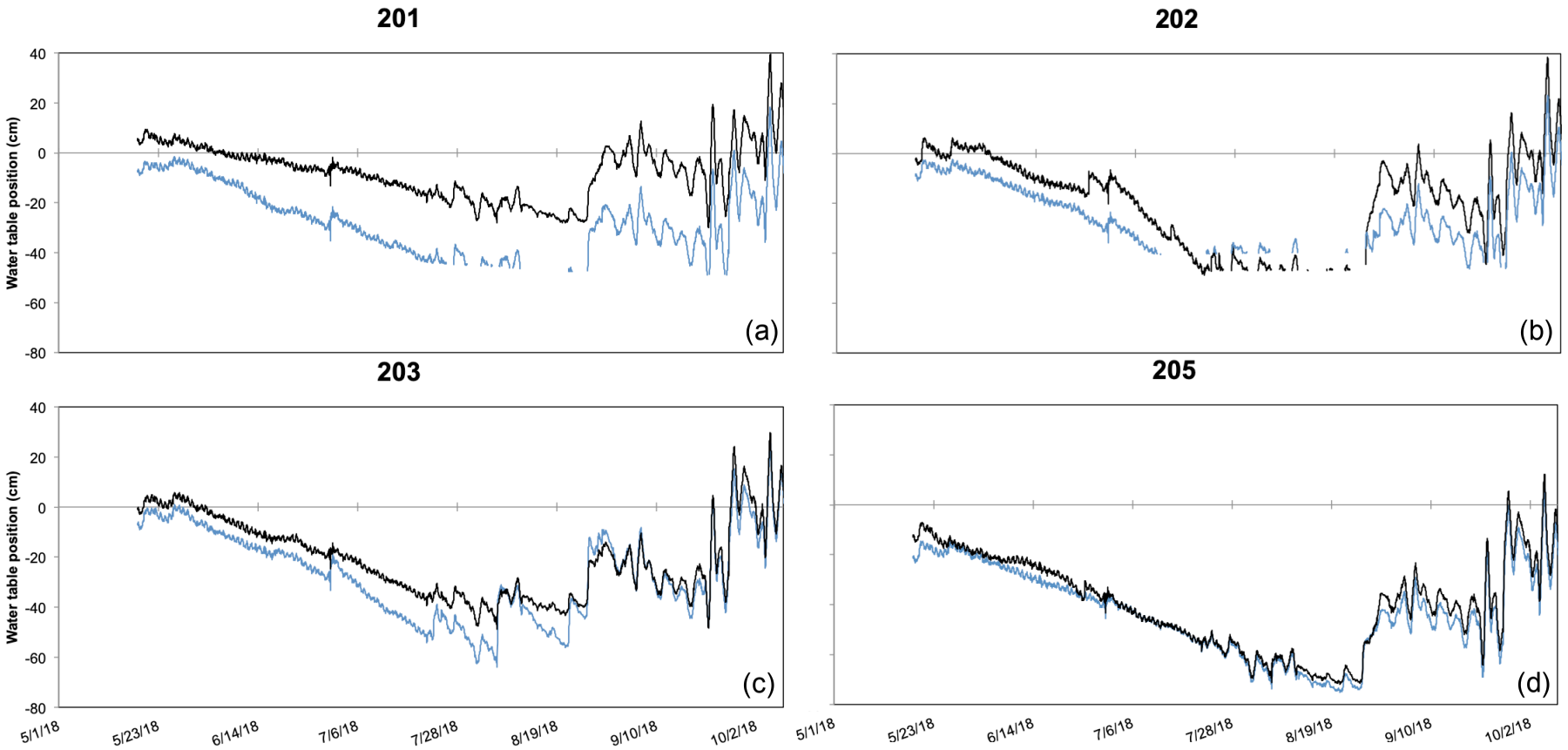

Figure 2-11 (a-d): The water table position (where 0 = moss surface) upstream (black) and downstream (blue) of the road cut-through in all four wetlands. The water table position within each wetland was expressed to a common datum (culvert) and subsequently moved back to a single moss surface to identify flooding events (WT > 0 cm). The upstream and downstream water table position was statistically significant in all four wetlands (Wilcoxon signed rank, $p<0.0001$)

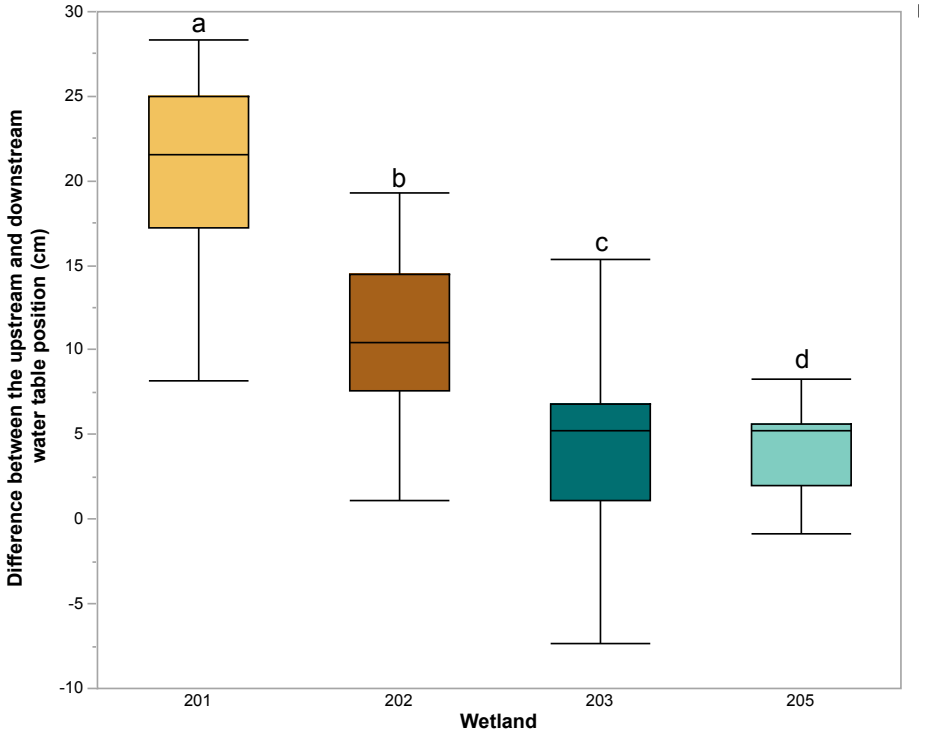

Figure 2-12: The difference between the upstream and downstream water table position (ΔWT) using the mean daily water table. The ΔWT was used as an indicator to assess the severity of the disturbance. The ΔWT within and between all four wetlands were statistically different (Wilcoxon/Kruskal-Wallis, $p<0.0001$).

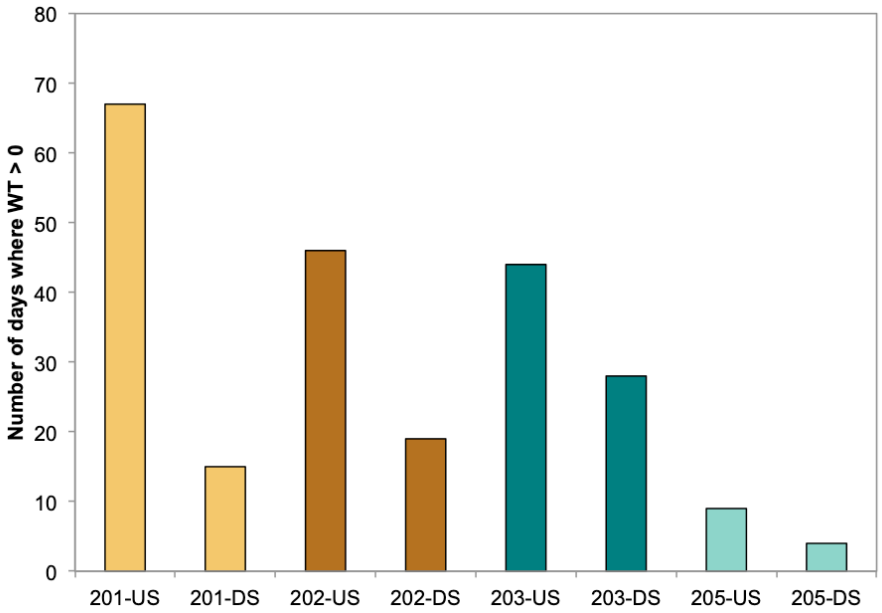

Figure 2-13: Number of days where the water table position was above the moss surface as measured using the daily maximum water table position.

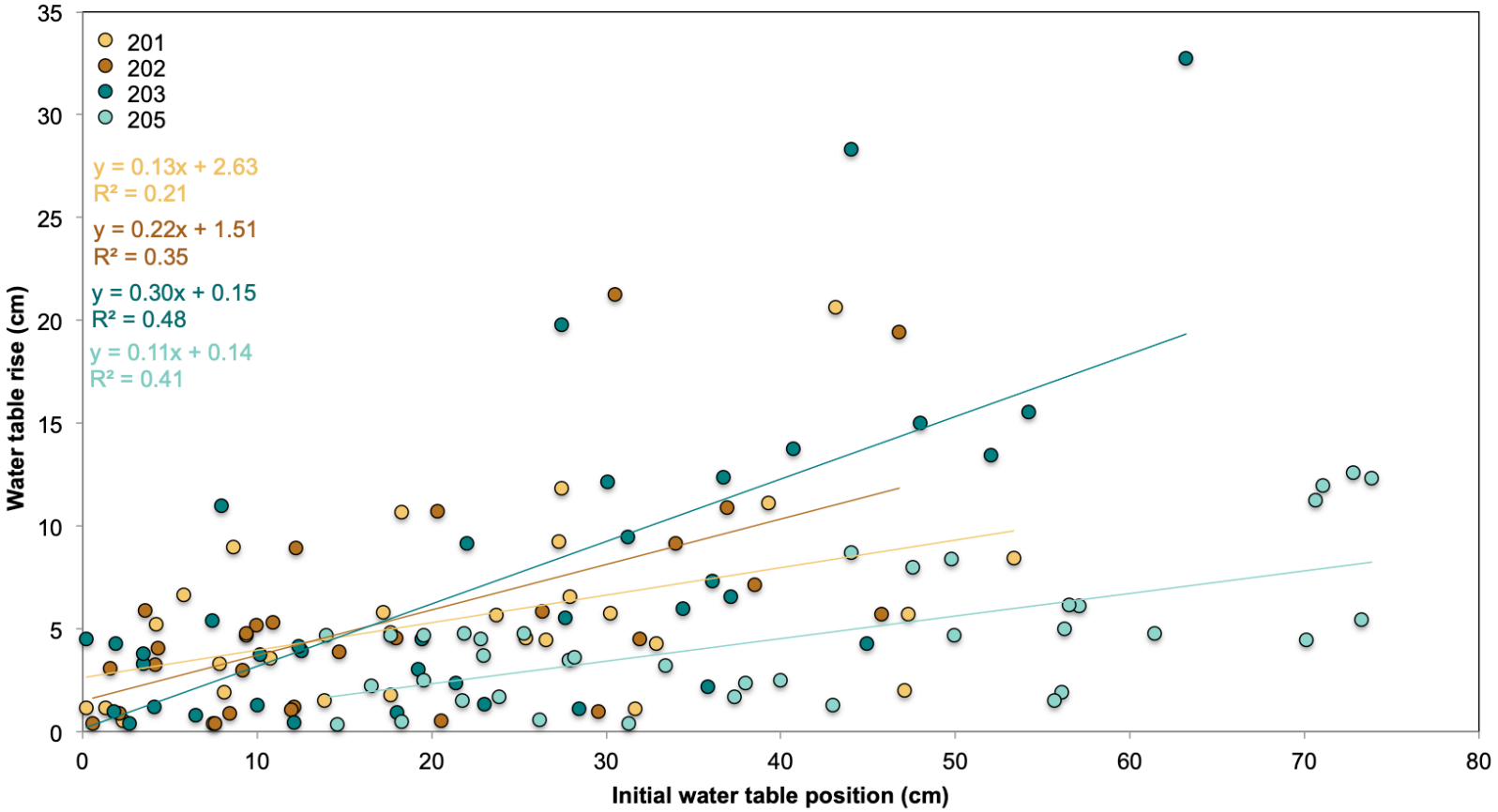

Figure 2-14: Relationship between the initial water table position (cm) and water table rise in all four wetlands. The water table rise within all four wetlands was a function of both the size of the rain event and to a lesser degree the initial water table position. The predictor equation as established from the generalized linear model is as follows: 201 = 0.09 $WT_{initial}$ + 0.22 rain size + 0.4593, 202 = 0.10 $WT_{initial}$ + 0.35 rain size – 0.63, 203 = 0.28 $WT_{initial}$ + 0.23 rain size – 2.59, 205 = 0.08 $WT_{initial}$ + 0.19 rain size – 0.91.

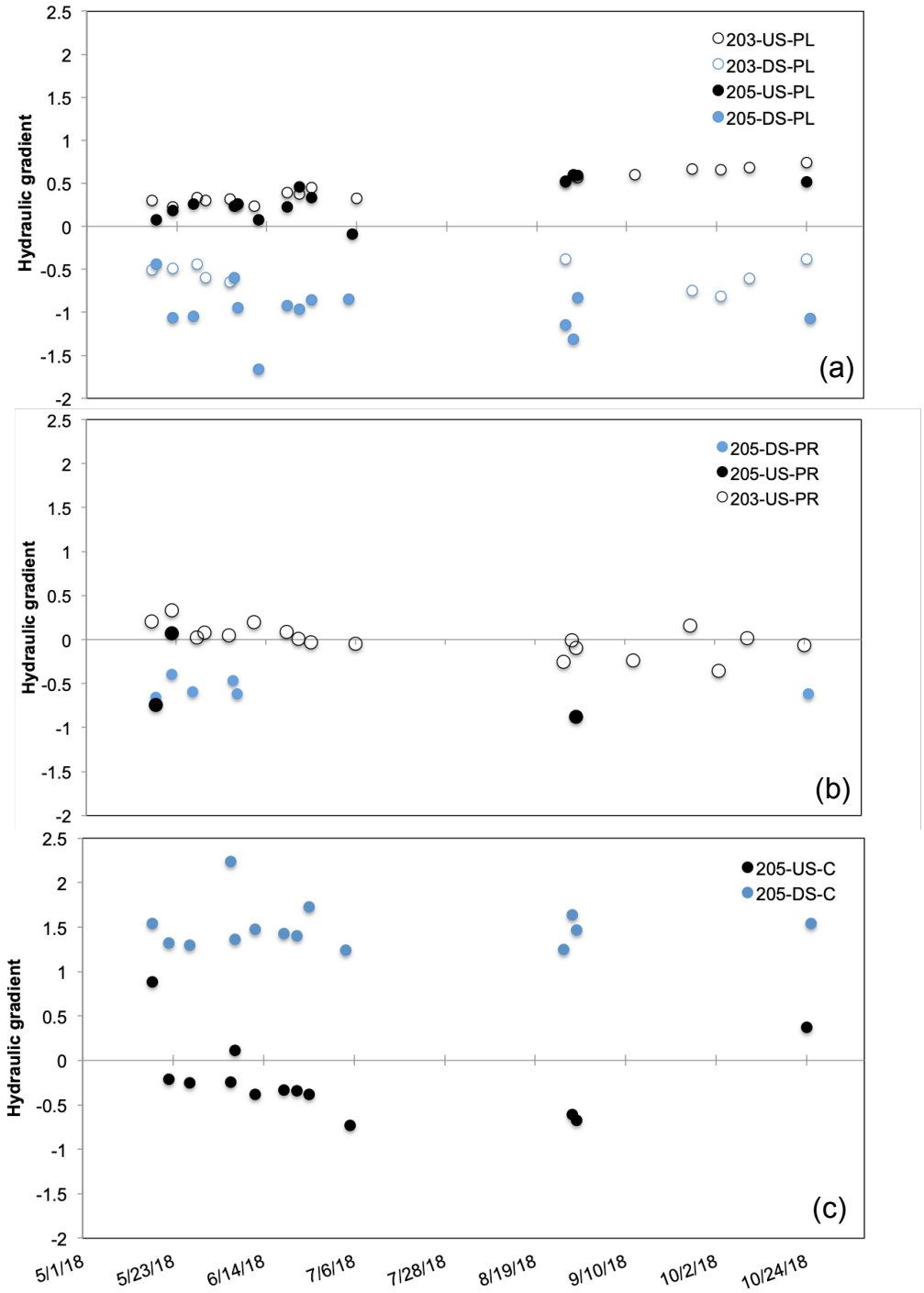

Figure 2-15 (a-c): Hydraulic gradient measured in the piezometer nest upstream (black) and downstream (blue) of the road as water encountered a boundary (a) or culvert (c). The hydraulic gradient in the nest furthest away from the road (b) was included to show vertical hydraulic gradient in undisturbed substrates. Positive values indicate discharge, and negative values indicate recharge.

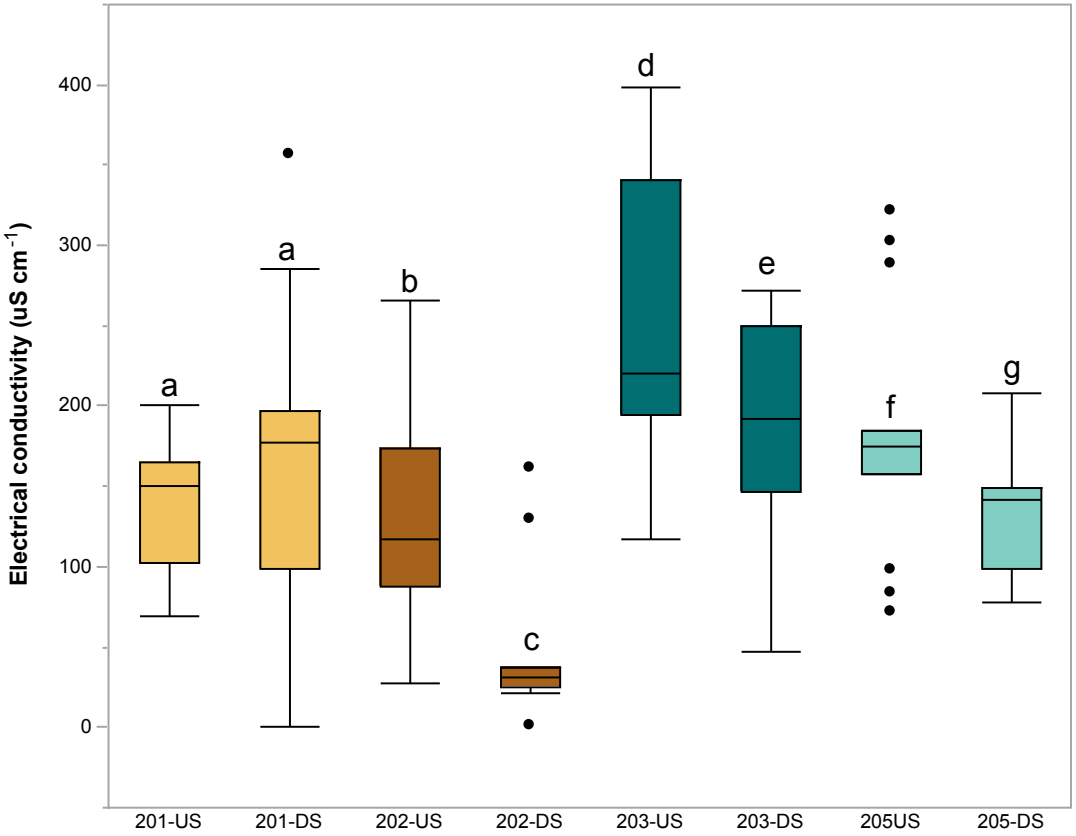

Figure 2-16: Electrical conductivity (uS cm^{-1}) measured in the wells closest to the culvert upstream and downstream of the road. Letters denote statistical difference (Wilcoxon signed rank, $p<0.0005$) between the groups.

2.8 APPENDICES

Appendix A: Instrumentation details for 201

Orientation	US/DS	Nest	Depth (cm)	Material
NE	US	C	25	Organic
			50	Organic
			75	Mineral soil
			105	Mineral soil
		PR	25	Organic
			50	Organic
			66	Mineral soil
SW	DS	C	25	Organic
			50	Organic
			75	Mineral soil
		PR	25	Organic
			50	Organic
			75	Mineral soil
			113	Mineral soil

Appendix B: Instrumentation details for 202

Orientation	US/DS	Nest	Depth (cm)	Material
W	US	C	25	Organic
			50	Organic
		PR	25	Organic
			61	Mineral soil
E	DS	C	25	Organic
		PR	25	Organic
			50	Organic
			77	Mineral soil

Appendix C: Instrumentation details for 203

Orientation	US/DS	Nest	Depth (cm)	Material
E	US	C	25	Organic
			50	Organic
			75	Organic/Mineral soil
			100	Mineral soil
			134	Mineral soil
		PL1	25	Organic
			50	Organic
			75	Organic/Mineral soil
			100	Mineral soil
			141	Mineral soil
		PR	25	Organic
			50	Organic
			75	Organic/Mineral soil
			100	Mineral soil
			183	Mineral soil
		PL2	25	Organic
			50	Organic
			75	Mineral soil
			100	Mineral soil
			135	Mineral soil
W	DS	C	25	Organic
			50	Organic
			75	Organic/Mineral soil
			84	Mineral soil
		PL1	25	Organic
			50	Mineral soil

Appendix D: Instrumentation details for 205

Orientation	US/DS	Nest	Depth (cm)	Material
SE	US	PL1	25	Organic
			50	Organic
			75	Organic/Mineral soil
			100	Mineral soil
			135	Mineral soil
		C	25	Organic
			50	Organic
			75	Organic/Mineral soil
			100	Mineral soil
			175	Mineral soil
		PL2	25	Organic
			50	Organic
			75	Organic/Mineral soil
			100	Mineral soil
			125	Mineral soil
		PR	25	Mineral soil
			50	Mineral soil
			166	Mineral soil
NW	DS	PL1	25	Organic
			50	Organic
			75	Organic/Mineral soil
			100	Mineral soil
			157	Mineral soil
		C	25	Organic
			50	Organic
			75	Organic/Mineral soil
			100	Mineral soil
			152	Mineral soil
		PL2	25	Organic
			50	Organic
			75	Organic/Mineral soil
			100	Mineral soil
			124	Mineral soil
		PR	25	Organic
			50	Organic
			169	Mineral soil

CHAPTER 3: A GIS APPROACH TO ASSESS WETLAND FLOODING POTENTIAL TO GUIDE ACCESS ROAD CROSSINGS IN WETLAND-DOMINATED ROCK BARREN LANDSCAPES

3.1 INTRODUCTION

Near-northern Ontario consists of a unique landscape where vast expanses of wetlands are formed in bedrock depressions and topographic valleys on the Precambrian shield. Unlike wetlands found in other regions, the development and formation of these wetlands are constrained by the underlying bedrock geology, where water contributions to the depression originates from precipitation, groundwater inflow, surface water inflow, snowmelt, and overland flow when the storage capacity of upland hydrologic response units (HRU) are exceeded (Spence and Woo, 2003). This landscape also serves as a biological hotspot for numerous species-at-risk (SAR) reptiles, including the eastern Massasauga rattlesnake (EMR), which utilizes *Sphagnum* hummocks found in wetlands as overwintering habitat (Johnson et al., 2000; Shine and Mason, 2004). Historically, environmental protection has been placed on wetlands due to the ecosystem services that are provided (Lemly, 1996). In the case where access roads do need to cross wetlands, the number of crossings is commonly kept to a minimum (FP Innovations, 2011). Given that large wetland expanses are found across Ontario, and development is expected to accelerate due to developmental pressures from mineral extraction and energy infrastructure projects, complete wetland avoidance is unrealistic. The decision of when and where to cross a

wetland therefore becomes a large planning constraint (FP Innovations, 2011), especially when multiple crossings are required.

Access roads are an important infrastructure component associated with resource extraction projects (such as wind farms) as it allows the movement of material into the site and the operation of the facility. Although necessary, access roads are linear disturbances that can result in cumulative hydrological impact across the landscape (Trombulak and Frissell, 2000). Furthermore, a large cost can accumulate during the construction of access roads (Pearce, 1974), and as such proper planning of road networks are required to minimize both the economic and environmental cost associated with projects. While numerous studies have been conducted to identify the most suitable location for wind farms (van Haaren and Fthenakis, 2011; Tegou et al., 2010), less research has been published to micro-site the location of turbine pads (Xu et al., 2016), and even fewer studies on planning access roads. As hydrology is the dominant factor regulating the form, function, and development of wetlands (Mitsch and Gosselink, 1993), it is essential to identify hydrological processes that will be impacted as a consequence of road cut-through, and mitigation measures to minimize potential impact to the wetland form and function.

The hydrological impact of road crossings in wetlands formed in bedrock depressions manifests itself through a higher water table position upstream and a lower water table downstream of the disturbance (Chapter 1; Vu, 2019). Although mitigation measures (i.e. culverts) can be added to maintain drainage patterns within the bisected wetlands, the difference between the water table position upstream and downstream of the road (ΔWT) was statistically significant even in wetlands with the most optimal culvert design (partial burial; Phillips, 1997). A higher ΔWT was

also observed during the fall rewetting, suggesting that the culvert was incapable of allowing sufficient lateral flow downslope during large storm events and periods of overland flow (Vu, 2019; Chapter 1). Provided that the culvert design was standardized throughout the road network, wetlands that receive a greater contribution of overland flow would experience extended periods of flooding. Wetlands with a high flooding potential can therefore be assessed prior to planning a road network such that hydrological impact is minimized. The objective of this research is to therefore develop a GIS tool to assess the flooding potential of wetlands as a result of runoff generation on Precambrian shield landscapes.

3.2 METHODOLOGY

3.2.1 Study area

The Henvey Inlet Wind Energy Centre (HIWEC) is the largest wind farm development in Ontario, Canada. This 300-megawatt wind energy generation facility is being developed on the Henvey Inlet First Nation (HIFN) reserve, located along the eastern shore of Georgian Bay approximately 80 km south of Sudbury, Ontario (Figure 3-1). The surficial bedrock geology at HIWEC is composed of a complex suite of highly foliated migmatitic gneisses of granitic to granodioritic composition (Kor, 1994). The upper 10 to 20 m of the exposed bedrock is fractured, with hydraulic conductivities ranging from 4×10^{-7} to 8×10^{-4} m s^{-1} (AECOM, 2015). Mineral soil can be found in thin discontinuous deposits located along the exposed bedrock as well as thicker deposits under organic material in low-lying areas and bedrock depressions. The mineral soil originates from the final Late Wisconsinan glacial advance and retreat (Kor, 1989), and consists of glaciolacustrine deposits, ice-contact stratified deposits, and tills (OGS, 2003). Longitudinal ridges run throughout the study area in a northwest to southeast direction, where

elevation values range from 171 to 213 mASL. In general, water flows from an east to west direction, with the exception of the central portion of HIWEC where water flows towards Henvey Inlet.

HIWEC is located within the Georgian Bay Ecoregion, where the majority of the Ecoregion is dominated by mixed forest. Coniferous and deciduous forests make up a smaller portion of the Ecoregion. Wetlands can be found throughout the landscape in bedrock depressions isolated from water bodies, and as large wetland complexes within topographic valleys. The different wetland types found at HIWEC are swamps, marshes, fens, and bogs. Fens and bogs are dominated by peat mosses such as *Sphagnum* spp., and swamps and marshes are characterized as wetlands with occasional/frequent periods of inundation.

3.2.2 Instrumented wetlands

Four wetlands were randomly selected within HIWEC to validate the model. The wetlands were instrumented in the fall of 2017 to assess the water table position under natural conditions prior to the start of construction in the spring of 2018. The wetlands consisted of different wetland types including fens (HIS-059, HIS-108), bogs (HIS-100), and a transition between a marsh and fen (HIS-030). All four wetlands contained *Sphagnum* moss. The wetlands were surrounded by uplands where tree stands can be found along the bedrock perimeter. HIS-059, HIS-100, and HIS-108 were formed in isolated bedrock depressions, whereas HIS-030 was apart of a larger wetland complex.

3.2.3 Spatial data

All spatial analysis was completed in ArcGIS 10.5.1. Raster and vector files were projected into a Projected Coordinate System (NAD 1983 UTM Zone 17N) and clipped to the boundary of the project extent. Light Detection and Ranging (LiDAR) was flown over the study area. The last return points were extracted from the LiDAR dataset to create a Digital Elevation Model (DEM) with a pixel resolution of 1 m (provided by AECOM). Habitat types within HIWEC were classified according to the Ecological Land Classification (ELC) scheme (AECOM, 2015), and subsequently simplified into four categories: rock barren, forests, wetlands, and water bodies. The provincial stream network was acquired from Scholars GeoPortal.

3.2.4 Field data

3.2.4.1 Organic soil depth

In order to improve estimates of water storage and water table (WT) dynamics within the wetland, the organic soil thickness was measured. A 2 m rebar was inserted into the wetland until the mineral soil layer was reached. Multiple points along a single transect was measured until the organic soil thickness stopped increasing. The point at which the soil thickness stopped increasing was assumed to be the maximum value within the wetland. Due to site access limitations, organic soil depth measurements were only collected for a subset of wetlands along the road network (Figure 3-1).

3.2.4.2 Water table position

Monitoring wells were installed into the underlying mineral soil in HIS-030, HIS-059, HIS-100, and HIS-108. All pipes were constructed from slotted PVC (5 cm diameter), and lined with a

well sock to prevent sediment and material from entering. Logging pressure transducers (Solinst Junior Levelogger, Solinst, Georgetown, ON, CA, accuracy = ± 0.1%) were deployed in the wells to collect continuous water level measurements at 15-minute intervals. A barologger (Solinst Junior Levelogger, Solinst, Georgetown, ON, CA, accuracy = ± 0.1%) was suspended in a well (Figure 3-1) to correct for changes in atmospheric pressure. Rain events were captured using a tipping bucket rain gauge installed at HIS-030.

3.2.5 Model

3.2.5.1 Multi criteria decision analysis

It has been argued that there are three first-order controls on the regulation of streamflow generation within a catchment (T3 template; Buttle, 2006). This includes topography, which reflects the role of topographic gradients in propagating water movement through the catchment; topology, which measures the hydrological connectivity of HRUs within the catchment; and typology, which characterizes the residence time and ability of different surfaces to transmit water. Given that there are multiple controls influencing streamflow generation within the catchment, a multi-criteria decision analysis (MCDA) was used. The Analytical Hierarchy Process (AHP) was selected in particular as it breaks down the project goal into a hierarchy of criteria. The criteria was first organized into a pairwise comparison:

$$\begin{Bmatrix} w_i/w_i & w_i/w_j & w_i/w_n \\ w_j/w_i & w_j/w_j & w_j/w_n \\ \cdots & \cdots & \cdots \\ w_n/w_i & w_n/w_j & w_n/w_n \end{Bmatrix} \quad (2.1)$$

where $i, j = 1^{st}$ criteria, …, n^{th} criteria, and w_i/w_j (hereinafter referred to as an element) represents the relative importance of one criteria over the other as assessed using a numerical scale (Table

3-1). Each element within the pairwise comparison matrix was then divided by the sum of the column total in order to normalize the matrix. Lastly, the weights were calculated by summing the row of each criterion within the normalized matrix. Once the weights were derived, the model output was calculated using:

$$\sum_{n=1}^{n} (c_n * w_n) \tag{2.2}$$

where n = number of criteria included in the model, c = criteria, and w = derived weight. Each wetland within the study area would be given a flooding potential derived from the model output. The values range from 0 – 1, where 0 was associated with wetlands with a low flooding potential, and 1 was associated with wetlands with a high flooding potential. As the weights for each criterion were derived from ranks using expert evaluation and/or existing literature, inconsistencies can arise. Nevertheless, the ranks within the pairwise comparison matrix can be assessed using a consistency ratio (CR) as outlined in Saaty (1987). If the CR < 0.1, then the pairwise comparison matrix was determined to be consistent.

3.2.5.2 Model variables

Catchment area

A catchment refers to a topographic divide of an area of land where water is collected and drained to an outlet point. Whilst topography delineates the catchment and therefore the quantity of water that can be routed to the outlet, it is not synonymous with contributing area (Philips et al., 2011). Previous studies determined that the total catchment area explained less variation in runoff timing and magnitude for landscapes operating on a threshold-based runoff response (Lindsay et al., 2004). Instead, runoff is influenced by other factors such as the position, storage

capacity, and hydrological connectivity of HRUs within the catchment (McGuire et al., 2005; Buttle, 2006; Hrachowitz et al., 2009; Lindsay et al, 2004).

Catchments were delineated using raster datasets that were derived from the DEM, including flow direction and flow accumulation. The flow direction raster determines the direction that water will flow from each grid cell to its steepest downslope neighbor using an eight-direction flow model (D8 algorithm; O'Callaghan and Mark, 1984). The flow accumulation raster – based on the flow direction raster – calculates the number of upslope cells that flows into a given grid cell. In general, cells with high flow accumulation values correspond to areas of concentrated flow (e.g. streams). In Precambrian shield landscapes, streams are transient in nature and appear during periods of overland flow (Allan and Roulet, 1994). Therefore, water bodies were used as pour points to represent the outlet location, as these are areas where water will accumulate. Given that water bodies were clustered together and connect during periods of high flow (Rover et al., 2011), a single water body was used as the outlet for a given catchment.

Proportion of rock cover

Rainfall falling onto bedrock surfaces often results in rapid runoff generation as the relatively impervious surface of the bedrock limits the ability of water to infiltrate deeper into the subsurface (Allan and Roulet, 1994). While water infiltration into weathered bedrock systems can make up an estimated 18 – 55% of the total annual precipitation (Terajima et al., 1993), water infiltration can be restricted during high intensity rainfall events (Tromp-van Meerveld and McDonald, 2006). Assuming that precipitation falling onto the rock surface results in runoff generation, the ability of flow to be routed to the outlet is dictated by the storage capacity and

antecedent moisture conditions of wetlands found further downslope (Oswald et al., 2011). The proportion of rock cover within a given catchment can be used to estimate the proportion of the catchment that contributes to runoff. The inverse value would therefore represent the proportion of catchment that contributes to water storage. The proportion of rock cover (%Rock) was calculated by dividing the area of rock barren (derived from the habitat shapefile) by the total catchment area, where a higher %Rock value was associated with a greater proportion of area that can contribute to runoff.

Wetland position

Hydrological connectivity refers to the movement of water from one part of the catchment to another, and is related to whether a runoff response will be generated (Bracken and Crooke, 2007). In Precambrian shield landscapes, wetlands become hydrologically connected with the surrounding landscape and contribute to streamflow during periods of fill-and-spill. While previous studies have utilized flow path distance to the stream network as a proxy to assess whether the wetland will be hydrologically connected (Ali et al., 2015), distance is not a measure of hydrological connectivity in Precambrian shield landscapes (Vanderhoof et al., 2017). Rather, the spatial distribution and arrangement of wetlands plays a greater role. For instance, a study by Lindsay et al. (2004) determined that the maximum peak storm discharge was smaller in catchments that contained wetlands located near the outlet. This suggests that these wetlands were located in a suitable position to store overland flow that was being routed to the outlet (Leibowitz et al., 2019). Wetlands located near the outlet are therefore more likely to store runoff than wetlands located near the headwaters (McCauley et al., 2015). The stream order tool was used to assess the position of wetlands within the catchment (Martin and Soranno, 2006). Stream

order was calculated within each catchment using the flow direction raster, and by applying a threshold to the flow accumulation raster. A threshold was applied such that the stream network intersected all of the wetlands. The maximum stream order was applied if the wetland intersected multiple stream order values.

Surface water connection

The contribution of water source to wetlands varies on a spatial and temporal basis. The primary source of overland flow occurs during the spring freshet and fall rewetting when antecedent moisture conditions are met and the storage capacity of the depression is exceeded (Spence, 2003). During low moisture conditions, wetlands become hydrologically disconnected from the landscape and are susceptible to a complete loss of water table (Cohen et al., 2015). The ability of moss-containing wetlands to maintain moisture during this period of time is dependent on the hydrophysical properties of moss to minimize evapotranspiration, and persistent inflow from groundwater and surface water. Although groundwater discharge cannot be determined without field data, wetland connection to surface water can be assessed spatially. Wetlands were determined to have a surface water connection if they intersected with a water body and/or stream network. The resulting layer has a binary response where 1 = surface water (SW) connection, and 0 = absence of SW connection.

3.2.5.3 Normalization

The four criteria were normalized in order to maximize or minimize a value. In Precambrian shield landscapes, runoff is generated once the storage capacity of the HRU is exceeded. Given that there is a non-linear response to runoff generation (Phillips et al., 2011), a non-liner

approach to data normalization was used such that the values of each criterion was comparable. The resulting output would have values ranging from 0 to 1, where 0 indicated that the cell does not contribute to runoff, and 1 indicated that the cells do contribute to runoff.

In order to maximize the value such that higher values were more attractive, the following equation was used:

$$X_i = \frac{\left(x_i - {x_i}^{min}\right)}{{x_i}^{max} - {x_i}^{min}} \tag{2.3}$$

where X_i = criterion score of factor *i*, x_i = original value of factor *i*, x_i^{min} = minimum of factor *i*, and x_i^{max} = maximum of factor *i*.

Conversely, in order to minimize a value such that lower values were more attractive, the following equation was used:

$$X_i = \frac{({x_i}^{max} - x_i)}{{x_i}^{max} - {x_i}^{min}} \tag{2.4}$$

where X_i = criterion score of factor *i*, x_i = original value of factor *i*, x_i^{min} = minimum of factor *i*, and x_i^{max} = maximum of factor *i*

The stream order ranged from 1 – 5 where 1 indicated a location near the headwaters, and 3 – 5 indicated a location near the outlet, depending on the size of the catchment. The stream order was linearly normalized such that the highest stream order value within each catchment was given a value of 1.

3.2.5.4 Sensitivity analysis

To assess the influence of each criterion on the model output, a sensitivity analysis was completed. The criteria were given equal weights (0.25) and held constant as one of the criteria weights was adjusted by increments of 0.1. The flooding potential associated with the four instrumented wetlands were used to assess the influence of the criteria on the model output.

3.2.5.5 Model evaluation

Field data was used to evaluate the model by comparing the model output with the water table position of instrumented wetlands during the winter period. The winter period was selected as it represented a period of time when antecedent soil moisture conditions were quite high, evapotranspiration was minimized, and overland flow occurred (Spence and Woo, 2008). Data points were extracted when air temperatures were above 0°C to initiate melt, in the absence of precipitation events, and there was a change in water table position following the end of the melting period. The instrumented wetlands were subsequently ranked from high to low water table positions to correspond with a high and low flooding potential, respectively. The model was also evaluated by comparing the flooding potential of wetlands to organic soil depth, and wetland types.

3.2.6 Statistical analysis

Statistical analysis was completed to assess whether the model was capable of estimating the relative flooding potential of different wetland types, and depression depths that are associated with higher hydroperiods. All statistical analysis was completed in JMP 14 (SAS, Cary NC, USA). The datasets were first tested for normality using the Shapiro-Wilk test. Given that the

dataset failed the test for normality, non-parametric tests were used. The slope of the sensitivity analysis was used to evaluate the relative importance of one criterion over the other using the Wilcoxon/Kruskal-Wallis test. It is important to note that this analysis consists of a small sample size (n = 4). Once the model was created, the Wilcoxon/Kruskal-Wallis test was used to evaluate the relationship between the flooding potential of wetlands and depth class, and flooding potential and wetland type.

3.3 RESULTS

3.3.1 Water table position

While air temperature was consistently below 0°C from December 5 2017 to February 15 2018, there were a few days during the winter period when air temperature was above 0°C (Figure 3-2). The largest water table spike during the winter was on January 12 and February 21 (Figure 3-3), coinciding with a maximum air temperature of 6.5°C and 11.1°C, respectively. There were 11 – 26 days between January 10 and March 28 where air temperature was above 0°C, in the absence of precipitation events, and the water table position increased following the end of the melting period. The water table position for these days was highest in HIS-030, followed by HIS-059, HIS-108 and lastly HIS-100 (Figure 3-4). While the water table position was higher in HIS-030 than in HIS-059, it was not statistically different (Wilcoxon/Kruskal-Wallis test, $p=0.32$). Of the four monitored wetlands, the water table was consistently above the moss surface in HIS-030 and HIS-059 during the fall rewetting and winter period (Figure 3-3), indicating flooding conditions. Conversely, the water table in HIS-100 and HIS-108 did not exceed the moss surface, indicating a low flooding potential.

The summer was characterized by unusually dry conditions that persisted until August 24 2018, followed by numerous consecutive rain events during the fall that added large water inputs to the landscape (Figure 3-2). The historical rainfall between May and August was 340 mm (1981 – 2010; Environment Canada, 2015) as measured in the Monetville Station located approximately 30 km northwest of HIWEC. In comparison, 170 mm of rain fell between May and August in 2018. The minimum water table was reached on August 1 in HIS-108 (WT_{min} = -64.2 cm), and on August 20 in HIS-100 (WT_{min} = 52.0 cm) and HIS-030 (WT_{min} = -55.7 cm). There were two large water table spikes during the fall rewetting following the end of the summer drought. The first water table spike was initiated on August 25 following a 17 mm storm event. While this provided water to the wetlands, the water table in all three wetlands fell to pre-storm water table positions following the end of the rain events. The largest water table spike during the fall rewetting occurred on September 26 following a 71 mm rain event.

3.3.2 Criteria

Catchment area

There were 24 catchments that extended over the study area (Figure 3-5). The average catchment in the study area was 92 ha, with the largest and smallest area being 289 ha and 11 ha, respectively. The largest catchments were located along the south/southeastern portion of the study area. The smallest catchments were located in the centre of the study area where there was a higher concentration of water bodies.

%Rock

The average proportion of rock cover throughout the study area was 54% (Figure 3-6). Higher rock cover was found at the western portion of HIWEC. The maximum value was 85% coinciding with a catchment area of 25 ha, and the smallest value was 5% coinciding with a catchment area of 120 ha.

Stream order

In general, wetlands with higher stream orders were located close to water bodies and/or the stream network (Figure 3-7). The mean stream order for wetlands that were isolated from surface waters was 0.32. This was statistically different (Wilcoxon/Kruskal-Wallis test, $p<0.0001$) for wetlands physically connected to the surface water, which had a mean stream order of 0.55. Higher stream orders were also associated with larger wetlands (Tukey HSD, $p<0.05$).

Surface water connection

Of the 215 wetlands included in the study area, 120 were connected to an upland water body and/or a stream network (Figure 3-8). On average, larger wetlands were connected to surface waters. The average area was 3.98 ha for wetlands with a connection, and 1.7 ha for wetlands without (Tukey HSD, $p<0.05$).

3.3.3 Sensitivity analysis

A sensitivity analysis was first created when three criteria (%Rock, stream order, catchment area) was included in the model. The slope of the regression line (Table 3-5) was used as an indicator to assess the influence of a criterion on the model output (Figure 3-9). In all four

wetlands, the model was most sensitive to %Rock, followed by stream order and lastly catchment area. The slopes were statistically different between %Rock and catchment area, and %Rock and stream order (Wilcoxon/Kruskal-Wallis test, $p<0.05$), suggesting that catchment area and stream order have an equal importance to one another (Table 3-1) in the pairwise comparison matrix. The ranks established for a 3-criteria model is as follows: %Rock, stream order, and catchment area.

The sensitivity analysis was re-assessed when SW connection was added to the model (Table 3-6). Of the three criteria used in the first model, %Rock had the greatest influence on the model in all four wetlands (Figure 3-10). In HIS-059 and HIS-100 the stream order had a greatest influence on the model output than the catchment area. However, the slopes were not statistically different between the stream order and catchment area criteria. For wetlands that were connected to surface waters (HIS-030 and HIS-059), the SW connection criteria had the greatest influence on the model output, where the slope was similar to %Rock (Table 3-6). However, as SW connection was a binary variable, it did not have a consistent influence on the model output. Similar to the 3-criteria model, the slopes were statistically significant between %Rock and stream order, and %Rock and catchment area (Wilcoxon/Kruskal-Wallis test, $p<0.05$), suggesting that catchment area and stream order have an equal importance to one another (Table 3-1) in the pairwise comparison matrix. The ranks established for a 4-criteria model is as follows: %Rock, SW connection, stream order, and catchment area.

3.3.4 Model outputs

Various combinations of weights were run for the model in order to maintain the criteria ranking established from the sensitivity analysis, and the consistency ratio in the AHP. A final model was selected when the model output had a higher flooding potential for HIS-030, followed by HIS-059, HIS-108, and lastly HIS-100 (Figure 3-4). While a higher flooding potential should be associated with HIS-030, it could be similar to HIS-059 as the difference between the water table positions was not statistically significant (Wilcoxon/Kruskal-Wallis test, $p=0.32$). There should be a greater flooding potential difference between HIS-108 and HIS-100, however, as the water table position of these wetlands was statistically significant (Wilcoxon/Kruskal-Wallis test, $p<0.005$).

3-criteria model

The 3-criteria model was created (Figure 3-11) where %Rock had the largest influence on the model (weight of 41%), followed by stream order (33%) and lastly catchment area (26%). The flooding potential for HIS-030 and HIS-059 was 0.57 and 0.55, respectively. Conversely, the flooding potential was 0.42 for HIS-100 and 0.47 for HIS-108. As such, there exists a 0.08 flooding potential difference between the two groups. While the pairwise comparison matrix (Table 3-7) does indicate that stream order and catchment area had an equal importance over one another (value of 1), the model could not be created such that %Rock had the same ranking over stream order and catchment area (which had a value of 1 and 2, respectively). As such, a 3-criteria model could not be created to satisfy the ranks derived from the sensitivity analysis. Furthermore, there was no statistically significant relationship between flooding potential + wetland area, organic soil depth, and wetland type.

4-criteria model

The 4-criteria model was created (Figure 3-12) where %Rock had the largest influence on the model (weight of 34%), followed by SW connection (29%), stream order (20%), and lastly catchment area (17%). There was a 0.35 flooding potential difference between wetlands with a high water table position (HIS-030, HIS-059) and wetlands with a low water table position (HIS-100, HIS-108; Table 3-10). As such, there was a much larger flooding potential difference between the two groups than seen in the 3-criteria model. The flooding potential was 0.72 and 0.71 for HIS-030 and HIS-059, respectively. Conversely, the flooding potential was 0.32 for HIS-100 and 0.36 for HIS-108. The pairwise comparison matrix for the 4-criteria model was created such that stream order and catchment area had an equal importance over one another (value of 1), and %Rock had the same rank over stream order and catchment area (value of 2). As such, a 4-criteria model could be created such that the rank derived from the sensitivity analysis was satisfied.

There was no statistical significant relationship between wetland area and flooding potential, as well as between wetland area and organic soil depth. The flooding potential of wetlands with a shallow organic soil deposit (>60 cm) and deep organic soil deposit (<60 cm) was 0.47 and 0.60, respectively (Wilcoxon/Kruskal-Wallis test, $p<0.05$). The lowest flooding potential was associated with bogs, followed by swamps, fens, and marshes.

3.4 DISCUSSION

3.4.1 Runoff generation in Precambrian shield landscapes

Previous studies have determined that instead of identifying a threshold catchment area (topography) that initiates runoff, the focus should be on the spatial arrangement and distribution of wetlands (typology, topology) within the catchment (Buttle, 2006; Hrachowitz et al., 2009; McGuire et al., 2015; Ali et al., 2015). Hence, the model criteria were organized into the T3 template (Buttle, 2006) such that it corresponded with a hierarchy expected for Precambrian shield landscapes. The results of the model supported the idea that topography does not have a first-order control on runoff generation in Precambrian shield landscapes, as the ranks established from the sensitivity analysis and AHP could only be satisfied when catchment area was given the smallest weight (17%). Therefore, wetland metrics should be used instead of traditional basin metrics as predictor variables for runoff generation in depressional wetland dominated landscapes (Lindsay et al., 2004).

Runoff generation on rock barren landscapes operates on a threshold-based response, where the storage capacity of HRUs reduces the proportion of water that can be routed towards the outlet. It was therefore unsurprising that the primary control on runoff generation as identified in the model was typology. An assumption associated with the use of %Rock as a proxy to estimate the proportion of catchment that corresponded to runoff was that the inverse value corresponded to the storage capacity of the catchment. The storage capacity of HRUs, however, vary throughout the catchment, where it is a function of the depth and residence time of the material. For example, a study conducted by Spence and Woo (2002) determined that there was a 0.44 difference in runoff ratio between bare rock and slopes with soil patches. Furthermore, Peters et

al. (1995) determined that forests with deeper mineral soils corresponded with larger storage capacities. Given that forests found on Precambrian shield landscape are formed on thin mineral soil deposits (>20 cm), only small water inputs are needed to eliminate the storage deficit required to generate runoff (Spence and Woo, 2002). It was therefore inferred that the storage capacity of forests does not play a large role in reducing runoff magnitude. Instead, runoff generation is largely controlled by the storage capacity of wetlands. A depression depth of 60 cm was identified as the breakpoint for when the water table was never lost in wetlands in a similar rock barren landscape (Didemus, 2016). Although smaller depressions require smaller water inputs to exceed storage capacity, larger depressions rarely dry out and as such have higher water tables and hydroperiod (McCauley et al., 2015). When comparing the model output with the organic soil depths, it was determined that deeper depressions (>60 cm) were associated with higher a higher flooding potential. Therefore, %Rock was a suitable proxy for estimating the proportion of catchment that contributes to runoff generation.

3.4.2 Wetland selection for road crossing

The contribution of water source to wetlands varies on a spatial and temporal basis, where the subsequent wetland type that forms is a result of the hydrological regime found at that location. There are four wetland types (marshes, swamps, bogs, fens) in HIWEC, each with differing degrees of inundation. Marshes are defined as wetlands that experience prolonged inundation conditions. Swamps also experience periods of inundation, though the duration of flooding conditions varies seasonally. Whilst the water table position can be found at or near the moss surface in both bogs and fens, the water table is higher and more stable in fens due to continuous inflow from groundwater. The model was capable of identifying the average flooding potential

associated with different wetland types, where the highest and lowest flooding potential was associated with marshes and bogs, respectively (Figure 3-13). However, a large variability exists within each wetland type. For instance, the flooding potential of bogs ranged from 14 to 80%, suggesting varying contributions of water input to wetlands throughout the landscape. This difference in water input can result in the formation of microtopography within the wetlands. Bogs with a higher water table position (resulting from higher water inputs) may promote the establishment of hollow-forming species capable of withstanding flooded conditions (Wagner and Titus, 1984). Conversely, elevated hummock mounds may form in wetlands with deeper water table positions due to the drought-resistant traits of hummock-forming species (Breeuwer et al., 2008). For projects such as HIWEC where a large emphasis is placed on conserving habitat (hummocks) utilized by SAR reptiles, disturbance that promotes large WT variability that can subsequently reduce the availability of hummocks is not ideal. Therefore, assessing the flooding potential of wetlands (instead of predominantly assessing wetland type) can be completed in order to better meet project objectives.

Historically, isolated wetlands were targeted for drainage purposes as they were determined to have an insufficient contribution to the catchment as a result of discontinuous hydrological connections (Cohen et al., 2015). Smaller and shallower wetlands were also enticing sites for disturbance (Van Meter and Basu, 2015), as a smaller volume of material would need to be excavated and accounted for. However, there was no relationship between wetland size and flooding potential, and as such wetland size was not a suitable metric to assess wetland vulnerability. Furthermore, while a higher flooding potential was associated with wetlands with a surface water connection, the flooding potential for hydrologically isolated wetlands ranged from

0 – 76%, indicating hydrological connectivity at some point in time. Golden et al. (2015) indicated that isolated wetlands were significantly related to streamflow, especially during the winter period due to high antecedent moisture conditions (Acreman and Holden, 2013). Ameli and Creed (2017) also determined that isolated wetlands located 30 km away can influence the quality and quantity of the streamflow, further highlighting that distance is irrelevant when assessing hydrological connectivity in Precambrian shield landscapes. Therefore, instead of targeting smaller and hydrologically isolated wetlands, an evaluation of the flooding potential of wetlands can be completed.

3.4.3 Limitations

The ability of wetlands to maintain a water table during periods of prolonged drought conditions is dependent on water input entering the depression, as well as the hydrophysical properties of the moss (Vu, 2019; Chapter 1). A major limitation of the model was therefore assuming that the only contributing water source to the wetlands was via precipitation and overland flow, and that there was no groundwater connection and water loss through evapotranspiration. Through the use of isotope and hydrodynamic data, a groundwater connection was identified at HIWEC (Vu, 2019; Chapter 1). Not only does groundwater supply water to wetlands during periods of drought conditions, a groundwater connection was suggested to have played a role in minimizing ΔWT as well (Vu, 2019; Chapter 1). However, groundwater connection varied spatially throughout the landscape. Furthermore, while the model could estimate the average flooding potential associated with a given wetland type, uncertainties arise when comparing between swamps and fens. As such, quantifying groundwater contributions into the model can distinguish between the wetland types, and provide more information regarding the hydrology of wetlands.

Unfortunately, the identification of a groundwater connection cannot be completed spatially and would require fieldwork in order to collect and incorporate this data into the model. For instance, piezometers can be added to wetlands to obtain EC values, where high EC values are indicative of a groundwater source. Von-post values of organic soil can also be collected, which provides a quick and easy way to assess the degree of decomposition of moss and peat. This data, alongside with the depression depth, can provide estimates of the WT dynamics and storage capacity of the wetlands. Given that the project objective of HIWEC was to minimize disturbance to habitats (bogs) utilized by SAR reptiles, it was concluded that this model was sufficient in identifying the relative flooding potential of wetlands classified as bogs. Nevertheless, the GIS model can be used as an initial assessment of wetlands in order to focus field efforts.

3.5 CONCLUSIONS

A balance exists between the economic and environmental cost when planning an access road network. While environmental disturbance to wetlands should ideally be kept at a minimum due to the vast amount of ecosystem services that are provided, it is not always possible especially in wetland-dominated landscapes. Evaluation of wetlands is therefore required in order to assess potential sites that are vulnerable to road crossings due to ponding of lateral flow. Given that culvert design is standardized throughout the road network, a higher impact would occur for wetlands with a greater contribution of overland flow. Traditionally, basin metrics such as catchment area have been used as predictor variables to assess runoff generation. However, runoff generation in the Precambrian shield is largely controlled by the spatial arrangement and distribution of HRU within the catchment, suggesting that basin metrics is not applicable in this landscape. Instead, wetland metrics can be used. This includes an assessment of the storage

capacity, hydrological connectivity, and as identified by this study, the relative flooding potential of wetlands. Furthermore, the results of this study indicated the flooding potential instead of the wetland size and degree of isolation should be used, as small and isolated wetlands play an important role in the catchment response. While this model simplifies runoff and hydrological processes operating within the catchment, it can be used as a preliminary assessment of wetlands in order to focus field programs.

3.6 TABLES

Table 3-1: Fundamental scale adapted from Saaty, 1987.

Intensity of importance	Definition
1	Equal importance
3	Moderate importance of one over the other
5	Strong importance
7	Very strong importance
9	Extreme importance
2, 4, 6, 8	Intermediate values

Table 3-2: Objectives of the AHP organized into the T3 template (Buttle, 2006).

Criteria	Topography	Topology	Typology
Catchment area	X		
% Rock			X
Wetland position	X	X	
SW connection	X	X	

Table 3-3: Summary of the criteria selected for assessing water table position in the four wetlands.

Wetland	%Rock	SW Connection	Stream order	Catchment area (ha)
HIS-030	66	1	2	148
HIS-059	79	1	2	11
HIS-100	59	0	1	38
HIS-108	66	0	1	84

Table 3-4: Normalized value of the criteria selected for assessing water table position in the four wetlands. The values are normalized such that 0 = low flooding potential and 1 = high flooding potential.

Wetland	%Rock	SW Connection	Stream order	Catchment area
HIS-030	0.43	1	0.40	0.32
HIS-059	0.93	1	0.50	0.04
HIS-100	0.68	0	0.33	0.13
HIS-108	0.76	0	0.25	0.19

Table 3-5: Slope of the criteria following a sensitivity analysis for a 3-criteria model.

Criteria	HIS-030	HIS-059	HIS-100	HIS-108
%Rock	0.008	0.009	0.07	0.008
Stream order	0.004	0.005	0.003	0.003
Catchment area	0.003	0.0006	0.0004	0.0001

Table 3-6: Slope of the criteria following a sensitivity analysis for a 4-criteria model.

Criteria	HIS-030	HIS-059	HIS-100	HIS-108
%Rock	0.008	0.009	0.007	0.008
SW connection	0.01	0.01	0*	0*
Stream order	0.004	0.005	0.003	0.003
Catchment area	0.005	0.0004	0.001	0.003

* Not connected to surface waters

Table 3-7: Pairwise comparison of Model A using an AHP.

	%Rock	Stream order	Catchment area
%Rock	1	1	2
Stream order	1	1	1
Catchment area	0.5	1	1

Table 3-8: Pairwise comparison of Model B using an AHP.

	%Rock	SW connection	Stream order	Catchment area
%Rock	1	1	2	2
SW connection	1	1	1	2
Stream order	0.5	1	1	1
Catchment area	0.5	0.5	1	1

3.7 FIGURES

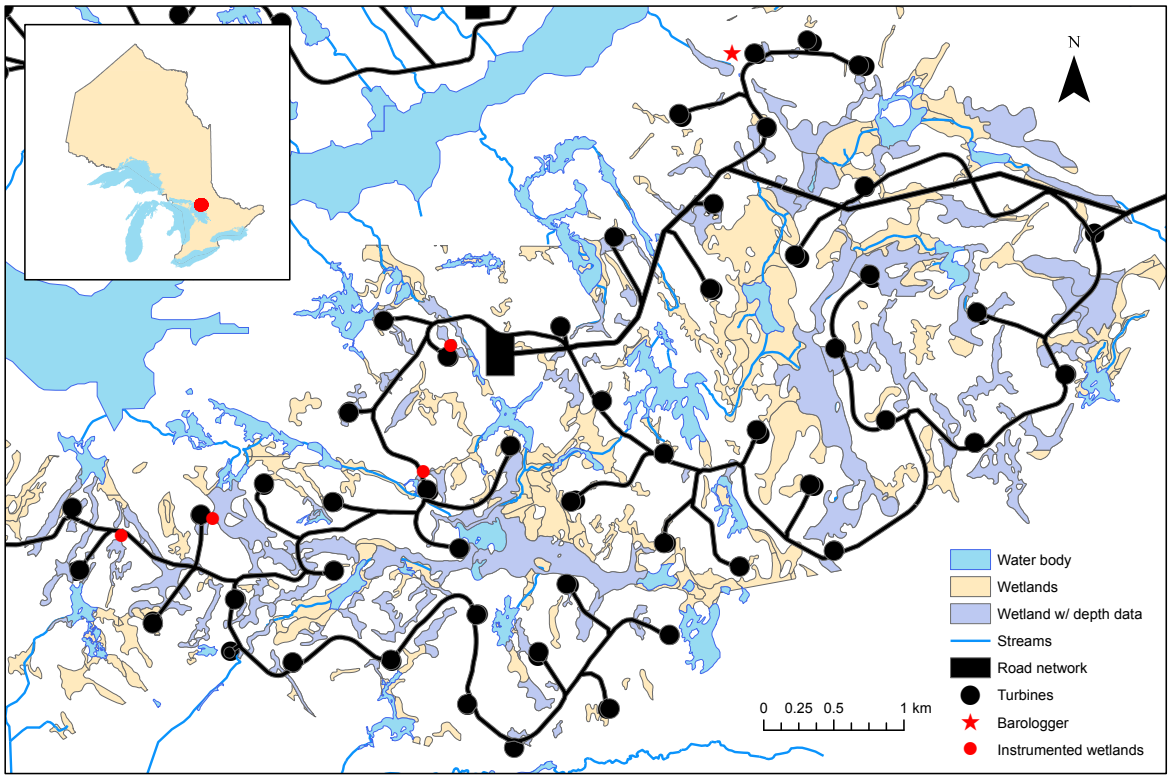

Figure 3-1: Map showing the boundary, road network, and instrumentation of the study area as located on the Henvey Inlet Wind Energy Centre.

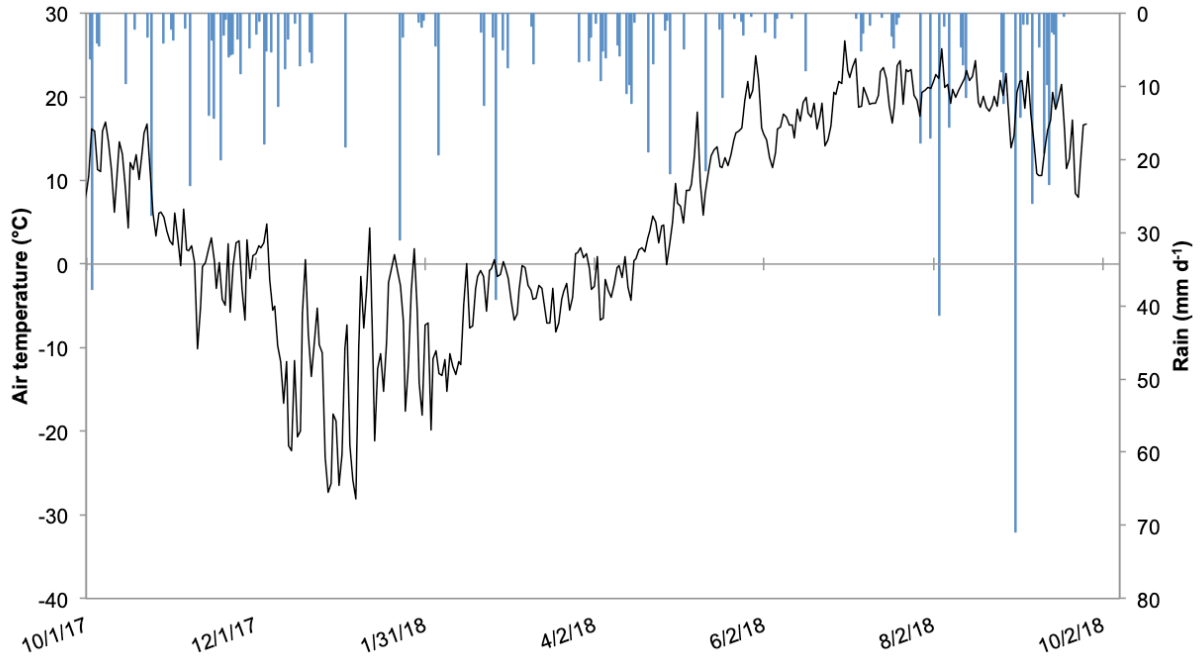

Figure 3-2: Air temperature (black, daily average, °C) and rainfall (blue, mm d^{-1}) measured over the study period from October 1st 2017 to October 2nd 2018.

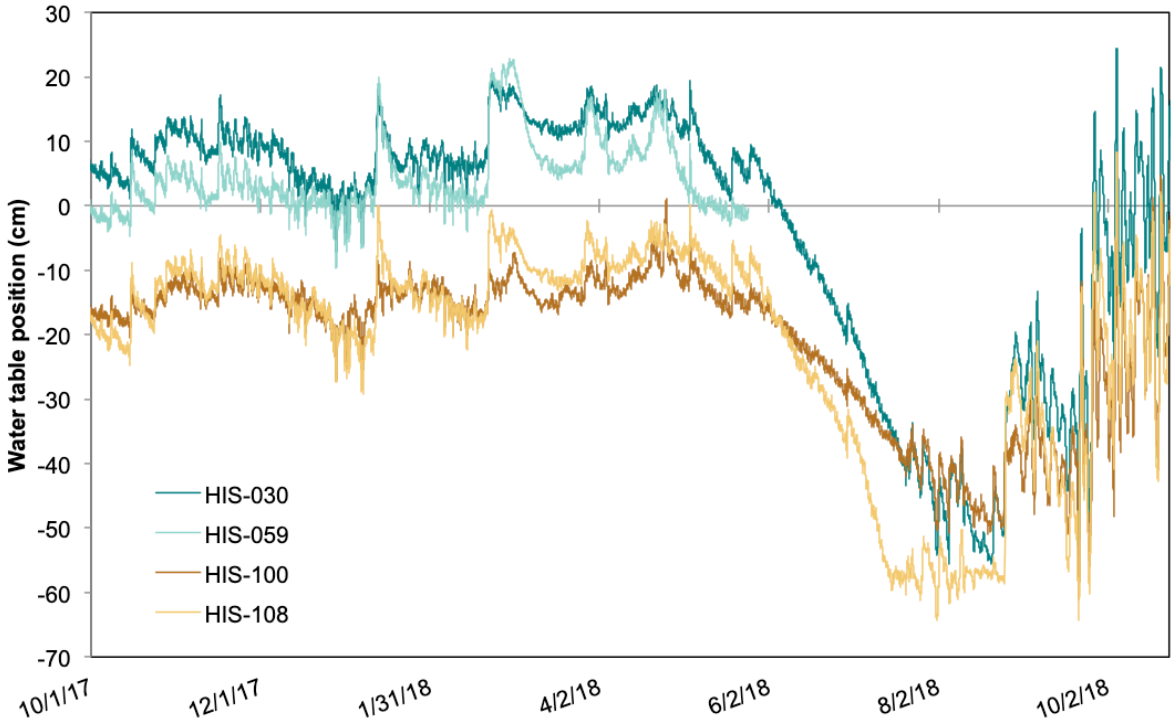

Figure 3-3: Water table position measured relative to the moss surface (0 cm). The wells were installed in October 2017 prior to construction in the spring.

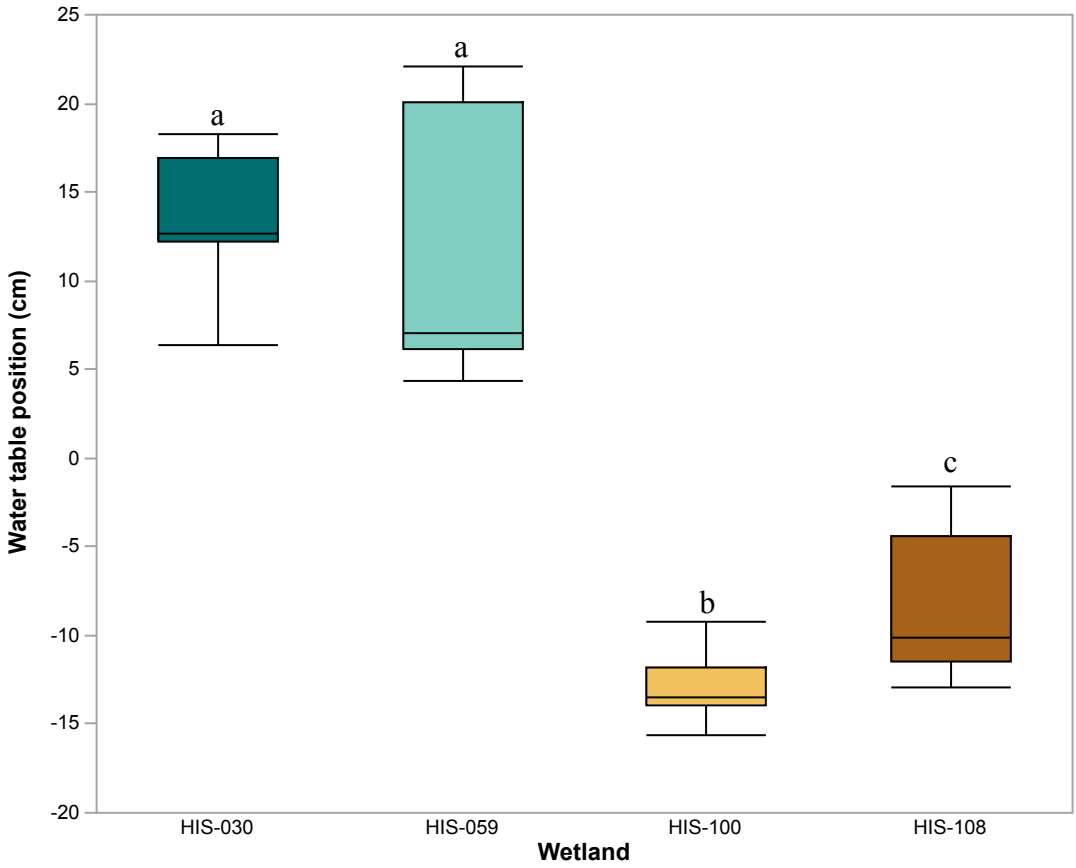

Figure 3-4: Water table position when the temperature was above 0°C, in the absence of precipitation events, during the winter period (January 12 to March 26). The letters denotes statistical difference between the groups (Wilcoxon/Kruskal-Wallis, $p<0.005$).

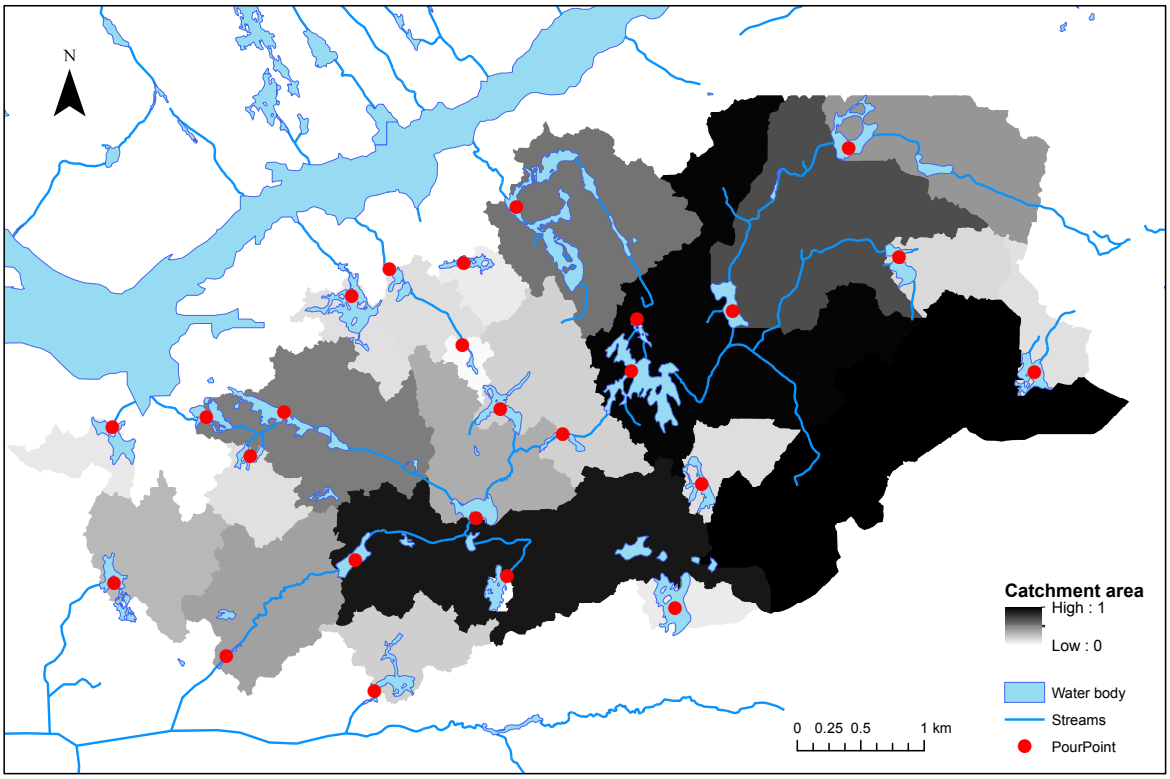

Figure 3-5: The catchment area criteria non-linearly normalized such that 1 equals to catchments with the largest area. The pour points (red circles) were used to delineate the catchments.

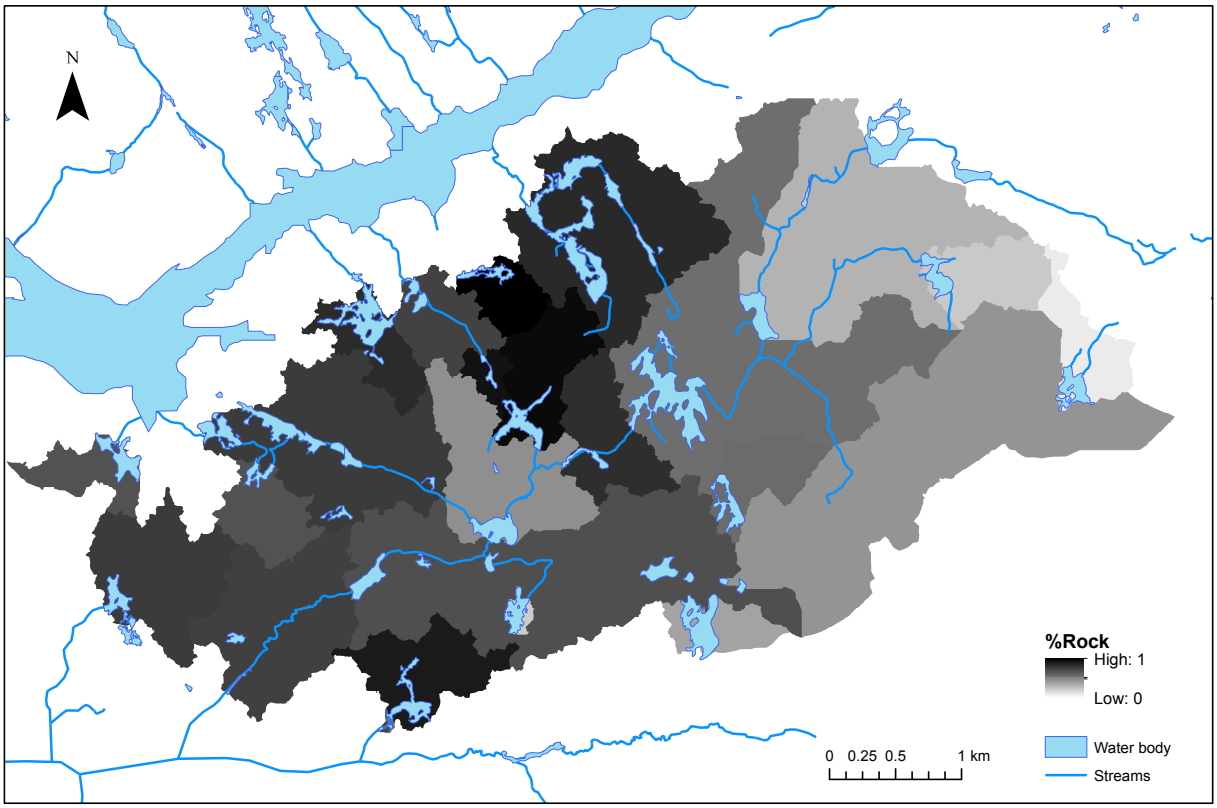

Figure 3-6: The %Rock criteria non-linearly normalized such that the maximum value (1) equates to catchments with the highest proportion of rock cover.

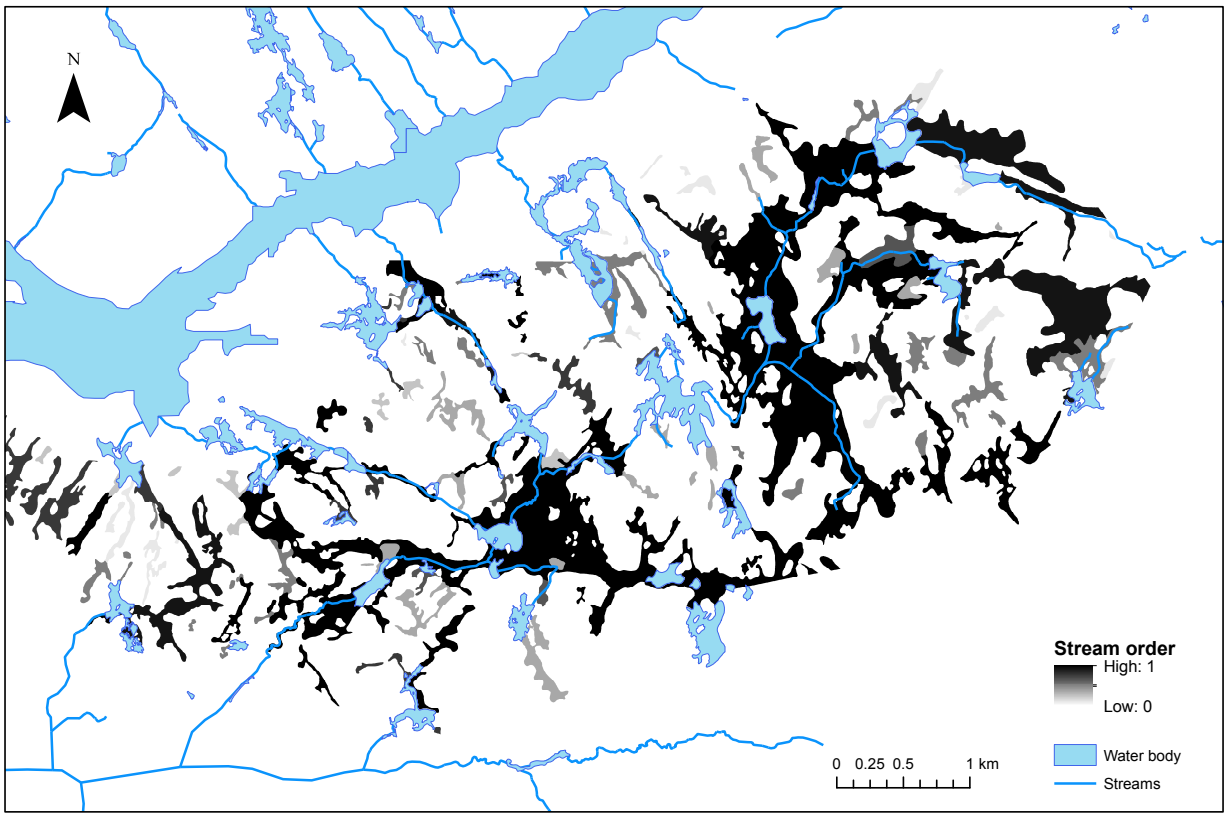

Figure 3-7: The stream order criteria linearly normalized such that the maximum value (1) equates to wetlands located near the outlet within a given catchment. A value of 0 refers to wetlands located within the headwaters.

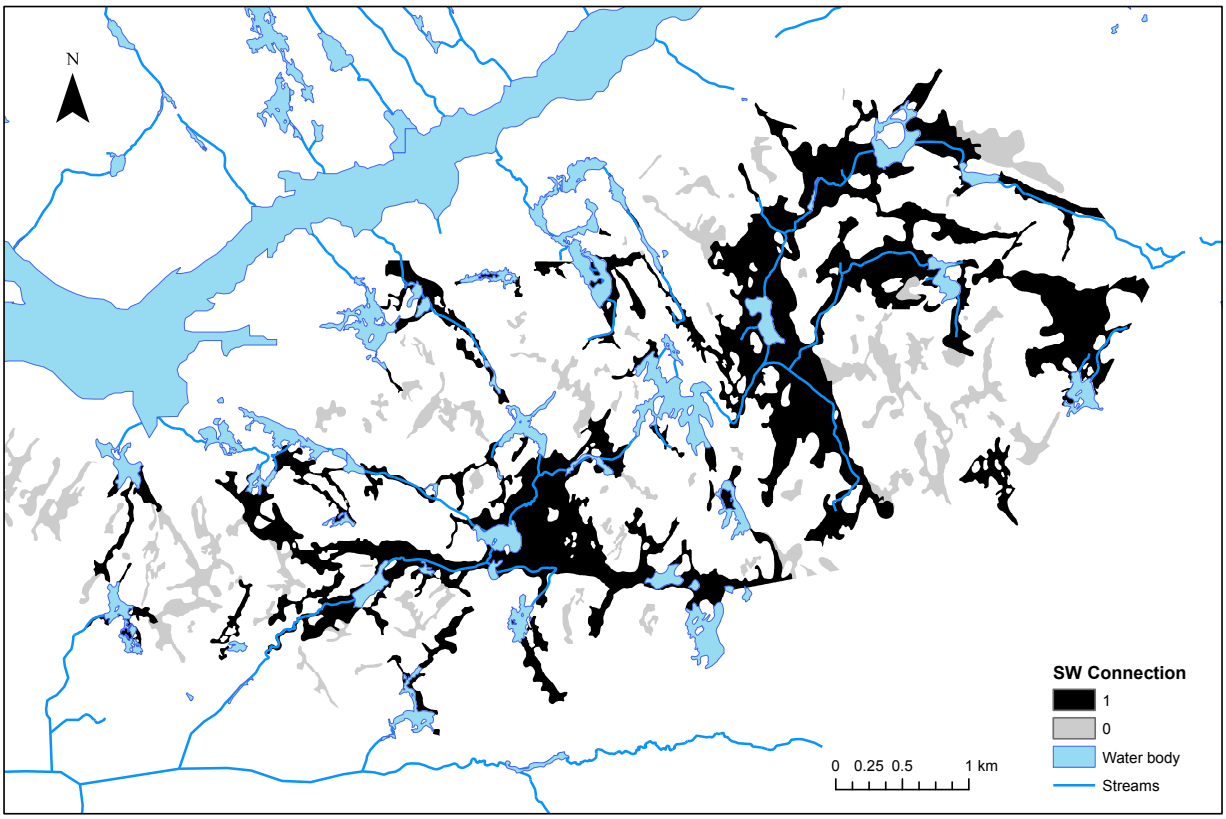

Figure 3-8: SW connection criteria where 0 indicates that wetlands were isolated from water bodies and/or the stream network, and 1 indicates wetlands with a connection to surface water.

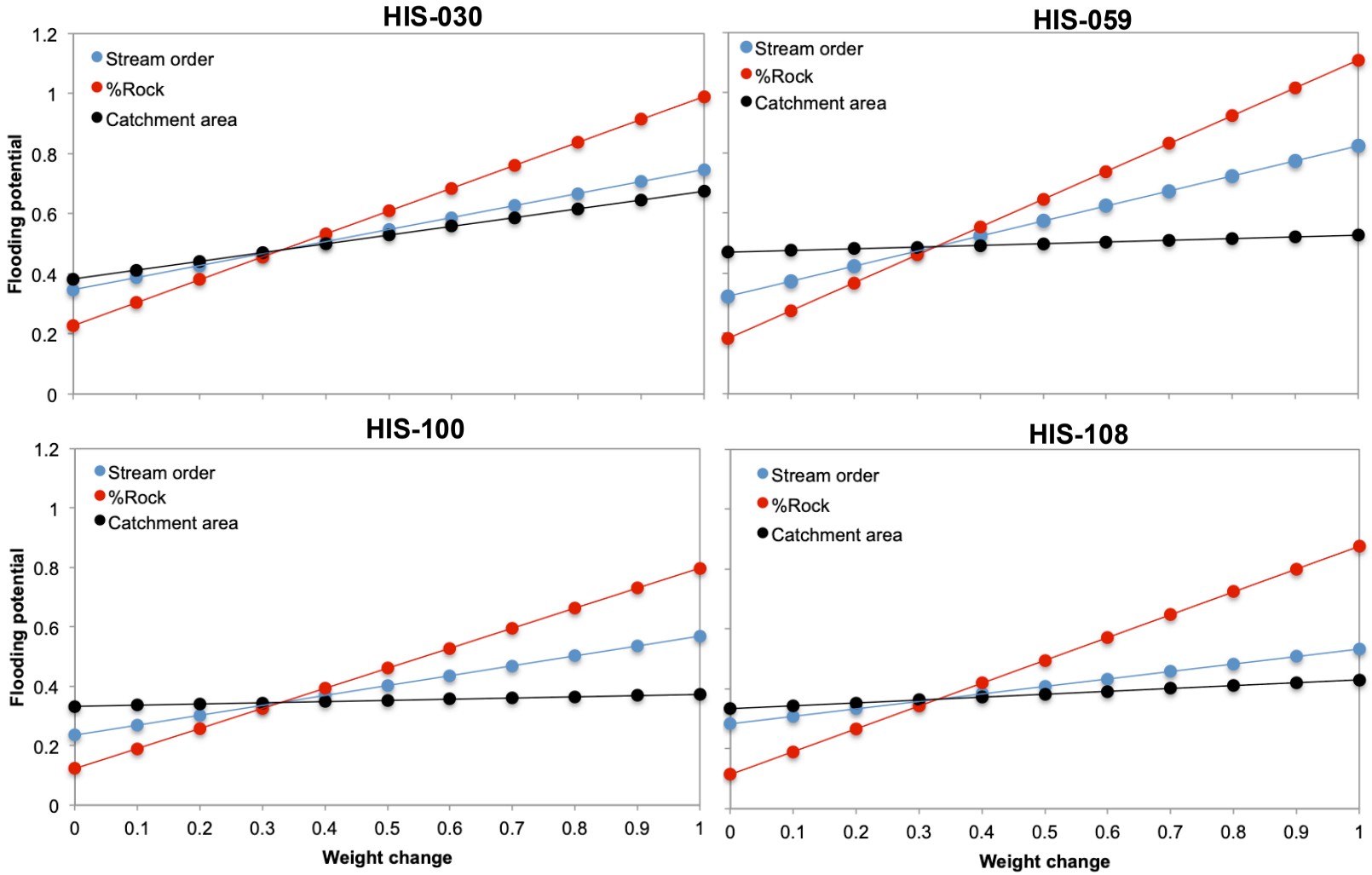

Figure 3-9: Sensitivity analysis for the 3-criteria model created by holding two criteria at an equal and constant weight, and changing the weight of one criteria by 0.1 increments. The slope of the regression line can be used to assess the influence of the criteria on the model output.

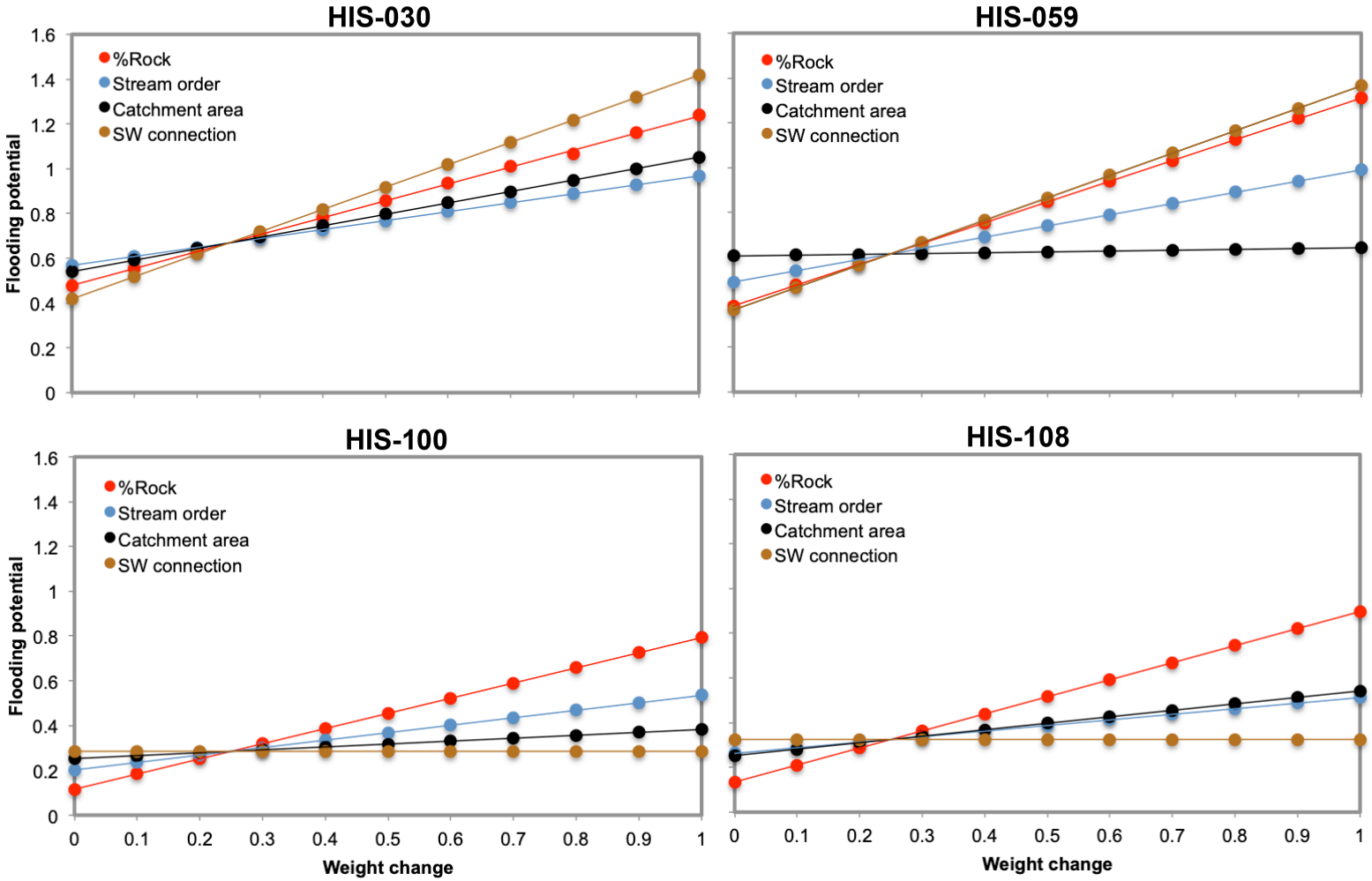

Figure 3-10: Sensitivity analysis for the 4-criteria model created by holding three criteria at an equal and constant weight, and changing the weight of one criteria by 0.1 increments. The slope of the line can be used to assess the influence of the criteria on the model output.

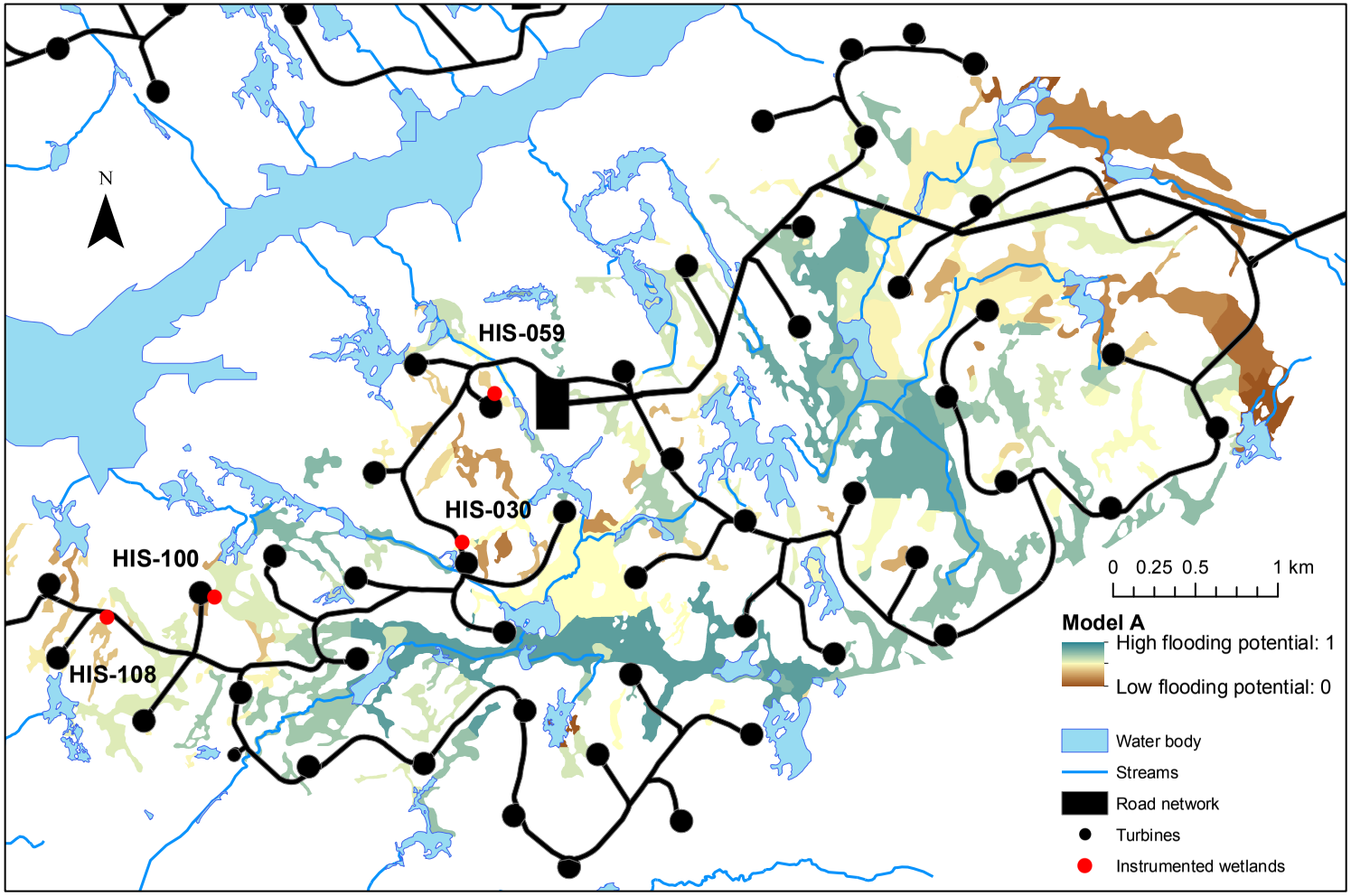

Figure 3-11: Results of the 3-criteria model (Model A) such that higher values (teal) indicates higher flooding potential, and smaller values (brown) indicates a lower flooding potential.

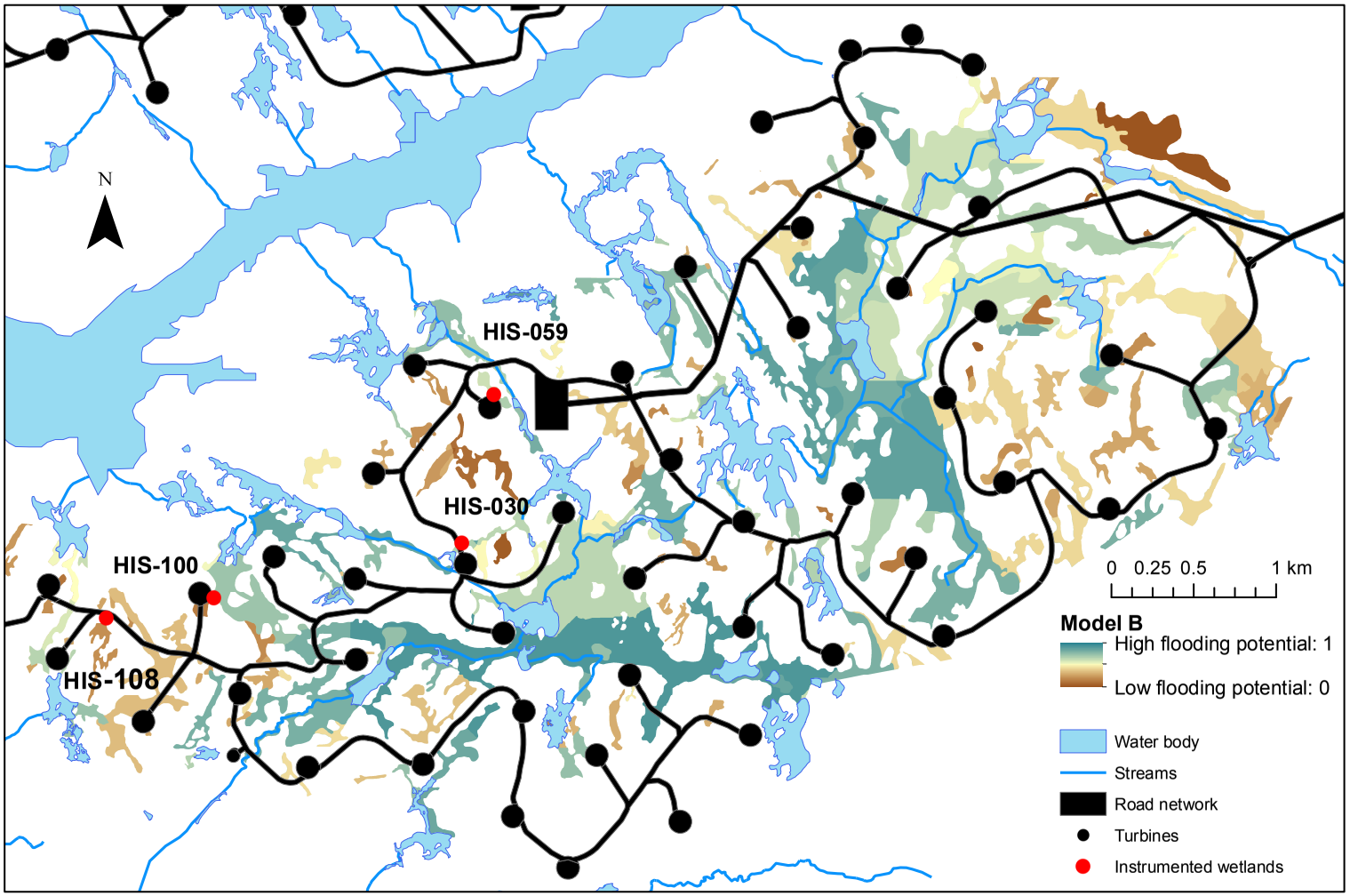

Figure 3-12: Results of the 4-criteria model (Model B) such that higher values (teal) indicates higher flooding potential, and smaller values (brown) indicates a lower flooding potential.

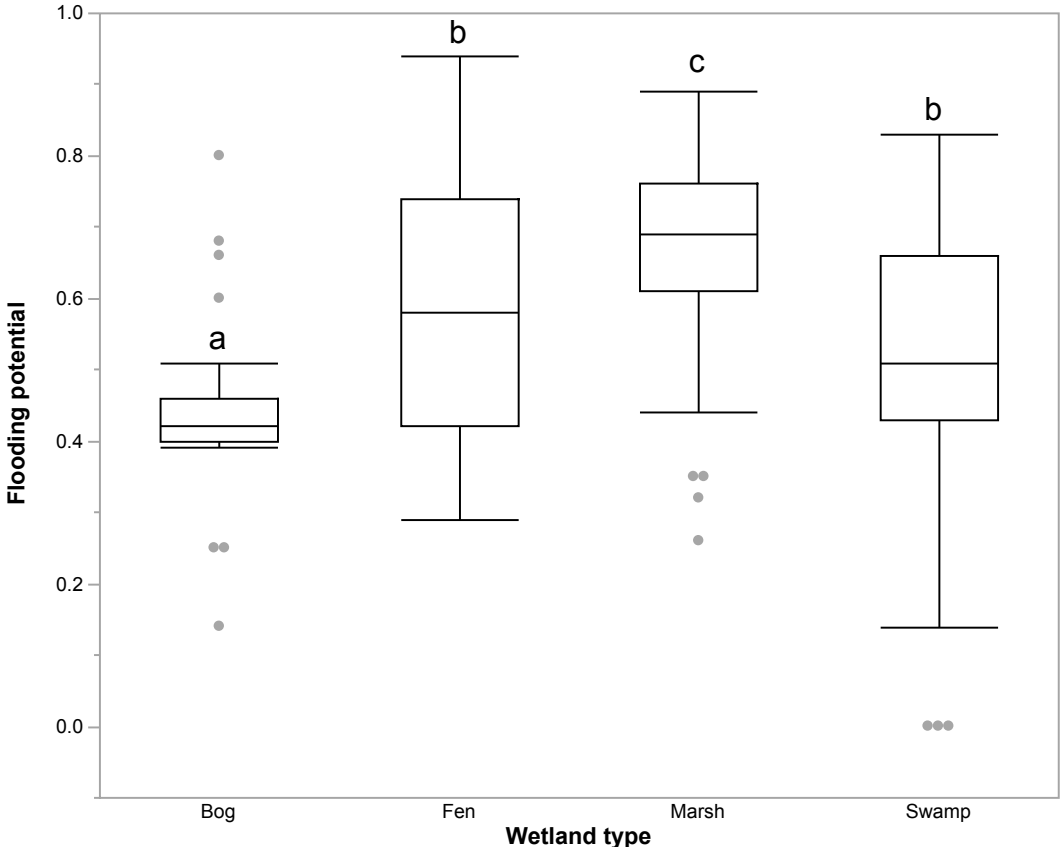

Figure 3-13: Flooding potential of the different wetland types. Letters denotes statistical significance between groups with different letters (Wilcoxon/Kruskal-Wallis test, $p<0.005$).

CHAPTER 4: CONCLUSIONS

Access roads are a large infrastructure component associated with natural resource and mineral exploration projects. Although necessary for the development and operation of these facilities, access roads are linear disturbances that can alter hydrological processes operating within wetlands. The addition of a road acts as a barrier to lateral flow, resulting in an increased water table upstream as water is discharged to the surface. The vertical gradient was small in piezometer nests installed in undisturbed substrates (~15 m away from the road), suggesting that this vertical water movement is a consequence of the road cut-through. Downstream of the road cut-through, the wetland experienced a lowered water table due to reduced water inputs from lateral flow. A lowered water table exposes the peat soils to aerobic condition, further degrading the wetland by increasing decomposition rates. While the wetland downstream of the road cut-through does not experience prolonged flooding conditions, a lower water table position prior to the start of a storm event are associated with a flashier water table response. This promotes the establishment of moss species that are capable of withstanding high WT variability. Given that wetlands found on the Precambrian shield are a biological hotspot for the EMR, changes in the wetland form and function can be detrimental to the future success of these species. Although hydrological change occurred throughout the landscape, the impact was not uniform across the landscape. It was observed that the difference between the water table position upstream and downstream of the road (ΔWT) was largest in wetlands (201) where the culvert was placed 20 cm above the moss surface, and smallest in wetlands (205) when the culvert was partially embedded into the subsurface. The results of this study supports a previous suggestion that

partial burial is the ideal culvert placement as it accounts for both surface and subsurface flow (Phillips, 1997). The placement of the culvert on the moss surface (202, 203) was also an improvement from 201, as the water table would only need to exceed the moss surface in order for flow to be permitted downstream. The moss would therefore not experience prolonged flooding conditions as a result of road cut-through. While the culvert design was similar between 202 and 203, the ΔWT was smaller in the wetland (203) that received not only water contributions from lateral flow, but from groundwater discharge and overland flow as well. This suggests that multiple water sources are important to provide water to the bisected unit downstream of the road cut-through.

In general, the ΔWT was higher during the fall rewetting than during the drought, suggesting that ponding occurred upstream during periods of high water input. Provided that culvert design is standardized throughout the road network, wetlands that receive large water inputs from overland flow would experience extended periods of flooding. A GIS model was therefore created to assess the relative flooding potential of wetlands using criteria (catchment area, proportion of rock cover, stream order, surface water connection) that represent the first-order controls of runoff (T3 template; Buttle, 2006) on Precambrian shield landscapes. The model output was evaluated using field data, where the wetlands were ranked based on its water table position during the winter period when snowmelt was assumed to occur. The model was capable of assessing the hydroperiod of different wetland types, where the highest and lowest flooding potential was associated with marshes and bogs, respectively. A higher flooding potential was also associated with deeper depressions (>60 cm), which was identified as the breakpoint for when the water table was never lost in wetlands (Didemus, 2016). Previously, smaller and

isolated wetlands were targeted for disturbance as it was assumed that these wetlands had a negligible impact on catchment response. However, the flooding potential of wetlands was variable throughout the landscape, and was not associated with a single wetland metric (i.e. hydrological connectivity, wetland type, wetland area). As such, this model suggests that flooding potential can be used in conjunction with wetland metrics to assess wetlands prior to road cut-through. Therefore, an understanding of wetland hydrology, and proper selection of wetlands and culvert design can be completed to minimize hydrological impact associated with access roads.

CHAPTER 5: REFERENCES

Acreman, M., Holden, J. (2013). *Wetlands*, 33, 773-786.

AECOM. (2015). *Henvey Inlet Wind Energy Centre – Hydrogeological Assessment and Effects Assessment.*

AECOM. (2016) *Henvey Inlet Wind Energy Centre – Environmental Assessment.*

Ali, G., Tetzlaff, D., McDonnell, J.J., Soulsby, C., Carey, S., Laudon, H., McGuire, K., Buttle, J., Seibert, J., Shanley, J. (2015). Comparison of threshold hydrologic response across northern catchments. *Hydrological Processes*, 28, 3575-3591.

Allan, C.J., Roulet, N.T. (1994). Runoff generation in zero-order Precambrian Shield catchments: the stormflow response of a heterogeneous landscape. *Hydrological Processes*, 8, 369-388.

Ameli, A.A., Creed, I.F. (2017). Quantifying hydrologic connectivity of wetlands to surface water systems. *Hydrology and Earth System Sciences*, 21, 1791-1808.

Bam, E.K.P. (2018). *Understanding hydrological processes and water fluxes linking wetland ponds and groundwater in the Prairie Pothole Region.* PhD dissertation, University of Saskatchewan, Canada.

Beven, K., Germann, P. (1982). Macropores and water flow in soils. *Water Resources Research,* 18(50), 1311-1325.

Bocking, E. (2015). *Analyzing the impacts of road construction on the development of a poor fen in Northeastern Alberta, Ontario*. MSc dissertation, University of Waterloo, Canada.

Bracken, L.J., Croke, J. (2007). The concept of hydrological connectivity and its contribution to understanding runoff-dominated geomorphic systems. *Hydrological Processes*, 21(3), 1749-1763.

Branfireun, B.A., Roulet, N.T. (1998). The baseflow and storm flow hydrology of a precambrian shield headwater peatland. *Hydrological Processes*, 12, 57-72.

Breeuwer, A., Heijmans, M.P.D., Robroek, B.J.M., Berendse, F. (2008). The effect of temperature on growth and competition between *Sphagnum* species. *Oecologia*, 156, 155-167

Brooks, R.T., Hayashi, M. (2002). Depth-area-volume and hydroperiod relationships of ephemeral (vernal) forest pools in southern New England. *Wetlands*, 22(2), 247-255.

Buttle, J.M., Sami, K. (1992). Testing the groundwater ridging hypothesis of streamflow generation during snowmelt in a forested catchment. *Journal of Hydrology*, 135, 53-72.

Buttle, J.M., Dillon, P.J., Eerkes, G.R. (2004). Hydrologic coupling of slopes, riparian zones and streams: an example from the Canadian Shield. *Journal of Hydrology*, 287, 161-177.

Buttle, J. (2006). Mapping first-order controls on streamflow from drainage basins: the T^3 template. *Hydrological Processes*, 20, 3415-3422.

Christensen, W. (2013). *Hydrologic characterization and modeling of a montane peatland, Lake Tahoe basin, California.* PhD dissertation, University of California, USA.

Clay, A., Bradley, C., Gerrard, A.J., Leng, M.J. (2004). Using stable isotopes of water to infer wetland hydrological dynamics. *Hydrology and Earth System Sciences*, 8(6), 1164-1173.

Cohen, M.J., Creed, I.F., Alexander, L., Basu, N.B., Calhoun, A.J.K., Craft, C., D-Amico, E., DeKeyser, E., Fowler, L., Holden, H.E., Jawitz, J.W., Kalla, P., Kirkman, K., Lane, C.R., Lang, M., Leibowitz, S.G., Lewis, D.B., Marton, J., McLaughlin, D.L., Mushet, D.M., Raanan-Kiperwas, H., Rains, M.C., Smith, L., Walls, S.C. (2015). Do geographically isolated wetlands influence landscape functions? *Proceedings of the National Academy of Sciences of the United States of America*, 113(8), 1978-1986.

Constanzo, J.P. (1988). Effects of humidity, temperature, and submergence behavior on survivorship and energy use in hibernating garter snakes, *Thamnophis sirtalis*. *Canadian Journal of Zoology,* 67, 2486-2492.

Crins, W.J., Gray, P.A., Uhlig, P.W.C., Wester, M.C. (2009). *The ecosystems of Ontario, part 1: ecozones and ecoregions*. Ontario Ministry of Natural Resources, Peterborough Ontario, Inventory, Monitoring and Assessment, SIB TER IMA TR-01.

Dansgaard, W. (1964). Stable isotopes in precipitation. *Tellus*, 16, 436-468.

Datta, P.S., Bhattacharya, S.K., Tyagi, S.K. (1996). 18O studies on recharge of phreatic aquifers and groundwater flow-paths of mixing in the Delhi area. *Journal of Hydrology*, 176, 25-36.

Delgado, J.D., Arroyo, N.L., Arévalo, J.R., Fernández-Palacios, J.M. (2007). Edge effects of roads on temperature, light, canopy cover, and canopy height in laurel and pine forests (Tenerife, Canary Islands). *Landscape and Urban Planning*, 81(4), 328-340.

Didemus, B.R. (2016). *Water storage dynamics in peat-filled depressions of Canadian Shield rock barrens: implications for primary peat formation.* MSc dissertation. McMaster University, Canada.

Environment Canada. (2015). Station results – 1981-2010 climate normal and averages – Monetville. Retrieved from http://climate.weather.gc.ca/climate_normals/results_1981_2010_e.html?stnID=4125&lang=e&StationName=Monetville&SearchType=Contains&stnNameSubmit=go&dCode=5&dispBack=1 MOECC,

Findlay, C.S., Bourdages, J. (2000). Response time of wetland biodiversity to road construction on adjacent lands. *Conservation Biology*, 14(1), 86-94.

Fitzjohn, C., Ternan, J.L., Williams, A.G. (1998). Soil moisture variability in a semi-arid gully catchment: implications for runoff and erosion control. *Catena*, 32, 55-70.

FP Innovations. (2011). *Water management techniques for resource roads in wetlands: a state of practice review.* Prepared for Ducks Unlimited Canada.

Fraser, C.J.D., Roulet, N.T., Lafleur, M. (2001). Groundwater flow patterns in a large peatland. *Journal of Hydrology*, 246, 142-154.

Freeze, R.A., Cherry, J.A. (1979). Groundwater. New Jersey: Prentice Hall.

Furukawa, A. (2018). *Pore-water feedbacks and resilience to decay in peat-filled bedrock depressions of the Canadian Shield*. MSc dissertation, McMaster University, Canada.

Gay, D.E. (1998). *A comparison of the hydrology and aqueous geochemistry of temporary ponds on the Prescott Peninsula of the Quabbin Reservoir watershed in central Massachusetts*. MSc dissertation. University of Massachusetts, USA.

Golden, H.E., Sander, H.A., Lane, C.R., Zhao, C., Price, K., D'Amico, E., Christensen, J.R. (2015). Relative effects of geographically isolated wetlands on streamflow: a watershed-scale analysis. *Ecohydrology*, 9(1), 21-38.

Gray, D.M., Landine, P.G., and Granger, R.J. (1984). Simulating infiltration into frozen prairie soils in streamflow models. *Canadian Journal of Earth Sciences*, 22(3), 464-472.

Gröning, M., Lutz, H.O., Roller-Lutz, Z., Kralik, M., Gourcy, L., Pöltenstein, L. (2012). A simple rain collector preventing water re-evaporation dedicated for δ18O and δ2H analysis of cumulative precipitation samples. *Journal of Hydrology*, 448-449, 195-200.

Haddad, N.M., Brudvig, L.A., Clobert, J., Davies, K.F., Gonzalez, A., Holt, R.D., Lovejoy, T.E., Sexton, J.O., Austin, M.P., Collins, C.D., Cook, W.M., Damschen, E.I., Ewers, R.M.,

Foster, B.L., Jenkins, C.N., King, A.J., Laurance, W.F., Levey, D.J., Margules, C.R., Melbourne, B.A., Nicholls, A.O., Orrock, J.L., Song, D., Townshend, J.R. (2015). Habitat fragmentation and its lasting impact on Earth's ecosystems. *Science Advances*, 1(2), 1-9.

Hare, D.K. (2015). *Hydrogeological control on spatial patterns of groundwater seepage in peatlands*. MSc dissertation, University of Massachusetts, USA.

Harvey, D.S., Weatherhead, P.J. (2006). Hibernation site selection by Eastern Massasauga Rattlesnakes (*Sistrurus catenatus catenatus*) near their northern range limit. *Journal of Herpetology,* 40(1), 66-73.

Hewlett, J.D., Hibbert, A.R. (1967). Factors affecting the response of small watersheds to precipitation in humid areas. In *International Symposium on Forest Hydrology*, Sopper W, Lull H. (eds) Pergamon: New York; 275-290.

Hogg, E.H. (1993). Decay potential of hummock and hollow *Sphagnum* peats at different depths in a Swedish raised bog. *Oikos*, 62, 269-278.

Holden, J., Chapman, P.J., Labadz, J.C. (2004). Artificial drainage of peatlands: hydrological and hydrochemical process and wetland restoration. *Progress in Physical Geography*, 28(1), 95-123.

Hvorslev, M.J. (1951). Time lag and soil permeability in groundwater observations. *Waterways Experimental Station Bulletin*, 36, Corps of Engineers, United States Army, Vicksburg, Mississippi.

Hrachowitz, M., Soulsby, C., Tetzlaff, D., Dawson, J.J.C., Malcom, I.A. (2009). Regionalization of transit time estimates in montane catchments by integrating landscape controls. *Water Resources Research*, 45, 1-18.

Ivanov, K. (1981). *Water movement in mirelands.* New York: Academic Press.

Johnson, G., Kingsbury, B., King, R., Parent, C., Seigel, R., Szymanski, J. (2000). *The Eastern Massasauga rattlesnake: A handbook for land managers.* Fort Snelling, MN.

Kor, P.S.G., Delorme, R.J. (1989). *Quaternary geology of the Key Harbour Area, Southern Ontario*. Ontario Geological Survey, Map P3145, Geological Series Preliminary Map, scale 1:50,000.

Kor, P.S.G. (1991). *The quaternary geology of the Parry South-Sundridge area, Central Ontario*. Ontario Geological Survey, Open File Report 5796.

Ketcheson, S.J. (2015). *Hydrology of a constructed fen watershed in a post-mined landscape in the Athabasca oil sands region, Alberta, Canada.* PhD dissertation. University of Waterloo, Canada.

La Marche, J.L., LettenMaier, D.P. (2001). Effects of forest roads on flood flows in the Deschutes River, Washington. *Earth Surface Processes and Landforms,* 26, 115-134.

Lehmann, P., Hinz, C., McGrath, G., Tromp-van Meerveld, H.J., McDonnell, J.J. (2007). Rainfall threshold for hillslope outflow: an emergent property of flow pathway connectivity. *Hydrological and Earth System Sciences*, 11, 1047-1063.

Leibowitz, S.G., Brooks, R.T. (2008). Hydrology and landscape connectivity of vernal pools. *Science and Conservation of Vernal Pools in Northeastern North America.* Florida: CRC Press.

Leibowitz, S.G., Wigington, P.J., Schofield, K.A., Alexander, L.C., Vanderhoof, M.K., Golden, H.E. (2018). Connectivity of streams and wetlands to downstream waters: an integrated systems framework. *Journal of the American Water Resources Association*, 54(2), 298-322.

Lemley, D.A. (1996). Risk assessment in the regulatory process for wetlands. *Ecotoxicology and Environmental Safety*, 35, 41-56.

Lindsay, J.B., Creed, I.F., Beall, F.D. (2004). Drainage basin morphometrics for depressional landscapes. *Water Resources Research*, 40, 1-9.

Mader, K. (2014). *Mitigating impacts of new forest access roads on water levels in forested wetlands: are cross-drains enough?* MSc dissertation. Dalhousie University, Canada.

Martin, S.L., Soranno, P.A. (2006). Lake landscape position: relationships to hydrologic connectivity and landscape features. *Limnology and Oceanography,* 51(2), 801-814.

McCauley, L.A., Anteau, M.J., van der Burg, M.X., Wiltermuth, M.T. (2015). Land use and wetland drainage affect water levels and dynamics of remaining wetlands. *Ecosphere*, 6(6), 1-22.

McGuire, K.J., McDonnell, J.J., Weiler, M., Kendall, C., McGlynn, B.L., Welker, J.M., Seibert, J. (2005). The role of topography on catchment-scale water residence time. *Water Resources Research*, 41(5), 1-14.

Megahan, W.F., (1972). Subsurface flow interception by a logging road in mountains of central Idaho. In *National Symposium on Watershed in Transition*. American Water Resources Association: Minneapolis, USA, 350-356.

Mitsch, W.J., Gosselink, J.G. (1993). *Wetlands*, 2nd ed. New York: John Wiley

Natural Resources Canada. (2018). Energy and the economy. Retrieved from https://www.nrcan.gc.ca/energy/facts/energy-economy/20062

Noss, R.F., Cooperrider, A.Y. (1994). *Saving nature's legacy*. Island Press, Washington, D.C.

O'Callaghan, J.F., Mark, D.M. (1984). The extraction of drainage networks from digital elevation data. *Computer Vision, Graphics, and Image Processing*. 28(3), 323-344.

Ontario Geological Survey (2003). *Surficial geology of Southern Ontario*. Ontario Geological Survey, MRD128.

Oswald, C.J., Richardson, M.C., Branfireun, B.A. (2011). Water storage dynamics and runoff response of a boreal shield headwater catchment. *Hydrological Processes*, 25, 3042-3060.

Payne, R.J., Malysheva, E., Tsyganov, A., Pampura, T., Novenko, E., Volkova, E., Babeshko, K., Mazei, Y. (2016). A multi-proxy record of Holocene environmental change, peatland development and carbon accumulation from Staroselsky Moch peatland, Russia. *Holocene*, 26, 314-326.

Pearce, J.K. (1974). *Forest engineering handbook: a guide for logging planning and forest road engineering*. Bureau of Land Management, Oregon State Office, US Department of the Interior.

Peters, D.L., Buttle, J.M., Taylor, C.H., LaZerte, B.D. (1995). Runoff production in a forested, shallow soil, Canadian Shield basin. *Water Resources Research*, 31(5), 1291-1304.

Phillips, M.J. (1997). *Forestry best management practices for wetlands in Minnesota.* Retrieved from https://www.srs.fs.usda.gov/pubs/ja/ja_phillips001.pdf

Phillips, R.W., Spence, C., Pomeroy, J.W. (2011). Connectivity and runoff dynamics in heterogeneous basins. *Hydrological Processes*, 25, 3061-3075.

Piehl, B.T., Beschta, R.L., Pyles, M.R. (1988). Ditch-relief culverts and low-volume forest roads in the Oregon coast range. *Northwest Science*, 62(3), 91-98.

Saaty, R.W. (1987). The analysical hierarchy process – what it is and how it is used. *Mathematical Modelling*, 9(3-5), 161-176.

Shantz, M.A., Price, J.S. (2006). Characterization of surface storage and runoff patterns following peatland restoration, Quebec, Canada. *Hydrological Processes*, 20, 3799-3814.

Shine, R., Mason, R.T. (2004). Patterns of mortality in a cold-climate population of garter snakes (*Thamnophis sirtalis parietalis)*. *Biological Conservation*, 120, 201-210.

Siegel, D.I., Reeve, A.S., Glaser, P.H., Romanowicz, E.A. (1995). Climate-driven flushing of pore water in peatlands. *Nature*, 374, 531-533.

Singer, S.N., Cheng, C.K. (2002). *An assessment of the groundwater resources of Northern Ontario: Areas draining into Hudson Bay, James Bay, and Upper Ottawa River* (Hydrogeology of Ontario Series, Report 2). Ministry of the Environment, 188 pp.

Smolarz, A.G., Moore, P.A., Markle, C.E., Waddington, J.M. (2018). Identifying resilient Eastern Massasauga Rattlesnake (*Sistrurus catenatus*) peatland hummock hibernacula. *Canadian Journal of Zoology*, 96, 1024-1031.

Snodgrass, J.W., Komorowski, M.J., Bryan, A.L., Burger, J. (2000). Relationships among isolated wetland size, hydroperiod, and amphibian species richness: implications for wetland regulations. *Conservation Biology*, 14, 414-419.

Spence, C. (2000). The effect of storage on runoff from a headwater subarctic shield basin. *Arctic*, 53(3), 237-247.

Spence, C., Rouse, W.R. (2002). The energy budget of Canadian Shield subarctic terrain and its impact on hillslope hydrological processes. *Journal of Hydrometeorology*, 3(2), 208-218.

Spence, C. Woo, M. (2002). Hydrology of subarctic Canadian shield: bedrock upland. *Journal of Hydrology*, 262(1-4), 111-127.

Spence, C. (2003). *Hydrological and energy budget processes of the subarctic Canadian Shield*. PhD dissertation. McMaster University, Canada.

Spence, C., Woo M. (2003). Hydrology of subarctic Canadian shield: soil-filled valleys. *Journal of Hydrology*, 279(1-4),151-166.

Spence, C., Woo, M. (2008). *Hydrology of the northwestern subarctic Canadian Shield*. Cold Region Atmospheric and Hydrologic Studies. Springer, Berlin, Heidelberg.

Spence, C., Guan, X.J., and Phillips, R. (2011). The hydrological functions of a boreal wetland. *Wetlands*, 31, 75-85.

Redding, T.E., Devito, K.J. (2006). Particle densities of wetland soils in northern Alberta, Canada. *Canadian Journal of Soil Science*, 86, 57-60.

Reeve, A.S., Siegel, D.I., and Glaser, P.H. (2000). Simulating vertical flow in large peatlands. *Journal of Hydrology*, 227, 207-217.

Rover, J., Wright, C.K., Euliss, N.H., Mushet, D.M., Wylie, B.K. (2011). Classifying the hydrologic function of Prairie Potholes with remote sensing and GIS. *Wetlands*, 31, 319-327.

Taylor, J.A., Tucker, R.B. (1970). The peat deposits of Wales: an inventory and interpretation. *Proceedings of the 3rd international peat congress 1968, Quebec.* Department of Energy, Mines and Resources, Ottawa, 163-173.

Tegou, L., Polatidis, H., Haralambopoulos, D.A. (2015). Environmental management framework for wind farm siting: methodology and case study. *Journal of Environmental Management*, 91(11), 2134-2147.

Terajima, T., Mori, A., Ishii, H. (1993). Comparative study of deep percolation amount in two small catchments in granitic mountain. *Japanese Journal of Hydrological Sciences*, 23, 105-118.

Tew, N., Hesselberg, T. (2017). The effect of wind exposure on the web characteristics of a tetragnathid or b spider. *Journal of Insect Behavior*, 30(30), 273-286.

Thomas, R.B., Megahan, W.F. (1998). Peak flow responses to clear-cutting and roads in small and large basins, western Cascades, Oregon: a second opinion. *Water Resources Research*, 34(12), 3393-3403.

Tromp-van Meerveld, H.J., McDonnell, J.J. (2006). Threshold relations in subsurface stormflow: the fill and spill hypothesis. *Water Resources Research*, 42, 1-11.

Tromp-van Meerveld, H.J., Peters, N.E., McDonnell, J.J. (2007). Effect of bedrock permeability on subsurface stormflow and the water balance of a trenched hillslope at the Panola Mountain Research Watershed, Georgia, USA. *Hydrological Processes*, 21, 750-769.

Trombulak, S.C., Frissell, C. (2002). Review of ecological effects of roads on terrestrial and aquatic communities. *Conservation Biology*, 14(1), 18-30.

van Geldern, R., Barth, J.A.C. (2012). Optimization of instrument setup and post-run corrections for oxygen and hydrogen stable isotope measurements of water by isotope ratio infrared spectroscopy (IRIS). *Limnology and Oceanography Methods*, 10, 1024-1036.

van Haaren, R., Fthenakis, V. (2011). GIS-based wind farm site selection using spatial multi-criteria analysis (SMCA): evaluating the case for New York State. *Renewable and Sustainable Energy Review*, 15, 3332-3340.

Van Meter, K.J., Basu, N.B. (2015). Signatures of human impact: size distributions and spatial organization of wetlands in the Prairie Pothole landscape. *Ecological Applications*, 25(2), 451-465.

Vanderhoof, M.K., Christensen, J.R., Alexander, L.C. (2017). Patterns and drivers for wetland connections in the Prairie Pothole Region, United States. *Wetlands Ecology and Management*, 25, 275-297.

Verry, E.S., Boelter, D.H., Päivänen, Nicchols, D.S., Malterer, T., Gafni, A. (2011). *Physical properties of organic soils.* Peatland Biogeochemistry and Watershed Hydrology. CRC Press.

Waddington, J.M., Morris, P.J., Kettridge, N., Granath, G., Thompson, D.K., Moore, P.A. (2015). Hydrological feedbacks in northern peatlands. *Ecohydrology*, (8), 1137-127.

Wagner, D.J., Titus, J.E. (1984). Comparative desiccative tolerance of two *Sphagnum* mosses. *Oecologia,* 62, 182-187.

Wemple, B.C., Jones, J.A., Grant, G.E. (1996). Channel network extension by logging roads in two basins, western casades, Oregon. *Water Resources Bulletin*, 32(6), 1195-1207.

Xu, C., Chen, D., Han, X., Pan, H., Shen, W. (2016). The collection of the main issues for wind farm optimization in complex terrain. *Journal of Physics: Conference Series*, 753, 1-12.